Escuela Politécnica Superior de Jaén

Grado en Ingeniería Mecánica

UNIVERSIDAD DE JAÉN
Escuela Politécnica Superior de Jaén

Trabajo Fin de Grado

Theoretical-experimental study of the combustion chamber of a laboratory-scale jet engine

Alumno: Jabri Ilhem

Tutoras: Prof. Dr. Eloísa Torres Jiménez
Prof. Dr. Francisca María Guerrero Villar

Dpto: Ingeniería Mecánica y Minera

Septiembre,2023

UNIVERSIDAD DE JAÉN
Escuela Politécnica Superior de Jaén
Departamento de Ingeniería Mecánica y Minera

Doña ELOÍSA TORRES JIMÉNEZ, tutora del Trabajo Fin de Grado titulado: Thermal and fluid installations, que presenta JABRI ILHEM, autoriza su presentación para defensa y evaluación en la Escuela Politécnica Superior de Jaén.

Jaén, Septiembre de 2023

El alumna:

Las tutoras:

Firmado digitalmente por TORRES JIMENEZ ELOISA - 75019082M
Fecha: 2023.09.06 12:20:05 +02'00'

GUERRERO VILLAR FRANCISCA MARIA - 26019083B

Firmado digitalmente por GUERRERO VILLAR FRANCISCA MARIA - 26019083B
Fecha: 2023.09.06 13:02:47 +02'00'

JABRI ILHEM

Eloísa Torres Jiménez

Francisca María Guerrero Villar

Acknowledgments

I would like to express my heartfelt gratitude to the Professors and Doctors that assisted me in the preparation of my final graduation project, as well as the success of this fantastic academic internship experience.

First of all, my special thanks go to:

Prof. Dr. Eloisa Torres Jiménez, *deserves special recognition for the honor she bestowed upon me by consenting to oversee this project, as well as for the invaluable advice she provided. Her assistance and understanding were a genuine motivator to finish this project, and her availability during many phases of this effort, as well as her pertinent ideas, have consistently increased the quality of this paper. I owe her immense gratitude and great respect.*

Prof. Dr. Francisca Mara Guerrero Villar*, who ensured a large portion of this effort, deserves my admiration and appreciation for leading us in carrying out this research. thank you for guiding me throughout the entire process and providing valuable feedback and support.*

Prof. Dr. Fernando A. Cruz Peragon, *thank you very much for all of your efforts as well as suggestions in this work. May this effort provide witness to my thanks and sincere admiration.*

We would also want to thank the jury members who consented to take an interest in our work and provide us with their professional opinion.

Jabri Ilhem.

Table of Contents

Tables List

Figures List

Abbreviations and symbols List

Acronyms:

ECU:	Electronic control unit
EDT:	Engine data terminal
MGT:	Micro gas turbine
ATM:	Air Traffic Management
CNC:	Computer numerical control
EASA:	European Aviation Safety Agency
NATO:	North Atlantic Treaty Organization
THRO:	Throttle position
EGT:	Exhaust Gas Temperature
PRM:	Revolutions of shaft
APU:	Auxiliary power unit
GCV/PSC:	Gross calorific value
LCV/PCI:	Lower or net calorific
LIMS:	Laboratory information management systems
SCAI:	Central research support services
CICT:	Centre for Scientific-Technical Instrumentation
ICAO:	International Civil Aviation Organization
APU:	Auxiliary power unit
LTO:	landing and take-off
ISA:	International Standard Atmosphere
CAD:	Computer-aided design

CAM:	Computer-aided manufacturing
CAE:	Computer-aided engineering
FEA:	Finite element analysis
CFD:	Computational fluid dynamics
MAF:	Air mass flow
LTO:	Landing and take-off
In:	Inlet
Out:	Outlet
Num:	Numerical
Exp:	Experimental

Symbols:

T:	Temperature
P:	Pressure
s:	Enthalpy
°C:	Degrees Celsius
F:	Fahrenheit
K:	Kelvin
Psi:	Pounds per square inch
Pa:	Pascals
Hz:	Hertz
mph:	Miles per hour
kgf:	Kilogram-force
Ps:	Static pressure
P_a:	Ambient pressure

Ts:	Static temperature
T_a:	Ambient temperature
O_2:	Oxygen
CO:	Carbon monoxide
CO_2:	Carbon dioxide
NO:	Refers to nitric oxide
NO_2:	Nitrogen dioxide
NO_x:	Nitrogen oxides
HC:	Hydrocarbons
H_2:	Hydrogen
pa:	Pascal
ρ:	Density
η:	Mechanical efficiency
T:	Thrust
P_R:	Pressure ratio
u:	Viscosity
D_h:	Hydraulic diameter
A:	Area section
p:	perimeter
P:	Power
ε:	Error estimation
ppm:	Parts per million
rpm:	Revolutions per minute
C:	Speed

General Introduction

The air transport sector plays a vital role in connecting people and goods across the globe. However, it also contributes significantly to air pollution directly impacting human health. While air transport provides numerous benefits, it also contributes significantly to air pollution. The emissions from aircraft, including carbon dioxide (CO_2), nitrogen oxides (NOx), sulfur oxides (SO_2), and particulate matter, have detrimental effects on the environment and human health. It is crucial for the aviation industry to continue investing in research and adopting sustainable practices to mitigate the pollution caused by air travel and minimize its impact on the planet. That is why the Aviation Industry is actively exploring alternative fuels and jet engines parts to get cleaner energy sources to provide higher emissions compared to traditional jet fuels derived from fossil sources, as it aims to combat climate change, improve air quality, protect human health, ensure energy security, create economic opportunities.

Further, when it comes to engine design, one of the primary concerns is minimizing exhaust emissions, here where the numerical CFD simulation which is the Computational Fluid Dynamics, allows us as a future engineers to explore numerous design parameters and identify optimal configurations, providing information into how changes in engine geometry can affect emission levels, by altering variables like combustion chamber shape, and to represent the flow of fluids and gases within the engine, including fuel-air mixing, combustion, and exhaust gas flow. That is why I worked on this project, which aims to experimentally and numerically characterize the behavior of the fluid that passes through a jet engine, in particular as it passes through the combustion chamber of an Olympus HP jet engine.

To reach this target, it will be required to characterize the jet engine geometrically and to determine performance characteristics such as fuel consumption, thrust, engine speed, temperature, and pressure at serval points of the engine, as well as emissions characteristics such as nitrogen oxides, hydrocarbons, carbon monoxide, oxygen, and carbon dioxide. It will also be necessary to experimentally determine fuel properties and main flow thermodynamic properties. Based on the experimental results, the thermodynamic cycle will be calculated, providing the input data for the simulation that will be performed via Ansys-Fluent, and validated using the experimental data.

This work mainly consists of the following parts:

- First, we will study the literature on jet engines and how they operate. We will also present several types of jet engines and their features, as well as a comprehensive overview of the micro gas turbine thermodynamic cycle and how it works.

- Second, the details of the experimental investigation conducted on the test bench devices that we will used in our micro gas turbine test.

- Third, the fundamental process of fuel device characterization employing specific equipment that provides us with the required values.

- Fourth, we will discuss the process of implementing the engine under evaluation and attaching it to the experimental data that we acquired.

  Then we have a numerical validation of the engine to experimented values using the ANSYS software with Fluent solver and the theory of basic fluid flow in CFD will be presented.

- Finally, we finish this report by a general conclusion adding some perspectives and a few works that can be done in the future.

Chapter 1: Bibliographic studies

Introduction:

The primary goal of the bibliographic chapter is to establish a solid foundation for the research by identifying the key concepts, theories, methodologies, and findings that have been previously investigated. That is why we will examine and synthesize the knowledge about jet engines, which have played a crucial role in enabling faster and more efficient air travel, powering airplanes, helicopters, and even certain types of space crafts. Hence, in this chapter, we'll start with a broad definition and then go over the primary aspects that will impact jet engines.

1. What is a jet engine?

A jet engine (see Figure 1) is a machine that converts high energy, liquid fuel into a powerful pushing force called thrust [1]. A more technical name for a jet engine is a gas turbine, which is a type of propulsion system that utilizes the principle of jet propulsion to generate thrust. It works by expelling a high-velocity stream of heated gas, usually air, which produces forward motion in the opposite direction.

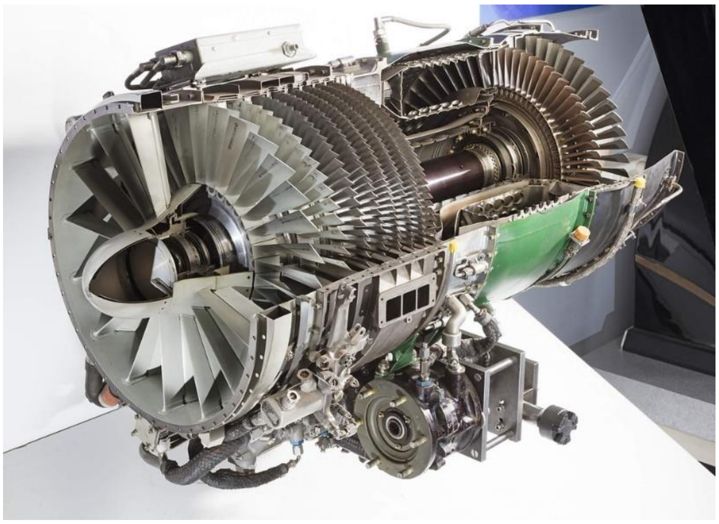

Figure 1: Jet Engine.

The jet engine works on the same principle: when air sucks back, it has the power to push the aircraft forward [2]. The air is not very heavy, so if you are using a lot of force to move a large object like an airplane, you will need a lot of air to do a small acceleration at a reasonable speed.

Besides are known for their high power, efficiency, and ability to operate at high altitudes and speeds. Thus, they have revolutionized air travel and play a critical role in aviation, enabling faster and more efficient transportation across the globe.

A jet engine is made up of numerous main components, each of them plays a specialized role in the engine's overall operation. The following are the key components of a typical jet engine:

- **Inlet:**

The inlet, also known as the intake, is placed at the front of the engine and is in charge of introducing fresh air into the engine. To maximize airflow and minimize deformation, it frequently features an intake lip or a cone-shaped structure.

- **Turbine:**

The turbine is one of the major parts of the jet engine. which consists of a series of blades or stages located after the combustion chamber. It is used to remove energy from the exhaust gases that is used to drive the compressor and other engine parts [3].

- **Fan:**

The fan is a large rotating component in the form of blades mainly constructed of titanium and located at the front of the engine and outside the core engine. It draws in a significant amount of air and provides bypass airflow that it helps to generate additional thrust and contributes to the engine's efficiency.

- **Fuel System:**

The fuel system contains a fuel pump, fuel lines, and valves. It is used to supply fuel to the combustion chamber.

- **Compressor:**

The compressor is the core of the jet engine. First part, it is a series of rotating blades or stages that compress the incoming air. It increases the air pressure and directs it towards the combustion chamber.

Compressors can be axial or centrifugal, and some engines have multiple stages of compression for higher efficiency.

- **Combustion Chamber:**

The combustion chamber also known as the burner or combustor, is where fuel is mixed with compressed air and burned. The burning fuel-air mixture generates high-pressure and high-temperature gases.

- **Nozzle:**

The exhaust nozzle is located at the rear of the engine and serves two main functions. It expands and accelerates the exhaust gases, generating thrust, and it helps control the direction and shape of the exhaust jet. There will be a mixer in front of the nozzle that mixes warm air coming from the heart of the engine with cool air flowing through the fan [3].

- **Lubrication System:**

Lubrication system has the responsibility to properly distribute the engine oil to different engine parts to reduce friction and wear [4].

- **Engine Control System:**

The engine control system is a combination of hydraulic, mechanical, and electronic parts that manage and control different functions of the engine and each playing a vital role in the engine's operation to produce thrust and power the aircraft. It may vary depending on the specific application, such as commercial aviation, military aviation, or industrial power generation, but the fundamental principles and main components remain consistent across most jet engines [4].

2. How a jet engine works?

In brief, each main part of the engine does a different thing to the air or fuel mixture passing through (see Figure 2). Simply put, jet engines have a core that is split into three main sections:

a. Compressor: Dramatically increases the pressure of the air.

b. Combustion chamber: Increases the temperature of the air-fuel mixture by releasing heat energy from the fuel.

c. Exhaust nozzle: Dramatically increases the velocity of the exhaust gases, so powering the plane.

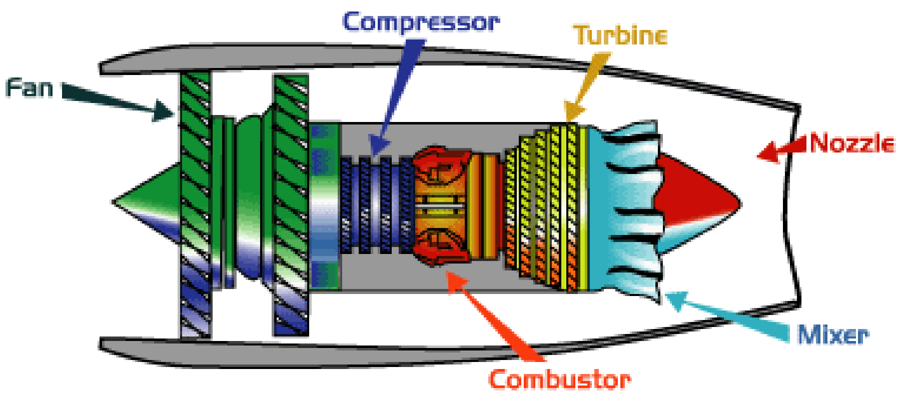

Figure 2: Jet engine operations.

3. Classification of Jet Engine:

Jet engines are typically divided into different types, including turbojet, turbofan, turboprop, and turboshaft engines. Each classification can be identified by its unique characteristics, such as the configuration of compressors, combustion chambers, and turbines. Each category is explained more below.

- **Turbojets Engine:**

The basic idea of the turbojet engine is simple (see Figure 3). Air taken from an opening in the front of the engine is compressed to 3 to 12 times its original pressure in the compressor. Fuel is added to the air and burned in a combustion chamber to raise the temperature of the fluid mixture to about 1,100 F to 1,300 F [5].

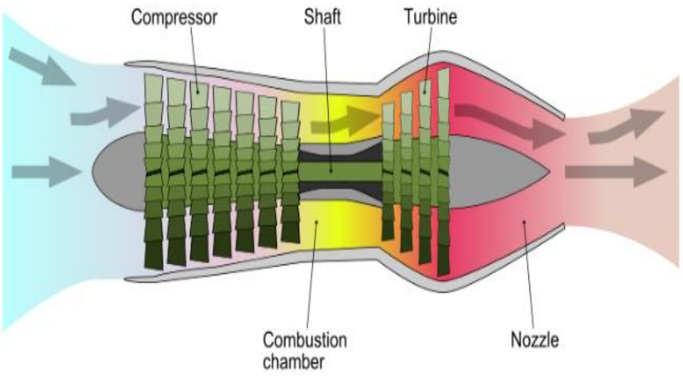

Figure 3: Turbojets engine.

- **Turboprop Engine:**

A turboprop engine is a jet engine attached to a propeller (see Figure 4). The turbine at the back is turned by the hot gasses, and this turns a shaft that drives the propeller. Some small airliners and transport aircraft are powered by turboprops [5].

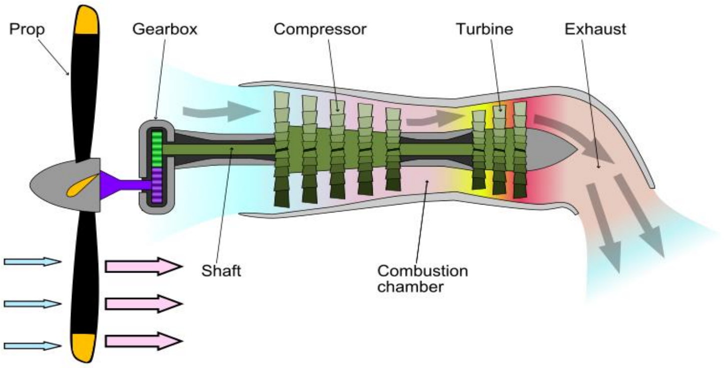

Figure 4: Turboprop engine.

- **Turbofan Engine:**

A turbofan engine (see Figure 5) has a large fan at the front, which sucks in air. Most of the airflow around the outside of the engine, making it quieter and giving more thrust at low speeds. In a turbofan engine, only a portion of the incoming air goes into the combustion chamber [5].

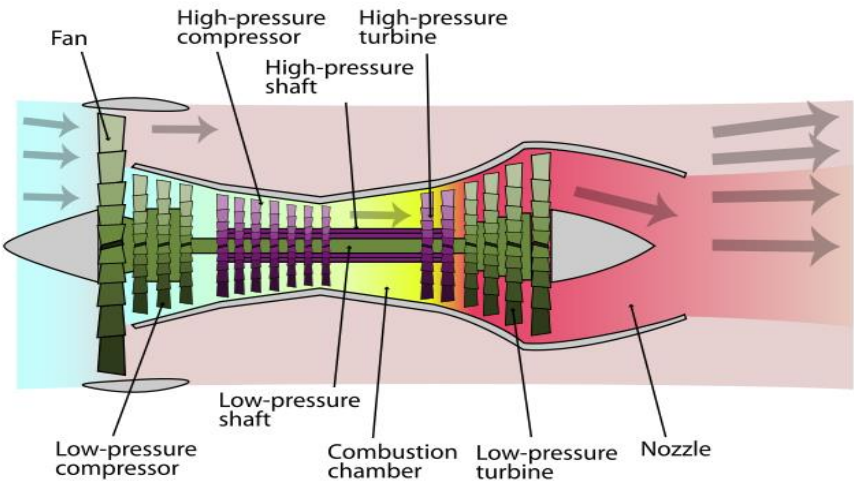

Figure 5: Turbofan engine.

- **Turboshaft Engine:**

This is another form of gas-turbine engine that operates much like a turboprop system. It does not drive a propeller. Instead, it provides power for a helicopter rotor. The turboshaft engine (see Figure 6) is designed so that the speed of the helicopter rotor is independent of the rotating speed of the gas generator [5].

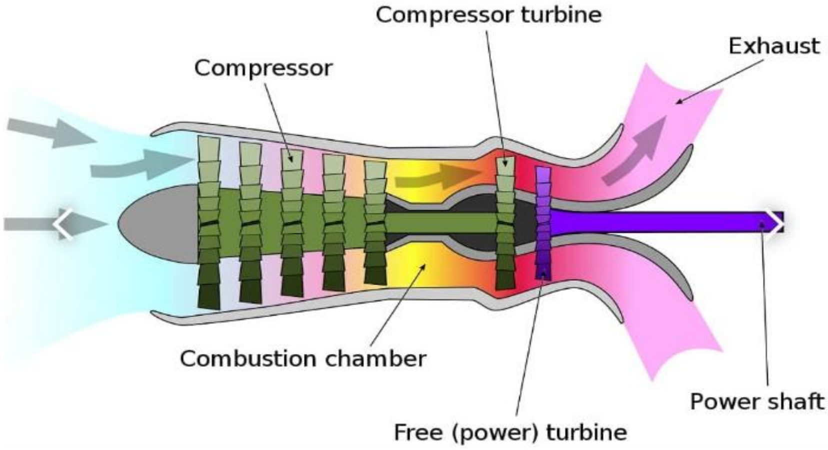

Figure 6: Turboshaft engine.

However, the fundamental principle of generating thrust by expelling high-velocity gases remains consistent across these engine types. The continuous and efficient operation of the jet engine allows aircraft to achieve high speeds, climb to higher altitudes, and provide the necessary thrust for takeoff, cruising, and landing.

4. Micro gas turbine thermodynamic working cycle:

Understanding the basic approach by which energy is converted inside a system is required when introducing the thermodynamic cycle. Thermodynamic cycles (see Figure 7) define the series of events that happen when a working substance changes pressure, temperature, and volume before returning to its starting condition. We obtain insights into efficiency, heat transfer, and work output by evaluating thermodynamic cycles, which helps to optimize and develop various energy conversion processes.

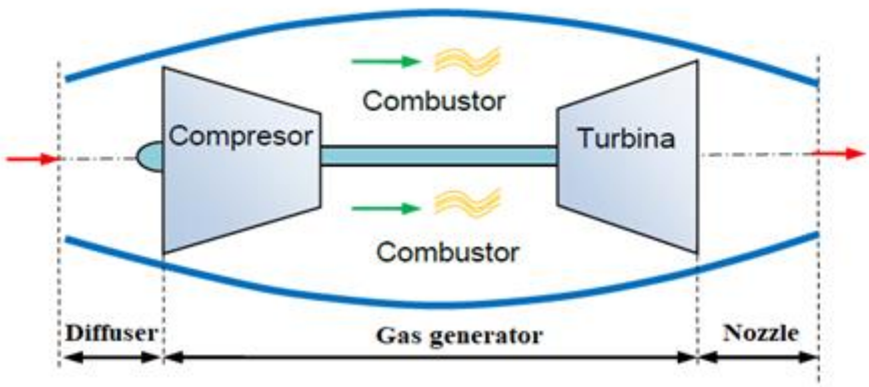

Figure 7: Turbo reactor gas turbine.

These engines move at high speeds, the influence of this speed is employed to partly compress the air at the inlet, at a static pressure Ps and temperature Ts, before it passes to the compressor (states 1, 10s, and 10) (see Figures 8). The enthalpy s of rest or stop of the air is maintained throughout the intake in this phase, as it would be in a diffuser.

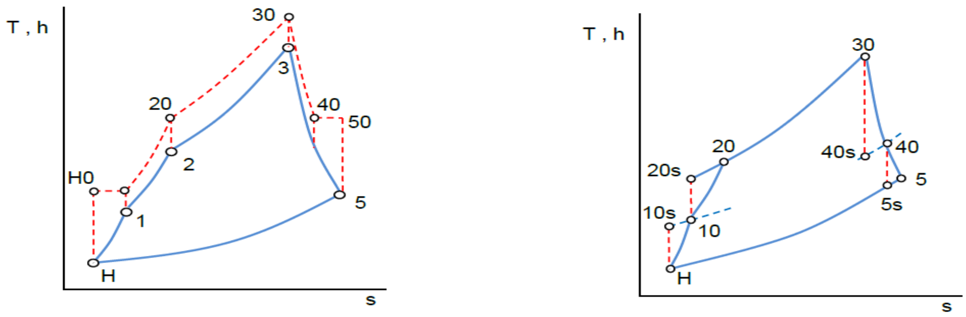

Figure 8: Micro gas turbine thermodynamic cycle.

Following that, a gas turbine's thermodynamic cycle (Baryton) is run, evaluating stop or rest circumstances. After compression (states 2, 20s, and 20), combustion takes place, and at its exit (state 3 and 30) it is passed to the turbine. The turbine's assignment is only to drive the compressor such that there is still enough energy in the gases exiting it (states 4, 40s, and 40) (see Figures 8).

Then, they travel via a nozzle, where they expand (while maintaining a constant enthalpy at rest) until they leave at static pressure Ps (which is equivalent to ambient pressure Pa) (states 5, 5s, and 50) (see Figures 8). This leads them to escape at a velocity, generating the thrust and power required for the propulsion of the device to which the motor is attached.

The overall, thermodynamic working cycle of a jet engine is crucial for engine design, performance analysis, and optimization. It allows engineers to evaluate factors such as compression ratio, turbine efficiency, and overall engine efficiency, contributing to the development of more efficient and high-performance jet engines.

Conclusion:

This chapter served to frame our project. It allowed us about the importance of jet engines and their evolution through time. We have studied about turbo-engines, their basic components, and how they function. Finally, we go over a jet engine's thermodynamic operating cycle. The following chapter has been retained to present and describe our test bench of this project.

Chapter 2: Test bench description

Introduction:

In this chapter, we will describe the micro turbine, which is mostly used in model aircraft, offer devices from our test bench, and indicating some additional measured thermodynamic equipment.

1. History of the micro gas turbine Jet Engines:

The use of micro gas turbine (MGT) engines is becoming more and more popular in the commercial aviation and industries. They are employed in unmanned aerial vehicles used in missions related to national security, telecommunications, real time acknowledgement, remote sensing, crime fighting, disaster management, agriculture and election monitoring.

MGTs are also used in hybrid electric vehicles and small combine heat and power generating plant applications as well as auxiliary power units (APUs) for modern aircraft. They are suitable for such applications due to their high power to weight ratio, multi fuel capability and simple design, low energy costs and emissions.

AMT Netherlands company (see Figure 9), designs and produces micro gas turbines which are primarily used for the propulsion of radio-controlled airplanes. The engines are also certified as a bring-home device for full size gliders, and various universities use the specially modified engines for research and educational purposes [4].

Figure 9: AMT Netherlands company.

AMT Netherlands is totally committed to developing efficient engines and associated equipment while continuously ensuring safety and reliability. All materials are carefully selected according to extensive calculations, operational tests, and our stringent quality control process. Every engine is assembled by skilled engineers and strictly tested before dispatch to ensure that it meets precise performance and safety parameters.

So, here are the main areas in this company that are responsible for producing and manufacturing these types of engines:

- CNC manufacturing: AMT Netherlands owns a state-of-the-art CNC machine park including 5-axis milling machines (see Figure 10) which can produce parts for 400-500 gas turbines engines per year, depending on engine type [4].

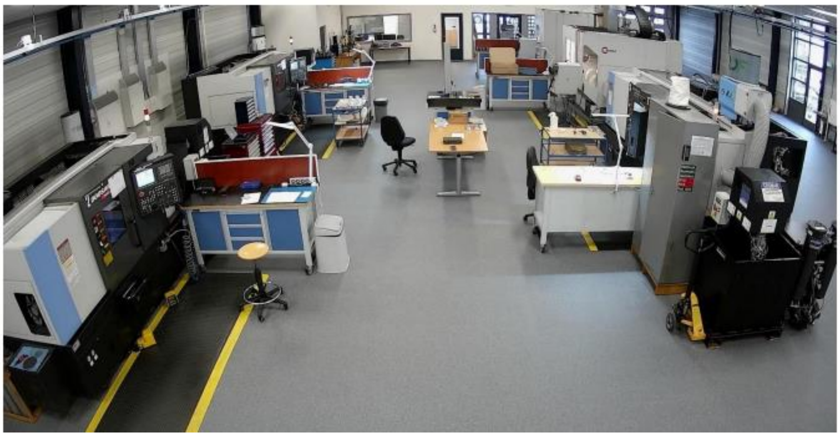

Figure 10: CNC manufacturing.

- Engine assembly: Presently they have 2 fully equipped engine assembly areas (see Figure 11) where their specialized engineers perform assembly, repair and maintenance [4].

Figure 11: Engine assembly.

- Balancing: For dynamic balancing of the rotor assembly, AMT Netherlands uses dynamic balancing machines (see Figure 12).

After the initial test run of each engine the rotor balance is measured and if necessary corrected before an engine is subjected to its final 3 test runs. All engines are balanced up to quality grade 6.3 which is normal for the use in aircraft gas turbine engines.

Grade 6.3 represents the result of the eccentricity in millimeters multiplied by the operating frequency in Hz (Hertz) [4].

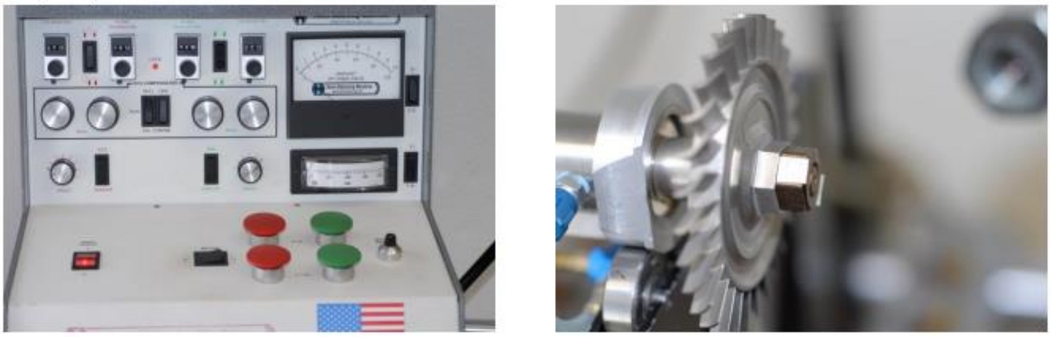

Figure 12: Balancing.

- Test facilities: Turbines are tested manually and during test runs fully automatically using professional customers [4] (see Figure 13).

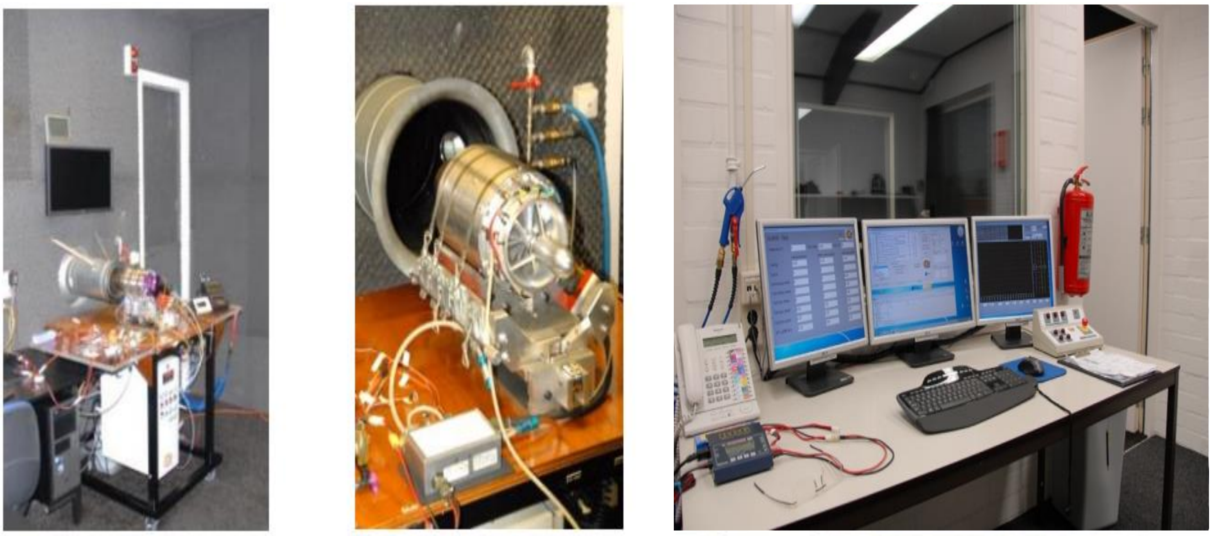

Figure 13: Test facilities.

2. Description of Olympus HP:

For more than 15 years AMT Netherlands also manufactures special university editions of the Olympus HP engine and develops small gas turbines for the propulsion of radio-controlled flying airplanes, remote heat/power generators, and auxiliary power units.

AMT’s latest version of these engines is the Olympus HP (see Figure 14) which has been developed from knowledge gained during design and operation of the Mercury HP, Pegasus HP and Olympus motors, and it has specifications and performance that have never been achieved before in a motor of this size [4].

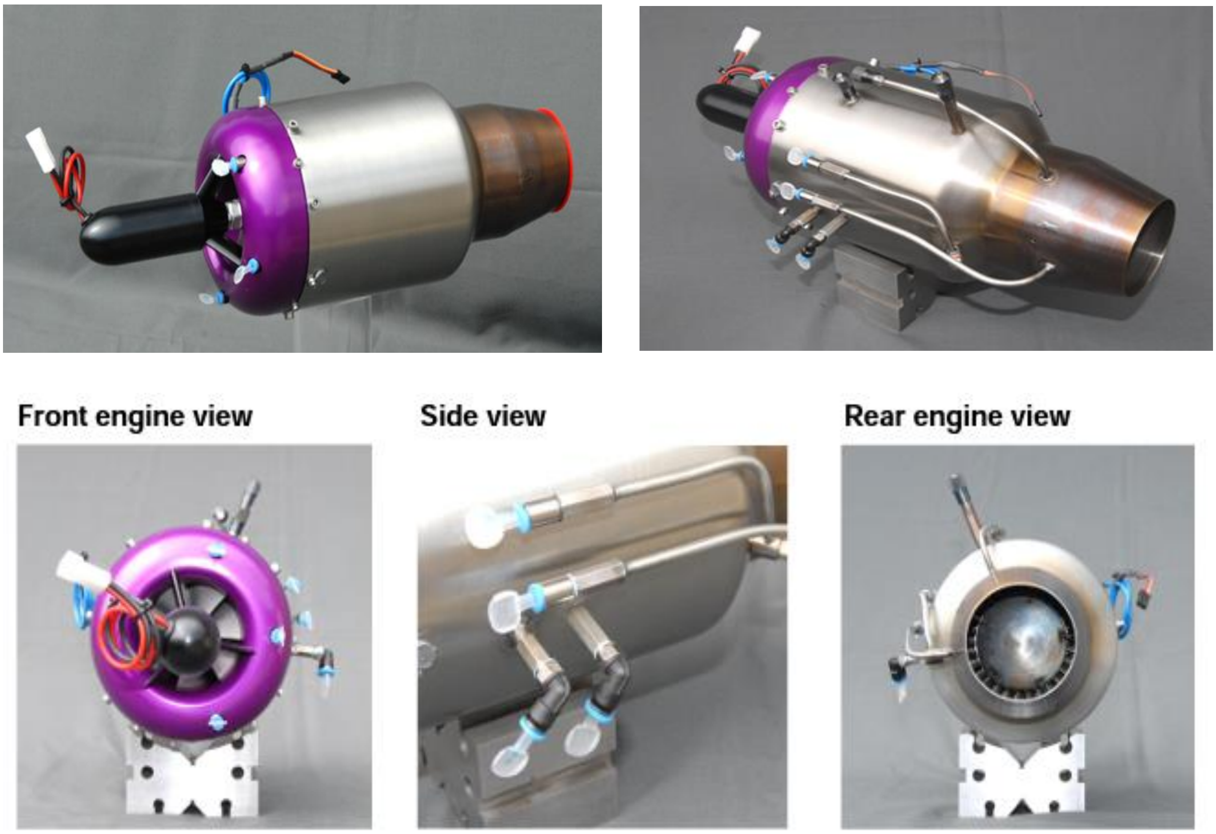

Figure 14: Olympus HP Views.

The Olympus HP owes much of its excellent performance and power to weight ratio to this turbine wheel which was designed by AMT staff. It is also positively influenced by the low mass of the axial turbine wheel, taking less than 4 seconds from min. to max. rpm and only 4 seconds from max. rpm to min. rpm [4].

Here is the Olympus HP on a full-size glider as a “bringing home” device (see Figure 15).

Figure 15: The Olympus HP on a full-size glider.

The turbine is protected from accidental damage by means of a microprocessor-based controller the electronic control unit (ECU) which regulates the maximum performance within preprogrammed software limits. The ECU is fully automatic and needs no adjustment by the operator.

3. Aviation fuels:

Currently, only a few fuels are utilized in commercial civil aviation, and they are all standard. Traditional fuels and biofuels presently used in air transport are examined to give a framework for gaseous emissions.

Since there have been numerous scientific review publications on aviation biofuels [6-7], this introduction will not analyze them in detail, but will only present a brief description.

Aviation fuels, frequently referred to as jet fuels, are standardized [8-9]. These standards, which define a set of tolerances, are mostly focused on the needs to be satisfied rather than the requirements on the chemical qualities of the fuels. There are several types of jet fuels available, depending on the engine to be used, the operating climate, or the place of manufacture. These are some examples:

- Alternative aeronautical engines: Av. Gas.
- Ramjet Engines: RJ-4, RJ-5, and RJ-6 JP-9, JP-10.
- Military Aviation: JP-4, JP-5, and JP-8.
- Commercial Aviation: Jet A-1, Jet A and Jet B.

Jet fuel is mostly made of hydrocarbons, primarily those with carbon chain distributions ranging from C8 to C16 [10]. Kerosene's, comprising paraffins, cycloparaffins or naphthene, aromatics, and olefins are the most significant hydrocarbons in the fuel [11]. The amount of each can vary depending on the kind of crude oil utilized and the refining procedure employed [12]. The manufacturing of conventional jet fuel has been the topic of research articles [13].

Jet fuel also contains, in parts per million, various sulfur, nitrogen, and oxygen compounds, the latter of which are primarily relevant to the fuel's oxidation and lubricity qualities [8]. Although the broad diversity of components in jet fuel makes modeling the combustion process challenging, simulations and models have been produced [14-15].

Our Olympus-HP engine runs on Jet A-1 fuel, which is why I'll go into more detail about it in the next section.

3.1. Description of the fuel tested Jet-A1:

- **Description:**

Jet A-1 is a liquid fuel used worldwide, whose approximate molecular formula is $C_{11}H_{21}$, used in jet engines for civil aviation worldwide, due to its high energy content and combustion quality, which makes it suitable for long international flights [16].

It responds to the following characteristics and properties (see Table 1):

- **Characteristics:**

- Colorless or slightly yellow fuel.
- Flammable at temperatures above 38 °C in the presence of flame or spark.
- High calorific value to obtain the maximum possible energy with the same weight.
- Low volatility to avoid evaporation losses and fire danger in the event of an accident.
- Very low crystallization point to favor cold behavior (very low temperatures at flight altitude).
- Oxidation stability, which means that it is not affected by oxidation processes.

- **Properties:**

Description	Value
Flash point	42 °C
Temperature of automatic ignition	210 °C
Freezing point	−47 °C
Burning temperature at standard atmospheric conditions	260–315 °C
Density at 15 °C	804 kg/L
Specific energy	43.15 MJ/kg
Energy density	34.7 MJ/L

Table 1: Jet A 1 jet fuel characteristics.

The use of aviation fuels in the internal combustion engines of road vehicles has been studied for a long time. Once the North Atlantic Treaty Organization (NATO) accepts JP-8 as a single fuel on the ground and in the air, most of these studies have focused on JP-8. For this reason, there are hardly any studies on the use of Jet A1, structurally very similar to JP-8, in the internal combustion engine. However, in obligatory cases such as during periods of war, it may be necessary to use Jet A1 in the same way as JP-8 in internal combustion engines.

Especially in cold climates, the Jet A1 can gain strategic importance due to its very low freezing point. In this study, both the effects of diesel and Jet A1 are combined on engine performance and exhaust emissions in both cylinders, and the direct injection diesel engine has been examined.

As a result, it has been determined that the use of Jet A1 reduces torque to 5.85% and increases specific fuel consumption to 8.77%. In addition, while there is an increase in smoke and carbon monoxide (CO) emissions 82% and 71.9%, respectively, there is a decrease in nitrogen oxide (NOx) emissions by 29%.

In conclusion, there is no positive effect of using Jet A1 in the diesel engine, except for the reduction in NOx emission and the decrease in freezing point [16].

4. Description of the measured variables:

The term "measured variables" refers to the physical quantities or parameters that are being measured or monitored in a given system or process. These variables can vary depending on the specific application or context. Measuring and monitoring these variables is essential for process control, scientific research, quality assurance, and various other purposes.

4.1. Variables provided by the test bench:

Already quickly, after the Olympus HP was launched, there came requests from universities and research institutes to modify this engine to an engine with extra measuring points (see Figure 16).

Figure 16: Olympus HP engine in the "university" configuration.

The contents of the Olympus HP configuration are:

-Turbine

-Electronic Control Unit (ECU)

-Fuel pump

-Owner's Manual

The Extra requirements:

-Fuel

-Compressed air

-Ignition system

-Fire extinguisher

This is the specialized setup that we used to evaluate and assess the performance, functionality of various mechanical and electronic systems and components of our engine. It provides a controlled environment where the professors and I can conduct experiments, measurements, and simulations to understand how the Olympus HP engine particular behaves under specific conditions related to the reality.

There is a specific variable of the Olympus HP engine provided by a test bench which will depend on the intended purpose of the testing, the complexity of the system under evaluation, and the capabilities of the test bench itself., and here below the performances of different parameters (see Figure 17) that we can experimentally obtain from our engine:

- Temperature (T): Temperature is a measure of the average kinetic energy of particles in a substance. It is commonly measured using devices like thermometers or temperature sensors and is expressed in units such as Celsius (°C) or Fahrenheit (°F).

- Pressure (P): Pressure refers to the force applied per unit area. It can be measured using devices like pressure gauges or transducers and is typically expressed in units such as pounds per square inch (psi) or pascals (Pa).

- Speed: Speed measures the rate of change of position of an object. It can be measured using speedometers or velocity sensors and is expressed in units such as meters per second (m/s) or miles per hour (mph).
- Throttle position (THRO): The throttle position refers to the position of the throttle valve in an internal combustion engine, is expressed as a percentage in our case (%) or can be an angle as well. Typically, it represents the opening of the throttle valve, at idle or when the engine is at rest, the throttle valve is usually closed or nearly closed, resulting in minimal airflow. As we press, the throttle valve opens, allowing more air into the engine. This increased airflow, in combination with the appropriate fuel delivery, leads to an increase in engine power and speed.

- Exhaust Gas Temperature (EGT): Exhaust Gas Temperature refers to the temperature of the gases exiting the combustion chamber of an internal combustion engine. It is a critical parameter expressed in (°C) used to monitor and manage the engine's performance and can provide valuable information about its operating conditions.
  We are going to measure it using a specific exhaust system near to a cylinder head which directly measure the temperature of the gases and same for its composition as they leave the engine.

- Revolutions of shaft (PRM): The revolutions of a shaft refer to the number of complete rotations the shaft makes within a given time frame. It is a measure of rotational speed and is typically expressed in revolutions per minute (RPM).

- Thrust: In the context of aviation, the thrust of an aircraft engine is what allows the aircraft to move forward and counteract the opposing forces of drag and gravity. By producing a high-velocity stream of gases, the engine generates an equal and opposite force known as thrust. This force is transmitted to the aircraft through the propulsion system, causing it to accelerate in the desired direction, and in our test, it is expressed in kilogram-force (kgf).

- Fueling: Fueling of our engine is expressed by milliliter per minute (ml/min), it refers to the process of supplying the engine with the appropriate fuel for combustion. It involves delivering the right amount of fuel to the engine's combustion chamber to support the combustion process and generate power.

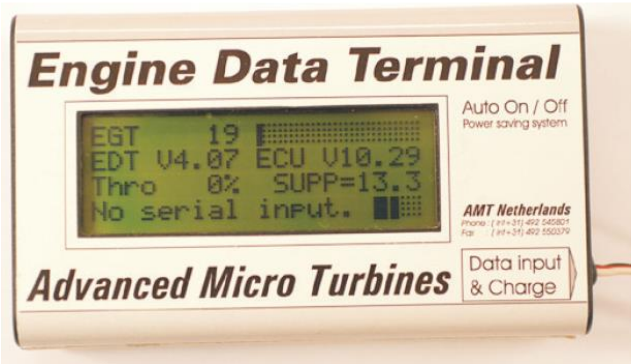

Figure 17: Engine Data Terminal.

The above system provides pressure data from Ps1, Ps3, Pt3, Pt4, Pt5 and temperature data from Tt1, Tt3, Tt4, Tt5, Tt6 [4]. Here are the positions of all the measuring points that Olympus HP offer (see Figure 18):

<u>Temperature:</u>

Tt3 - Temperature measurement behind diffusor stage.

Tt4 - Temperature measurement before nozzle.

Tt5 - Temperature measurement after turbine wheel.

Tt6 - Temperature measurement at exhaust nozzle.

<u>Pressure:</u>

Ps3 - Static pressure behind diffusor stage.

Pt3 - Total pressure behind diffusor stage.

Pt4 - Total pressure before nozzle.

Pt5 - Total pressure after turbine wheel.

Figure 18: The measuring points.

Furthermore, the technical graphic in the reference section explains all the measuring points placements in further detail (see Annex).

4.2. Additional thermodynamic properties measured:

These properties go beyond basic parameters and offer deeper insights into behavior and performance. Examples include thermal conductivity, viscosity, electrical resistivity, and more. By measuring these properties, we uncover essential information that aids in material selection, process optimization, and system design across various industries, from engineering and physics to chemistry and beyond. These properties provide valuable information about the system's energy, temperature, pressure, volume, and other related variables.

To perform the new connections, I will detail some of our extra test bench equipment and materials that we used in our test bench:

-The digital manometer:

This Digital Manometer (see Figure 19) handheld instrument is a microcontroller-based sensing device used to directly measure pressure of clean, dry, non-corrosive gases [18].

Pressure can be displayed in selectable engineering units of PSI, bar, mbar, kPa, mmHg, inHg, mmH2O or inH2O, as well as he can provide a convenient and accurate way to measure and monitor pressure in a wide range of applications [19].

Figure 19: CA 850 Manometer.

-The thermometer:

Thermocouples are versatile temperature sensors that provide reliable and accurate measurements in various environments, making them suitable for a wide range of applications in temperature monitoring and control systems. There are various types of thermocouples available, each made of different combinations of metals. The selection of our thermocouple type depends on the temperature range, accuracy requirements, chemical compatibility, and other factors specific to the application.

Into our test, we are using the TECPEL 307 thermometer below (see Figure 20) which is a device used to measure temperature, it consists of a temperature sensor and a scale or digital display to provide a numerical representation of the temperature being measured.

Figure 20: TECPEL 307 Thermometer.

-The Thermocouple Extensions Leads:

Thermocouple extension leads, also known as thermocouple extension wires or cables, are specialized cables used to connect a thermocouple sensor to a measuring instrument or control system. They are designed to maintain the integrity and accuracy of the temperature measurement while extending the distance between the thermocouple and the measuring device. In our test we used the type "RS PRO Type K Extension Cable, 2m, PVC Insulation, +220°C Max, 7/0.2mm" (see Figure 21).

Figure 21: Extension Cable.

-The tubes:

For chemical fuel oil applications, it is common to use pipes made from materials such as stainless steel, carbon steel, or certain types of plastic, these materials are chosen for their chemical resistance, durability, and ability to handle the pressure and temperature requirements of the application.

Considering our engine testing and our type of the fuel oil., we need to use two types of tubes (see Figure 22), the silicone fuel hose and the pneumatic air compressor pipe. We utilize it by reason of their high roundness, pressure resistance, explosionpro of, good flexibility and possess excellent performance.

Figure 22: The tubes.

Ultimately, the measurement and analysis of additional thermodynamic properties contribute to our understanding of the fundamental principles governing the behavior of matter, leading to advancements in various scientific and technological aviation domains.

4.3. Exhaust emissions measurement:

Exhaust emissions means substances emitted into the atmosphere from the exhaust discharge nozzle of an aircraft engine. Specifically, aircraft engine emissions include carbon dioxide (CO_2), water vapor (H_2O), nitrogen oxides (NOx), carbon monoxide (CO), Sulphur oxides (SOx), unburned hydrocarbons (HC), and other compounds [20]. Approximately 70% of these emissions are CO_2 and 30% H_2O, with the remaining compounds accounting for less than 1% [31].

The following figure (see Figure 23) provides a simple illustration of the effects of burning conventional aviation fuel [32].

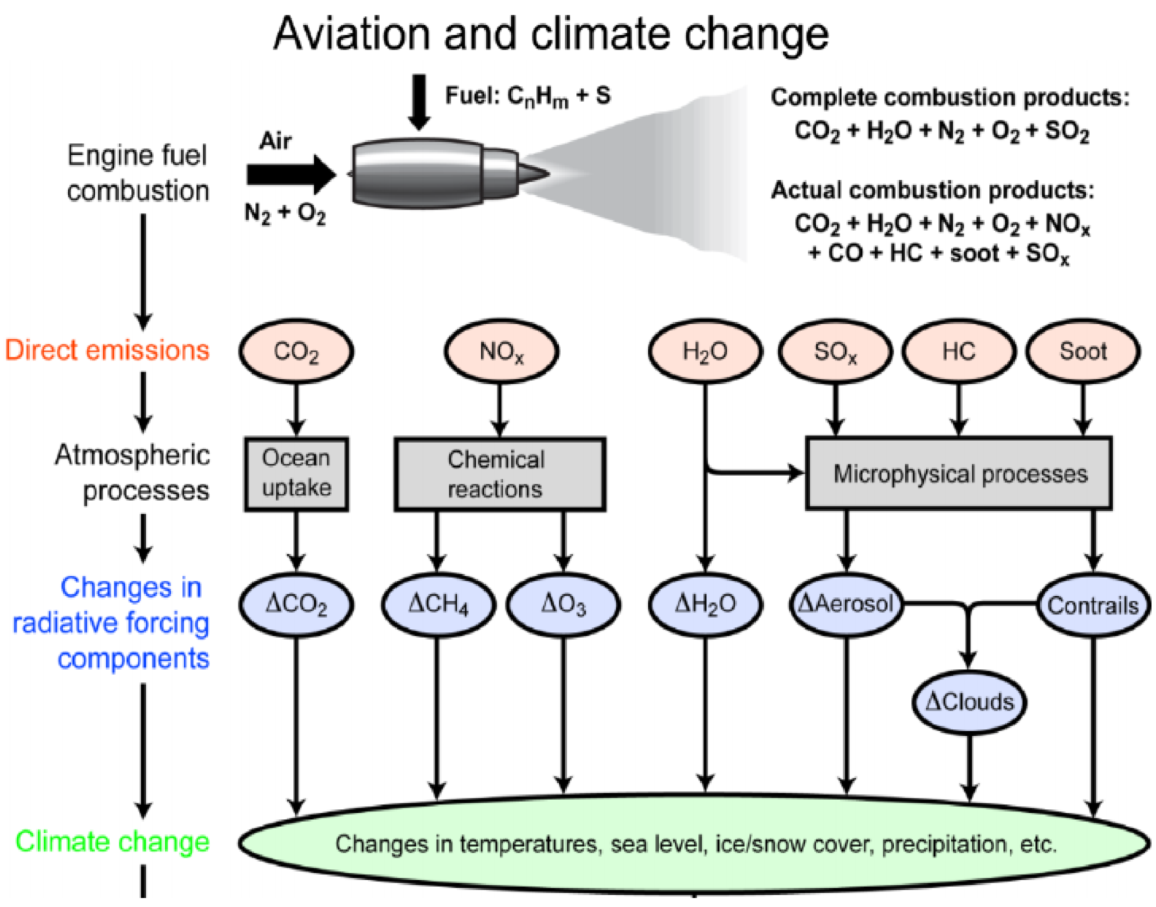

Figure 23: scheme of emissions and environmental impact resulting from air activity.

Exhaust emissions measurement is vital for evaluating the environmental impact of various combustion sources, including vehicles, power plants and industrial facilities. It helps in identifying sources of pollution, developing emission reduction strategies, and ensuring a healthier and cleaner environment.

As a result, in the following section, we will detail our fascinating equipment that may give us easily an exhaust emission finding.

- Testo 350 equipment:

The testo 350 exhaust gas analyzer (see Figure 24) is ideal for a wide range of professional industrial emission measurements and analysis applications, and is excellently suited for complex data compilation.

It used to control emission measurements, so it has a clearly structured graphic display, and four different menu applications to choose from, including burner / gas turbine / motors / user-defined applications [23].

Figure 24: Testo 350 Exhaust emissions equipment.

The testo 350 emissions equipment is a rugged, easy-to-use exhaust gas analyzer designed to meet the highest demands when it comes to carrying out precise industrial emission measurements and providing proper data administration.

The Analysis Box can be operated with up to 6 gas sensors, 5 of which are optional. This allows us to select freely from sensors for O_2, CO, NO, NO_2, NO_x, CO_2, HC and H_2 [24].

- O_2: Refers to oxygen, which is a colorless, odorless, and highly reactive gas that constitutes approximately 21% of the Earth's atmosphere and is essential for supporting life and combustion.

- CO: Refers to carbon monoxide, which is a colorless, odorless, and poisonous gas that is formed by the incomplete combustion of carbon-containing substances and poses a significant health risk when inhaled.

- CO_2: Refers to carbon dioxide, which is a colorless and odorless gas that is naturally present in the Earth's atmosphere. It is a greenhouse gas that plays a vital role in regulating the planet's temperature by trapping heat from the sun, but excessive CO2 emissions from human activities, such as burning fossil fuels, contribute to climate change and global warming.

- NO: Refers to nitric oxide, which is a colorless gas with a sharp odor and plays a crucial role in various biological processes in the human body, as well as being involved in atmospheric chemistry and air pollution.

- NO_2: Refers to nitrogen dioxide, which is a reddish-brown gas with a pungent odor that forms from the oxidation of nitric oxide (NO) in the atmosphere and is a significant air pollutant, contributing to respiratory problems and the formation of smog.

- NO_x: Refers to nitrogen oxides, which are a group of highly reactive gases that include nitric oxide (NO) and nitrogen dioxide (NO2). They are produced primarily from combustion processes in vehicles, power plants, and industrial activities, and are a major contributor to air pollution and the formation of smog.

- HC: Refers to hydrocarbons, which are organic compounds consisting of hydrogen and carbon atoms. They are found in various forms, including gases, liquids, and solids. It plays a significant role in the energy sector as fossil fuels, such as petroleum and natural gas.

- H_2: refers to molecular hydrogen, which is a colorless and odorless gas consisting of two hydrogen atoms. It is the lightest and most abundant element in the universe, and it plays a significant role in various applications, such as fuel cells, industrial processes, and potential energy storage solutions.

5. Operation with the Olympus HP engine:

Operating engines involves several key steps and considerations while the specific procedures may vary depending on the type of engine, so here is a general overview of the steps involved in operating Olympus HP engine:

5.1. Priming the fuel system:

For this “priming” are special software functions available, the two special functions needed are the “50%” and the “60%” priming function:

a. First prime the igniter system (60% function), we need to be sure that we do not prime into the igniter but disconnect the PP3 fuel line from the engine (G connection) before we prime and prime into a small fuel container.

b. Second prime the main fuel system (50% function), we need to be sure that we do not prime into the engine but disconnect the fuel line from the engine (F connection) before we prime and prime into a small fuel container and be sure that the there are no” air bubbles” visible [4].

5.2. Starting the Olympus HP:

The company recommends that we fully charge the ECU/pump lipo battery before every flight, to be sure that we have the maximum energy possible for powering the electric starter and igniter to ensure reliable starting.

a/ Power up the system

b/ Put the throttle in the idle position.

c/ Put the 3-position switch (or throttle trim lever for single channel operation) on the transmitter in the 'off' position.

d/ To start the turbine put the switch (or throttle trim lever) on the transmitter in the 'start/run' position (high-pitched beep). Now you will hear 5 beeps from the ECU, and then it will begin the start sequence and the electric starter motor will turn the turbine. The preheat of the igniter will be switched on automatically as soon as you “go” into the start sequence.

e/ After the 5 “count down beeps”, start the fuel pump and open the starter solenoid valve.

f/ At an EGT rise of 5 °C from the moment of “going into start” the main fuel valve will open and the electric starter motor will go to maximum RPM.

g/ At an RPM depending on a software setting the starter fuel valve will be closed and the igniter will be switched off.

h/ The ECU will automatically throttle up the turbine to its calibration point at approx. 50,000 RPM.

The ECU will keep the turbine at approx. 50,000 RPM for about 2 sec and then it will automatically throttle back down to idle RPM (36,000). Idle RPM is now calibrated [4].

5.3. Stopping the engine:

For the normal stopping of the engine, you should use the automatic “power-down” sequence which functions as follows:

a/ Put the nose of the model into the wind if possible.

b/ Put the switch (or trim lever) on your transmitter to the middle position to activate the automatic power-down sequence.

c/ The ECU now regulates the engine to 30 % throttle (approx. 60,000 RPM) for about 4 seconds and waits until the exhaust temperature stabilizes.

d/ After, the ECU will stop the engine.

e/ Then, the ECU will automatically switch the electric-starter on and off several times.

- The ECU is now ready for a new start-up [4].

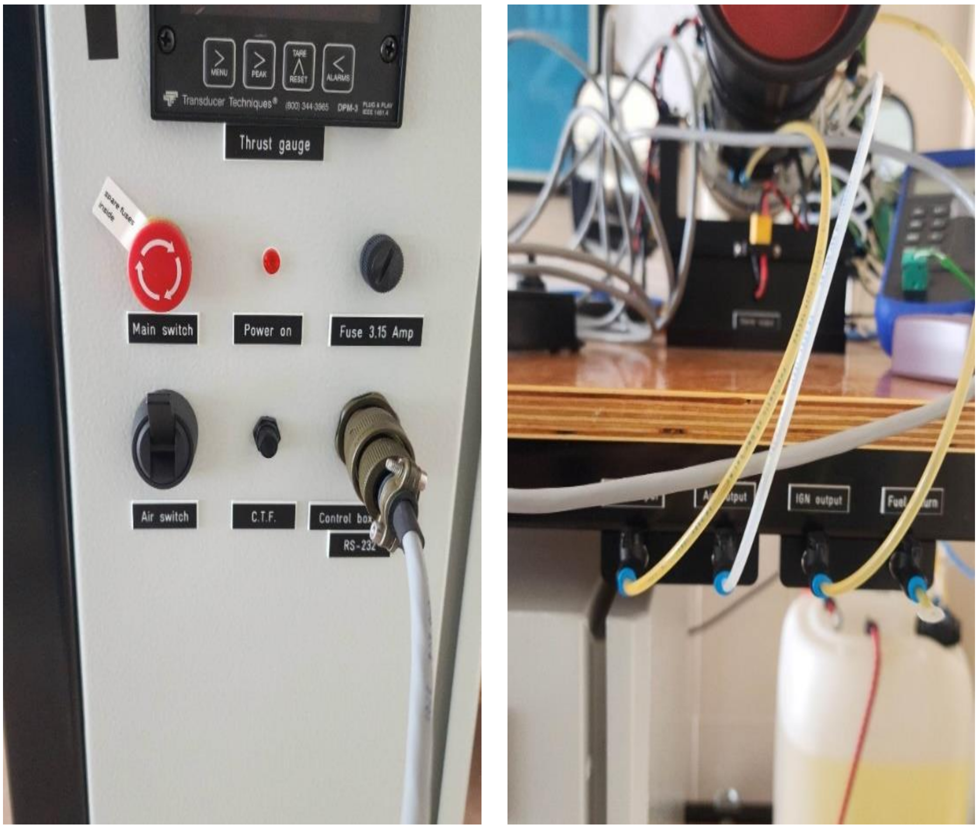

Figure 25: Operation with the Olympus HP engine.

The above steps are a general guideline from the Olympus HP catalogues, so I wanted to make it simple and short and make it easier for us to use.

Conclusion:

After conducting this literature study of the test bench, it can be concluded that there are many concepts of tests that can take the experiences to a better level of testing and by observing the engines already accomplished by various researchers in the company. In the next chapter we will talk about the devices of our fuel characterization that contains several necessary parts that will guides us to some important values we need in our experimental test.

Chapter 3: Devices for fuel characterization

Introduction:

Devices for fuel characterization play a crucial role in understanding and analyzing the properties of different types of fuels. It is essential for various industries, including aviation and research laboratories. These devices provide valuable information about fuel composition, quality, performance, and environmental impact. In this chapter we will introduce the operated equipment that we will going to use, explaining how every compound works and for what purpose.

1. Determination of Calorific Value:

One of the main characteristics of a fuel is its calorific value, which is defined as the amount of energy (kJ or kcal) produced by the combustion of 1 kilogram of fuel. Combustion is the oxidation of the carbon and hydrogen in the fuel to form water and carbon dioxide. The most commonly used units for calorific value are (kcal/kg), (kcal/m3). The calorific value of the same fuel does not change; however, there are different ways of measuring the heat generated when burning [25].

1.1. Superior calorific value:

The gross calorific value or the mean value (GCV or PCS) is the amount of heat produced in the combustion process, which includes the heat of condensation of the water vapor produced during combustion, it takes into account the latent heat [25].

The water vapor comes from:

- o the fuel's own moisture.
- o the water formed by the combustion of the hydrogen in the fuel.

1.2. Lower calorific value:

Lower or net calorific value (PCI or LCV) is the amount of heat produced in the combustion process, which is obtained by subtracting the heat of condensation or latent heat from the (PCS or GCV). The lower calorific value is of greater practical interest because under ordinary combustion conditions water vapor does not condense.

In the usual use of fuels in industrial processes, the gases are expelled at high temperatures, making cooling of the combustion products impossible. This means that the water vapor does not condense and, therefore, the heat of condensation of the vapor cannot be used due to the high temperature of the gases, which makes cooling of the combustion products impossible. change of state, so it is necessary to distinguish between the two types of calorific value. In practice, the lower calorific value is used, which does not take into account the latent heat of vaporization of the water formed [25].

Now I am going to describe the auxiliary equipment and devices used in the experiments carried out in the laboratory for getting these calorific values, as well as the methodology followed to determine the gross calorific value of liquid and solid samples.

❖ Calorimetric bomb: The calorimeter parr 6050:

The Parr 6050 calorimetric pump (see Figure 26) is the equipment used to carry out the experiments and with it we determine the gross calorific value.

The fuel is first combusted with Oxygen, under pressure, in a sealed “bomb”. Then, the heat of the subsequent reaction is measured from the temperature rise of a surrounding water bath.

Figure 26: Calorimetric bomb.

Main components of the Parr 6050 calorimeter:

1. Oxygen combustion vessel (1110).

2. Bucket (A1559DD).

3. Regulator block, oxygen (A570DD).

4. Oxygen solenoid valve (A1278DDD).

5. Power supply (1940E).

6. Capacitor, 40V, 81000uF (897E).

7. Male connector 1/8 NPTM-T-BT Nylon (538VB).

8. Fuse, snap-action 15A, 250V (139E23).

9. Card, I/O (A2140E).

10. Thermistor, cuvette (1417E3).

11. Main cable, ignition (A1564DD).

12. Thermistor, jacket (1416E).

13. Agitator motor assembly (A1268DD).

14. Cable, USB (A1560DDD).

Now we will discuss about the main components of the calorimeter equipment to learn more about how it works:

- Oxygen combustion vessel (1110) (see Figure 27):

Figure 27: Oxygen combustion vessel.

This is the composition of the Oxygen combustion vessel (see Figure 28):

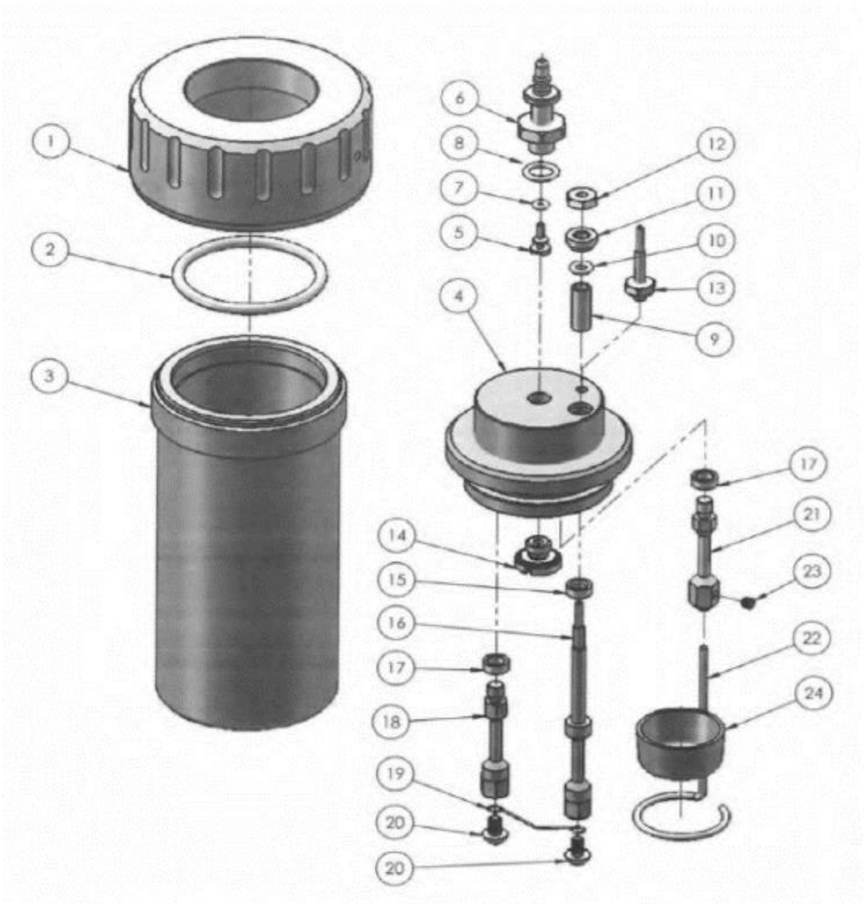

Figure 28: Composition of the Oxygen combustion vessel.

The oxygen combustion vessel (1110) is designed to withstand high pressures and temperature variations. The combustion of the samples takes place inside it. Here below here is the description of the components (see Table 2) that make up the oxygen combustion vessel:

Numeración	Código pieza	Descripción
1	1526DD	Tapón de rosca
2	1444DDJB	Junta tórica
3	1525DD	Cilindro, T313
	1524DDCC	Cilindro, C20
	1524DDCL	Cilindro, G-30 servicio de cloro
4	1525DD	Cabezal, recipiente T316
	1525DDCC	Cabezal, recipiente, C20
	1525DDCL	Cabezal, recipiente, G-30 servicio de cloro
5	1528DD	Pasador, válvula de retención
6	1527DD	Adaptador, tapa del recipiente
7	519AJV	Junta tórica
8	694DD	Junta tórica
9	658DD	Aislador

10	659DD	Junta tórica
11	663DD	Casquillo de contacto
12	SN1632HX	Tuerca hexagonal 8-32
13	1529DD	Electrodo de puesta a tierra
14	645DD	Difusor
15	654DD	Arandela de electrodo
16	1094DD2	Electrodo, largo
	1094DD2CH	Electrodo, largo (1110CL)
17	655DD	Electrodo, separador
18	1095DD	Electrodo
	1095DDCH	Electrodo (1110CL)
19	840DD2	Alambre térmico (2,0")
20	PA1332RD04	6-32 X ¼ RHMS
21	1095DD3CH	Electrodo
	1095DD3CH	Electrodo (1110CL)
22	906DD2	Portacápsulas
23	PC1332SC02	6-32 X 1/8 SHSS
24	43AS	Cazoleta, acero inoxidable

Table 2: Description of the components that make up the oxygen combustion vessel.

In the following, I will explain the most important elements of the oxygen combustion vessel.

(1) The screw plug is in charge of joining the head (4) with the cylinder (3).

(2) The O-ring, its function is to prevent possible oxygen leakage, it is important to take into account, replace the O-ring every 6 months or every 500 analyses. With the passage of time the O-ring deteriorates and leads to leakage due to juices.

(3) T316 stainless steel cylinder, this vessel contains 2.1% molybdenum so this material makes it more resistant to corrosive samples and high energy fuels.

(6) Adapter, it is a quick connector, when we carry out the combustion process, we will connect a terminal so that oxygen supply is produced.

(16) Electrode, it is an important element for the passage of electric current when we perform the combustion process, its purpose as well as the electrode (18) is to carry the electric current to the thermal wire (19).

Both electrodes close the electrical circuit, as the electric current passes through the heating wire (19) heat is generated, thus burning the cotton yarn and in turn proceeding to burn the sample. (22) Capsule holder, acts as a support for the stainless-steel cup (24), where the sample to be analyzed is added.

- Bucket (A1559DDD) (see Figure 29):

Figure 29: Bucket.

The bucket is a cylindrical container (see Figure 30) where inside we add a quantity of water specified by the manufacturer, in our case, 1 liter of water or 1 kg.

Figure 30: Special cuvette.

Inside the cuvette there are three main parts.

(1) Sensor protector in charge of taking data, it measures the water temperature (inside the tank).

(2) Base where the oxygen combustion vessel (1110) is placed.

(3) Holes for connecting the fluid to the water agitator pump.

- Regulator block, oxygen (A570DDD):

Its function is to provide the required pressure to the oxygen combustion vessel (1110), the manufacturer recommends 3000 kPa.

- Oxygen solenoid valve (A1278DD):

It is a normally closed valve, when no electric current is applied to it, it remains closed. When the calorimetric pump starts the process of analyzing a fuel, the control unit of the calorimetric pump sends an electric current to the oxygen solenoid valve producing the opening, therefore it starts supplying oxygen to the oxygen combustion vessel (1110), once it reaches the set pressure the oxygen regulator block sends the signal to the control unit, the control unit stops feeding electrically to the solenoid valve therefore it ends the process of supplying oxygen.

- Agitator motor assembly (A1268DDD):

Its function is to produce the recirculation of water in the cuvette when we perform the analysis process of a fuel, in order to obtain greater accuracy in the measurement of the temperature as a function of time when the combustion of the element we are analyzing occurs.

2. Determination of fuel density at different temperatures:

The density of the fuel depends on temperature, however, as for any other liquid: with increasing temperature, the density of the fuel decreases and vice versa - with a decrease in temperature, the density of the fuel increases, it varies with temperature, and its determination at different temperatures can be important for various applications [26].

It's worth noting that different fuels may have different density-temperature relationships, so it is important to refer to specific fuel properties or standards for accurate density determination. For highly precise density measurements of our test, we are going to determinate the fuel density of the fuel by the specialized laboratory equipment and techniques required which is the Mettler Toledo D4 density meter.

- Mettler Toledo D4 density meter:

It's important to note that different density meters may have different measurement ranges, accuracy levels, and operational considerations. The specific operating instructions and procedures for a particular density meter should be followed to ensure accurate density measurements. The density meters are used to measure slurries, sludges, and other liquids that flow through the pipeline. Industries such as mining, dredging, wastewater treatment, paper, oil, and gas all have uses for density meters at various points during their respective processes [27].

Developed for a broad range of industries, METTLER TOLEDO's Excellence Density Meters (see Figure 31) can measure almost any sample with a very high accuracy, it is a specific model of density meter manufactured by Mettler Toledo, known for its precision and reliability in density measurement.

Figure 31: Mettler Toledo D4 density meter.

Here below, the general overview of how density meters typically operate and some features commonly found in advanced density meters D4:

A/ Measurement Principle: Density meter employ various measurement principles to determine the density of a sample. Some common methods include oscillation, vibrating element, pressure, or optical principles.

B/ Sample Handling: The D4 density meter is likely equipped with a sample chamber or cell where the sample is placed for measurement. It may have a built-in mechanism for automatic sample handling, ensuring consistent and repeatable measurements.

C/ Temperature Control: Temperature can significantly affect the density of a sample, so density meters often feature precise temperature control mechanisms. The D4 is likely equipped with a temperature sensor and a temperature-controlled sample chamber to ensure accurate temperature readings and compensate for temperature variations.

D/ User Interface: The D4 density meter is likely equipped with a user-friendly interface, such as a touch screen or keypad, to allow operators to input parameters, select measurement modes, and view results. It may also have connectivity options for data transfer and integration with other systems.

E/ Calibration and Verification: Like any precision instrument, the D4 density meter would require periodic calibration and verification to maintain accurate and reliable measurements. It may include features such as automatic calibration routines, calibration reminders, or built-in reference standards.

F/ Data Handling and Analysis: D4 often offer data storage and analysis capabilities. It has internal memory for storing measurement data, as well as options for data export to a computer or other external devices. Additionally, the D4 might provide software for data analysis, reporting, and integration with laboratory information management systems (LIMS).

With highly accurate measurements of the D4, we can easily terminate inaccuracy and generate repeatable density results.

3. Determination of elemental analysis:

The elemental analysis refers to the quantitative determination of the elemental composition of a sample, further there are several techniques used for elemental analysis and there are some of the commonly used techniques for it. The choice of technique depends on the sample type required detection limits, element range, and other specific requirements. It is important to select the appropriate technique and follow established protocols and standards to ensure accurate and reliable elemental analysis results.

The University of Jaén has numerous university services and technical units for administrative and service staff, students and teachers, these include the famous central research support services (SCAI).

SCAI currently has 2 centers, these two centers share the management and administration functions. This provides a fluid channel for the exchange of information and experience between them, as well as facilitating the definition of strategies common to both centers, or seeking equity when these apply to only one of them.

The Centre for Scientific-Technical Instrumentation (CICT) at the University of Jaén is one of the two centers, designed to carry out scientific and technical tests and studies using its own instrumental resources, located and supervised in its own facilities, mainly in the west wing of the A2 building on the Jaén Campus [28].

There are certain chemical analysis units in this building, one of them that we will work on, is the ‘AQ07-CHNS 2 Automatic elemental analyzer’ (see Figure 32) which is an Elemental Analyzer based on the total combustion technique of micro-samples for the determination of the total content of Nitrogen, Carbon, Hydrogen and Sulfur, in various types of solid or liquid samples (organic, organometallic, pharmaceutical, plastics, polymers, soils and agricultural materials, sediments, oils, fertilizers...) [28].

Brand: Leco

Model: TruSpec Micro

Certificatic

Figure 32: AQ07-CHNS 2 Automatic elemental analyzer.

Analytical range for a 2 mg sample:

- For C: 0.002% to 100% of the total content of the element present in the sample.
- For H: 0.02% to 50% of the total content of the element present in the sample.

- For N: 0.02% to 50% of the total content of the element present in the sample.
- For S: 0.04% to 65% of the total content of the element present in the sample.

The analyzer consists of a primary combustion furnace where the sample is dropped and instant combustion takes place. This is followed by a secondary afterburner that traps the excess oxygen. Both furnaces have independent programmable temperature control up to 1100°C [28].

It features a detection system using independent detectors for each element:

- Carbon: CO_2 selective IR absorption detector
- Hydrogen: H_2O selective IR absorption detector
- Nitrogen: NO differential thermal conductivity detector
- Sulfur: SO_2 selective IR absorption detector

It is also equipped with an automatic sample loader with 2 carousels, each with 30 positions. These methods vary in terms of their sensitivity, precision, and suitability for different sample types. The selection of the appropriate method depends on the specific elements of interest, sample matrix, required detection limits, and available instrumentation.

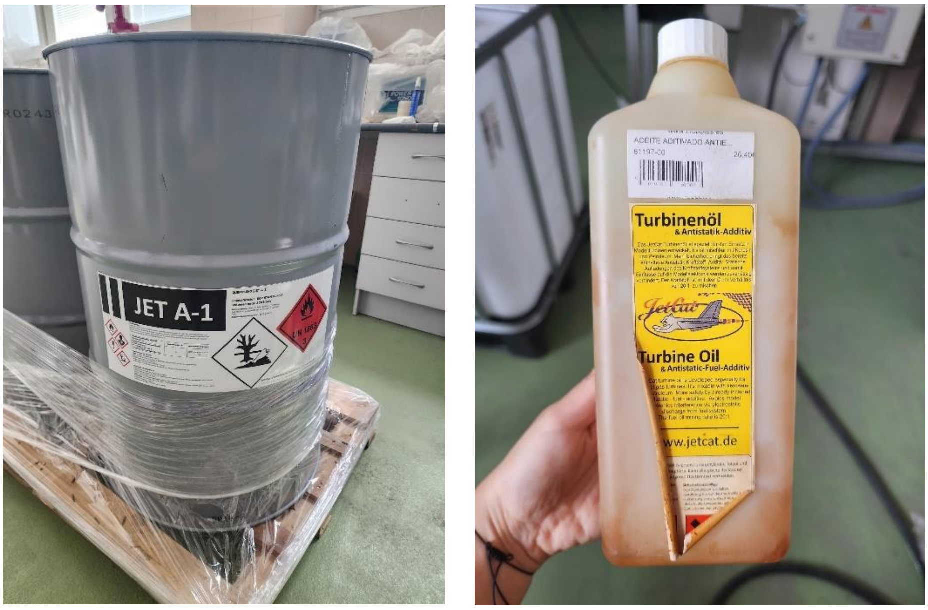

Figure 33: JETA1 and JETCAT OIL.

The samples that we are going to test after, is the pure JETA1 and pure and the blend of 95,5% Jet-A1 + 4,5% JETCAT OIL (see Figure 33) as documented in engine company papers, and it is the combination of two of these that we will utilize and store in the can, which is a closed container ideal for transporting and storing our fuel blend.

Conclusion:

The development and utilization of advanced fuel characterization devices continue to drive innovation and advancements in the energy sector, supporting the transition towards sustainable and cleaner fuel sources. Thus, in the coming chapter we will introduce the results of the operated equipment that we describe, as well as our engine setup that we did during the experiments and how all the devices connected.

Chapter4: Experimental study

Introduction:

The analysis and interpretation of the results provide valuable insights into the research questions or hypotheses, contributing to the overall understanding of the topic under investigation. Through this chapter, we will provide the experimental data obtained using the equipment discussed which demonstrate the performance of the Olympus-HP engine at different measurement points.

1. Operating regimes tested:

As mentioned above, the International Civil Aviation Organization (ICAO) recognizes that airport-related emissions sources have the potential to emit pollutants that can contribute to the deterioration of air quality in nearby communities. Similarly, attention should be paid to other potential environmental consequences, which will not be studied here, such as noise emissions, water quality, waste management, energy consumptions and local ecology in the vicinity of airports [20].

For some States, there is often a mix of regulations and standards in place covering many of the sources of emissions present at airports, but emissions standards for aircraft engines are agreed internationally through ICAO's and subsequently included in the national regulations of each Member State.

ICAO standards on engine emissions are applied through national and multinational certification processes for turbojet and turbofan engines with thrust greater than 26.7 kilonewtons (kN), but not for turboprop, reciprocating and auxiliary power unit (APU) engines [20]. These regulations are based on the performance of the engines in the idealized landing and take-off (LTO) cycle (see Figure 34) as shown below [22]:

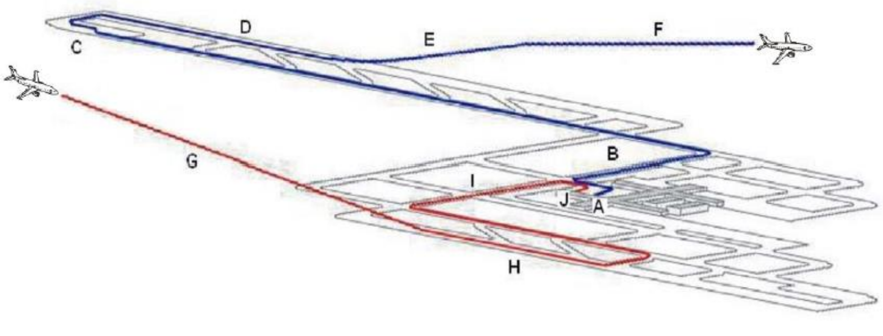

Figure 34: Landing Take Off cycle stages (LTO).

- EXIT:

A. Starting the engines. It is normal to start the main engines prior to or during the thrust maneuver, starting from the aircraft door or parking stand. When the aircraft does not require thrust, the main engines are started immediately prior to taxi.

B. Taxiing to the runway. Aircraft normally taxi with all engines running to the runway or holding area before entering the runway, although they may taxi with fewer engines running in certain circumstances. The taxi is normally performed at the idle power setting, apart from brief bursts of power to overcome initial inertia at the beginning of the taxi or, if necessary, to take sharp turns.

C. Waiting on the ground. When necessary, the aircraft may be asked to remain in a queue while awaiting clearance to enter the runway and taxi to the takeoff position. Normally, the main engines are placed at idle thrust with short bursts of power to taxi into position.

D. Takeoff run and initial lift. The aircraft accelerates along the runway at the predetermined rotational speed at the end of the takeoff run with the main engines trimmed for takeoff power. Operators use either takeoff thrusts that are not nominal or, more frequently, reduced thrust settings (flexible), which are determined by the actual takeoff weight of the aircraft, runway length, and weather factors at the time.

E. Initial climb to thrust reduction. After leaving the surface, the aircraft landing gear is folded and the aircraft climbs at constant speed with the initial takeoff power setting until it reaches the thrust reduction altitude at which the controls are retarded.

F. Acceleration, transition to clean configuration and in route climb. After thrust reduction, the aircraft continues to climb at a lower thrust setting than that used for takeoff, followed by retraction of flaps and flap overshoot as the aircraft accelerates and reaches cruise altitude.

- ARRIVAL:

G. Final approach and flap extension. The stabilized final approach from the final approach fix follows a relatively predictable glide slope at low engine thrusts. Thrust trims are increased to counteract additional forward drag as flaps and landing gear deploy, while speed decreases toward righting.

H. Righting, touchdown and landing run. Normally, the controls are retarded to idle during the righting and landing run. This is followed by application of wheel brakes and, when appropriate, thrust reversal to slow the aircraft on the runway.

I. Taxiing from the runway to the parking stand or gate. Taxiing from the runway is a similar process to the taxi to the runway described above; however, operators may shut down one or more engines, as appropriate, during taxi if the opportunity arises.

J. Engine Shutdown. The remaining engines are shut down after the aircraft has completed taxiing and power is available for the aircraft's onboard services. The certification procedures are carried out on a single engine in a test cell, with reference to a static sea level and International Standard Atmosphere (ISA) conditions.

For the characterization of gaseous emissions and the evaluation of their impact on the airport environment, the following analyses must be carried out:

- The emission inventories.
- The dispersion modeling of pollutant concentrations.

The emissions inventory provides the total mass of emissions released to the environment and forms the basis for reporting, compliance and mitigation planning. To relate emissions to pollutant concentrations, the spatial and temporal distribution of emissions must also be assessed. This mixed approach of using emission inventories and dispersion modeling allows for the assessment of historical, existing and future pollutant concentrations in the vicinity of airports due to specific meteorological conditions.

Aircraft remain a relatively small contributor to regional pollution [31]. Consequently, while reductions in aircraft emissions (through measures to reduce the emissions from aircraft) could be achieved in the short term, aircraft emissions are still a relatively small contributor to regional pollution [32]. operational and air traffic or more stringent ICAO engine standards [33] can contribute to improving local air quality in the vicinity of airports, it is also important to consider emissions from both regional and local ground vehicles.

Understanding that the technology has reached a stage of maturity with little scope for new developments and already has advantages over historical values [30], CAEP anticipates further increases in stringency of aircraft engine emission standards in the LTO cycle.

The timeframes and percentages of power at which we will test our engine are listed below for each stage of the LTO cycle (see Table3):

Stage	Duration	Percentage of power (%)
Approach	4	30
Taxi	26	7
Take-off	0,7	100
Climb	2,2	85

Table 3: Duration in minutes of the LTO cycle stages and the associated power percentage [34].

Except for the two inputs, throttle and switch, we can vary the proportion of power and cause the engine to run at the desired speed using this ECU analog (see Figure 35).

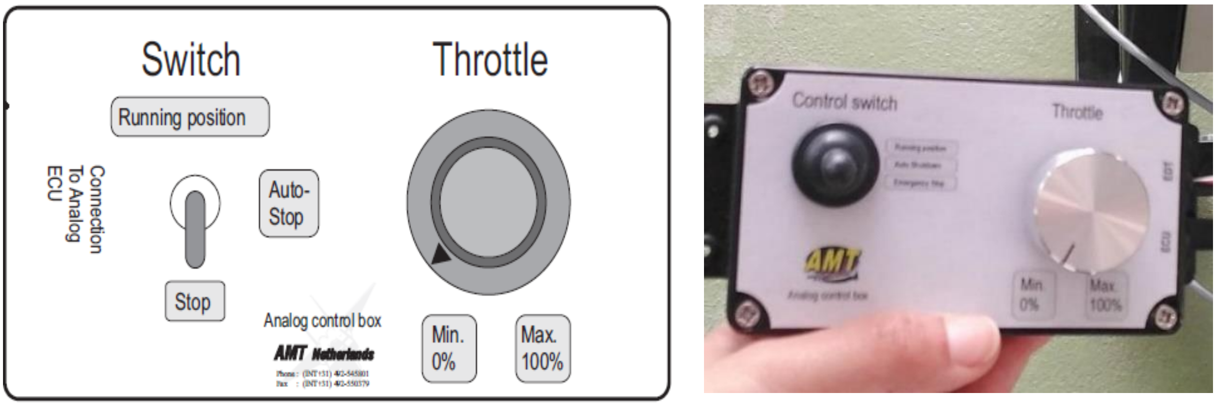

Figure 35: The ECU analog.

2. Thermodynamic properties and performance experimental results:

In this section we will going to introduce the purpose and objective of our experimental test which explain why the test is being assisted and what specific parameters or variables are being investigated describing the equipment, apparatus, materials and reagents used in the experiments carried out in the laboratory, as well as the methodology followed to determine our objective.

This project aims to study the behavior of the fluid that passes through a jet engine, in particular, as it passes through the combustion chamber, that’s why we need to demonstrate our installation for the experimental test involves providing a detailed overview of the setup and procedures used in the test.

Here's a step-by-step approach to describing our overall setup of the installation for this Olympus HP engine experimental test (see Figure 36), including the equipment, instruments, and apparatus used that we have previously discussed.

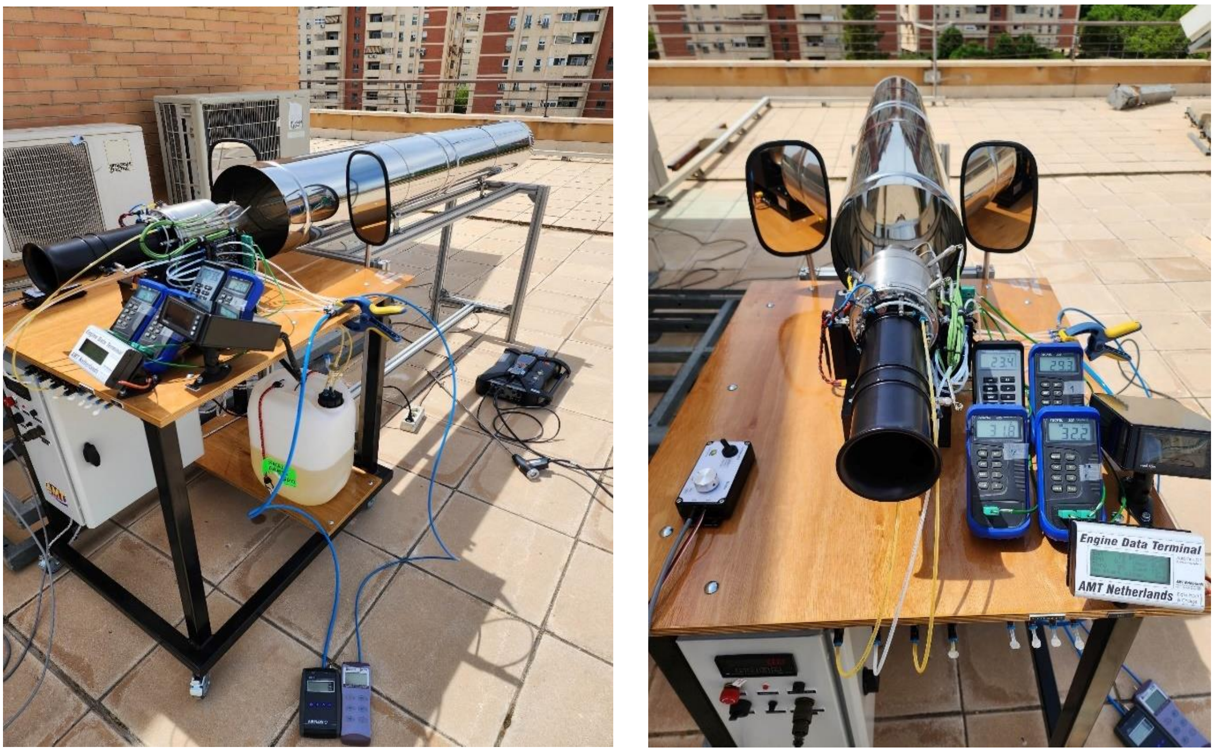

Figure 36: The Setup of Olympus-Hp engine.

For conducting experimental test on our turbine installation, we must go through a process of carefully selecting a suitable place, which is why we decided to test it on the roof of one of the university buildings, because it provides an excellent wind condition for accurate data collecting, and that’s must be carefully crafted to ensure accurate results.

After, we will be starting the work of connecting the equipment we have to the installation. we will carefully establish the appropriate connections, ensuring that each component is properly integrated for seamless functioning.

These components represented by:

- 2 digital manometers type **CA 850.**

- 4 thermometers type **TECPEL 307.**

- 1 Exhaust emissions equipment type **Testo 350**.

Which we have discussed in the previous section, and which are linked together via extension cables and specific tubes.

Additionally, a tube structure (see Figure 37) was constructed and was modeled by me and a specialist laboratory technician to collect the outside gases as they passed through the tube hole. This is how the results of the exhaust emissions were achieved utilizing the heat resistant handle of the Testo350 equipment and here below his design:

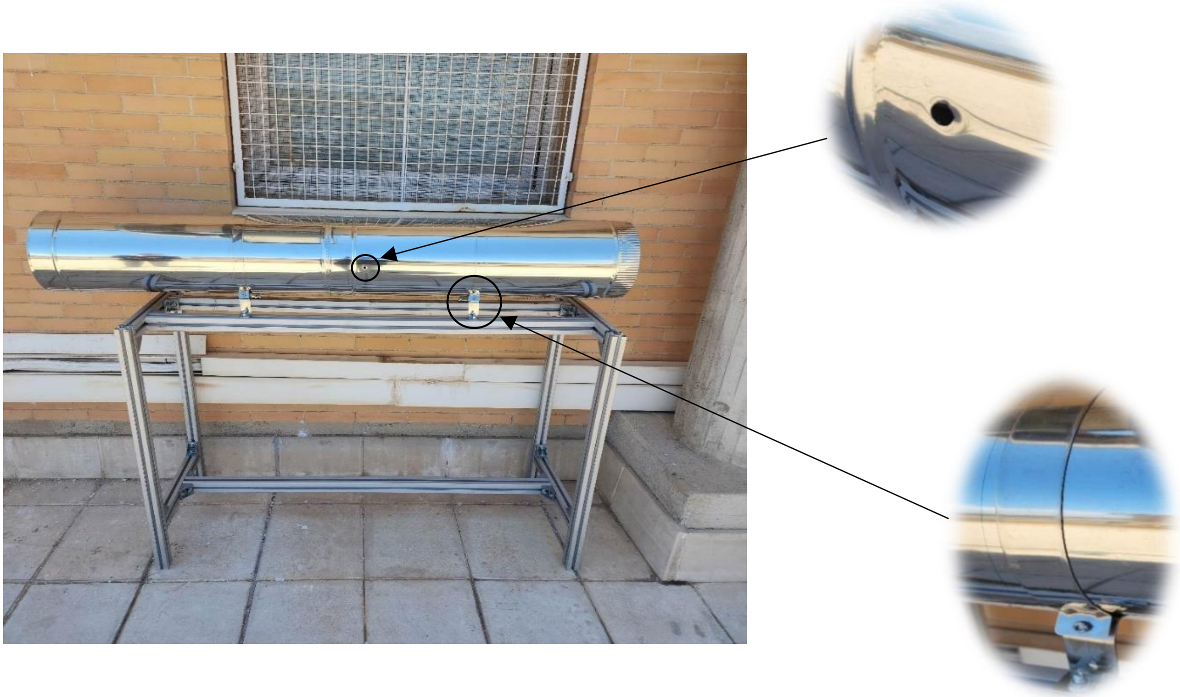

Figure 37: The tube structure.

The laboratory technician used a technic method to secure and stabilize the tube in place. Whether it involves fastening components together, affixing an item to a surface, or ensuring structural integrity and the choice of fixing method ii was dictated by the specific requirements of our task at hand.

Common techniques include screwing, bolting, welding, gluing, or using mechanical clamps., each method possesses its own unique advantages, such as strength, flexibility, or ease of disassembly.

The selection of our suitable fixing method of the tube demands careful consideration of factors such as load-bearing capacity, environmental conditions, material compatibility, and desired permanence, so that it may be properly positioned, aligned, and supported of the engine's exhaust gas emissions. Therefore, we wanted to clarify more his shape and measurements below (see Figure 38):

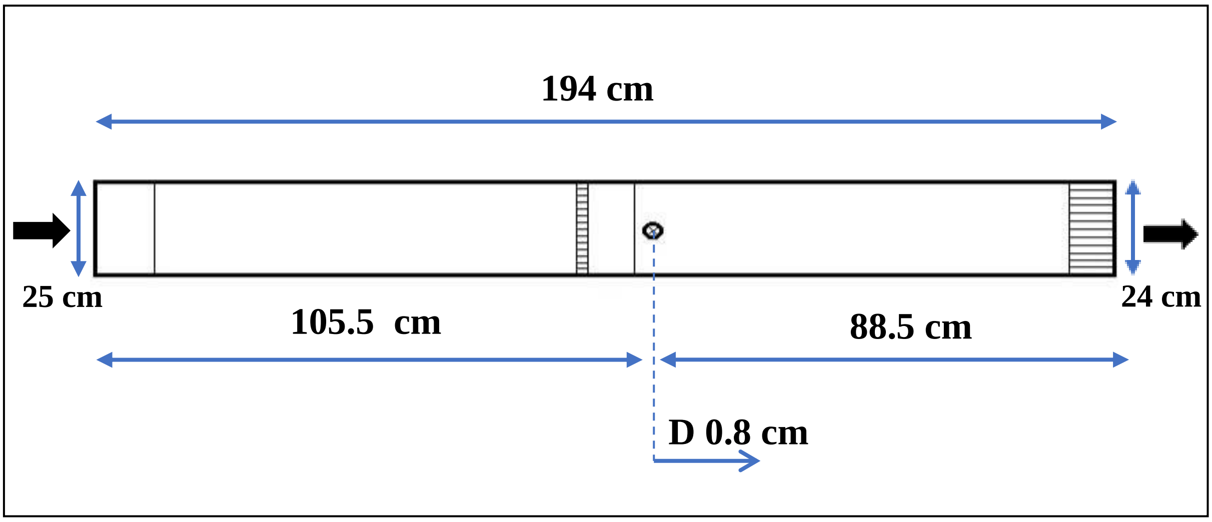

Figure 38: Scheme adopted for the tube measurement according to standards.

Once the tube is built and everything is precisely installed, ensuring proper position and secure anchoring to resist wind forces, a wide range of measurements, such as Speed, Thrust, RPM, Exhaust Gases, Pression, Temperature, and Fuel flow, are collected to assess the turbine's performance, which I have expressed in the form of tables below.

For turbine test number 1:

In this test, we analyze the turbine when the throttle position is on Idle (0%), 30% and 50% (see Table 4,5 and 6).

- Initial ambient temperature (digital thermometer): Ta = 25.9ºC
- Final ambient temperature (digital thermometer): Ta = 26.3ºC
- Initial relative humidity = 51%
- Final relative humidity = 53 %
- Ambient Pressure Pa= 972 mbar (hpa)

For one the thermometer measurements type (TECPEL 307), we have: T1=Tt3 and T2=Tt6:

First measurement on Idle (0%)		
The pression (bar)	**The temperature (°C)**	**The other Data**
PS1 = -0,0014	Tt1 = 22,3	Exhaust Gas Temperature (EGT) = 594°C
PS3 = 0,154	Tt3 =130	Revolutions of shaft (PRM) = $36,5.10^3$RPM
PT3 = 0,174	Tt4 = 63,9	Throttle position (THRO) = 0%
PT4 = 0,162	Tt5 = -278	Thrust = 0,8 kgf
PT5 = 0,0258	Tt6 = 489	Fueling = 144 ml/min

Table 4: First measurement on Idle (0%) of test number 1.

Second measurement on (30%)		
The pression (bar)	**The temperature (°C)**	**The other Data**
PS1 = -0,0172	Tt1 = 22,4	Exhaust Gas Temperature (EGT) = 529°C
PS3 = 1,114	Tt3 =132	Revolutions of shaft (PRM) = $80,0.10^3$RPM
PT3 = 1,315	Tt4 = 65,7	Throttle position (THRO) = 30%
PT4 = 1,098	Tt5 = -279	Thrust = 7,9 kgf
PT5 = 0,2182	Tt6 = 497	Fueling = 374 ml/min

Table 5: Second measurement on (30%) of test number 1.

Third measurement on (50%)		
The pression (bar)	**The temperature (°C)**	**The other Data**
PS1 = -0,028	Tt1 = 22,6	Exhaust Gas Temperature (EGT) = 561°C
PS3 = 1,706	Tt3 =160	Revolutions of shaft (PRM) = $92{,}5.10^3$RPM
PT3 = 1,906	Tt4 = 67,9	Throttle position (THRO) = 50%
PT4 = 1,651	Tt5 = -281	Thrust = 12,0 kgf
PT5 = 0,4612	Tt6 = 553	Fueling = 511 ml/min

Table 6: Third measurement on (50%) of test number 1.

According to the trend curve found from the test expressed earlier, we have a light regression between the temperature and the pressure in vacation entered on the temperature and the pressure because these are the two main parameters of our test, and we will try to find a correlation between these two parameters and the speed.

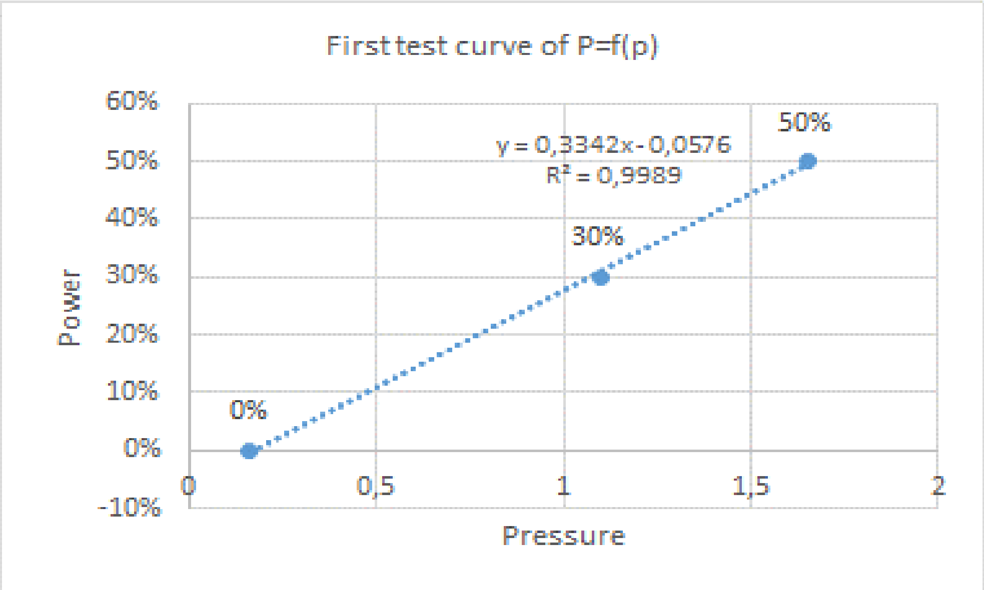

Figure 39: First test curve of P=f(p).

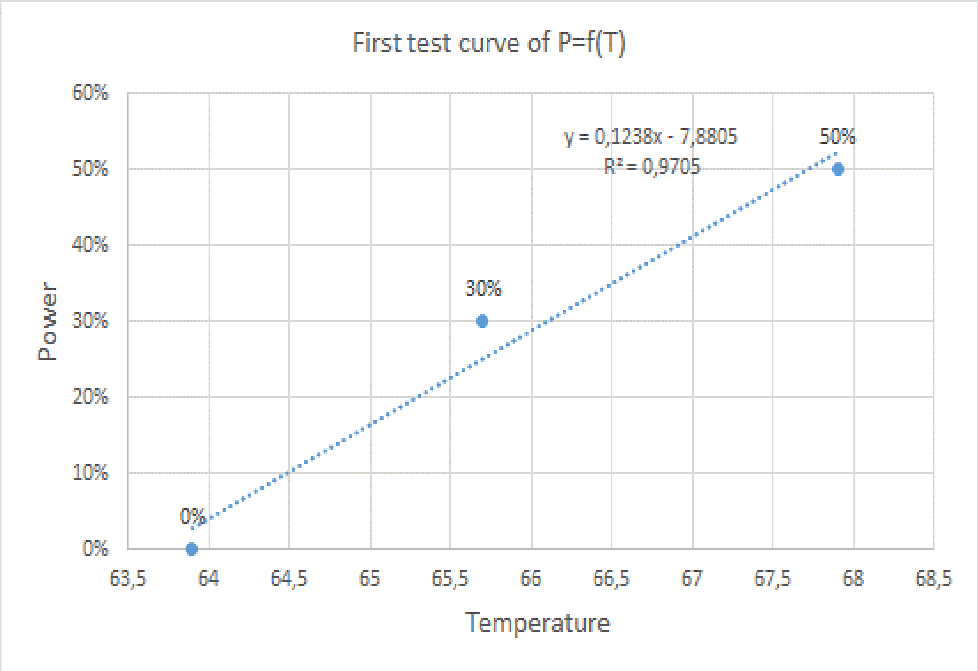

Figure 40: First test curve of P=f(T).

We are working on an experimental part that's why we chose to make a curve with a cloud of points, we have a trend curve that gives us the closest curve that passes through the most points

We got a decent linear trend curve since the confession of determination R^2 approached to 1.

For turbine test number 2:

In this test, we analyze the turbine when the throttle position is on 7%, 30% and 50% (see Table 7, 8, 9 and 10).

- Initial ambient temperature (digital thermometer): Ta = 24.1ºC
- Final ambient temperature (digital thermometer): Ta = 24.8ºC
- Initial relative humidity = 57%
- Final relative humidity = 61 %
- Ambient Pressure Pa= 963 mbar (hpa)

For one the thermometer measurements type (TECPEL 307), we have: T1=Tt3 and

First measurement on Idle (0%)		
The pression (bar)	**The temperature (°C)**	**The other Data**
PS1 = -0,0051	Tt1 = 20,2	Exhaust Gas Temperature (EGT) = 589°C
PS3 = 0,301	Tt3 = 42,5	Revolutions of shaft (PRM) = 36,0.10^3RPM
PT3 = 0,328	Tt4 = 635	Throttle position (THRO) = 0%
PT4 = 0,297	Tt5 = 551	Thrust = 0,9 kgf
PT5 = 0,0404	Tt6 = 512	Fueling = 144 ml/min

Table 7: First measurement on Idle (0%) of test number 2.

Second measurement on (7%)		
The pression (bar)	**The temperature (°C)**	**The other Data**
PS1 = -0,0051	Tt1 = 26,7	Exhaust Gas Temperature (EGT) = 566°C
PS3 = 0,301	Tt3 = 068	Revolutions of shaft (PRM) = $49,0.10^3$RPM
PT3 = 0,328	Tt4 = 638	Throttle position (THRO) = 7%
PT4 = 0,297	Tt5 = 544	Thrust = 1,9 kgf
PT5 = 0,0404	Tt6 = 508	Fueling = 200 ml/min

Table 8: Second measurement on (7%) of test number 2.

Third measurement on (30%)		
The pression (bar)	**The temperature (°C)**	**The other Data**
PS1 = -0,0177	Tt1 = 27,6	Exhaust Gas Temperature (EGT) = 538°C
PS3 = 1,067	Tt3 =121,1	Revolutions of shaft (PRM) = $79,0.10^3$RPM
PT3 = 1,249	Tt4 = 689	Throttle position (THRO) = 30%
PT4 = 1,044	Tt5 = 512	Thrust = 7,0 kgf
PT5 = 0,2059	Tt6 = 494	Fueling = 371 ml/min

Table 9: Third measurement on (30%) of test number 2.

Fourth measurement on (50%)		
The pression (bar)	**The temperature (°C)**	**The other Data**
PS1 = -0,0272	Tt1 = 28,8	Exhaust Gas Temperature (EGT) = 566°C
PS3 = 1;578	Tt3 =160,4	Revolutions of shaft (PRM) = $92{,}0.10^3$RPM
PT3 = 1,806	Tt4 = 696	Throttle position (THRO) = 50%
PT4 = 1,551	Tt5 = 542	Thrust = 11,1 kgf
PT5 =0,3163	Tt6 = 559	Fueling = 494 ml/min

Table 10: Fourth measurement on (50%) of test number 2.

And here are the temperature and pressure diagrams as well:

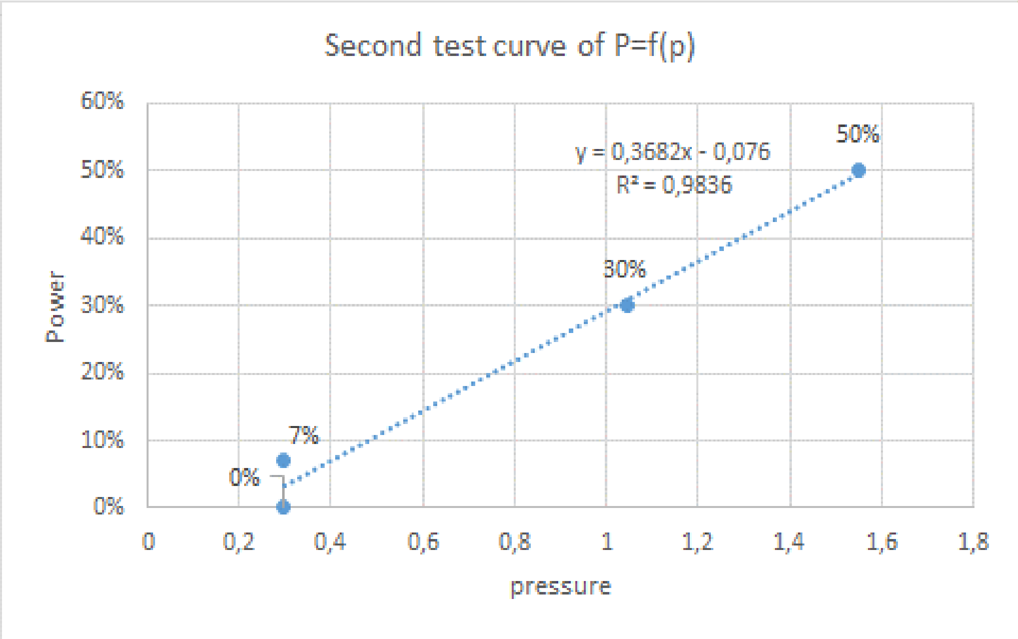

Figure 41: Second test curve of P=f(p).

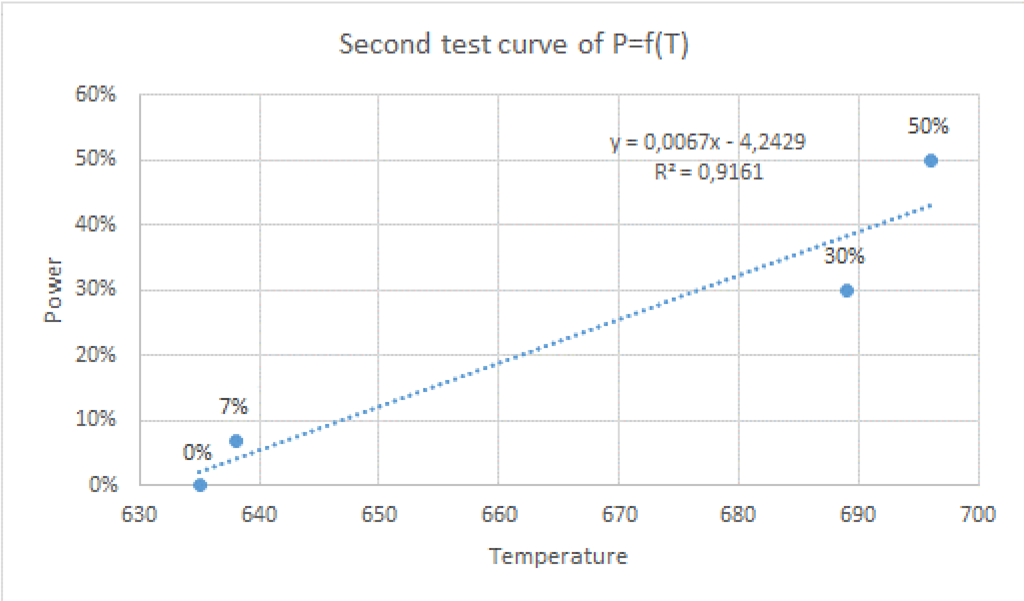

Figure 42: Second test curve of P=f(T).

For turbine test number 3:

In this test, we analyze the turbine when the throttle position is on 7%, 30%, 85% and 100% (see Table 11, 12, 13, and 14).

- Initial ambient temperature (digital thermometer): Ta = 23,2ºC
- Final ambient temperature (digital thermometer): Ta = 24.7ºC
- Initial relative humidity = 59%
- Final relative humidity = 63 %
- Ambient Pressure Pa= 964 mbar (hpa)

For one the thermometer measurements type (TECPEL 307), we have: T1=Tt3 and T2=Tt6:

First measurement on Idle (7%)		
The pression (bar)	**The temperature (°C)**	**The other Data**
PS1 = 0,011	Tt1 = 16,4	Exhaust Gas Temperature (EGT) = 515°C
PS3 = 0,185	Tt3 = 48	Revolutions of shaft (PRM) = $49{,}0.10^{3}$ RPM
PT3 = 0,159	Tt4 = 563	Throttle position (THRO) = 0%
PT4 = 0,108	Tt5 = 507	Thrust = 2,4 kgf
PT5 = 0,034	Tt6 = 478	Fueling = 200 ml/min

Table 11: First measurement on Idle (7%) of test number 3.

Second measurement on (30%)		
The pression (bar)	**The temperature (°C)**	**The other Data**
PS1 = 0,003	Tt1 = 16	Exhaust Gas Temperature (EGT) = 511°C
PS3 = 1,207	Tt3 = 110	Revolutions of shaft (PRM) = $79,0.10^3$ RPM
PT3 = 1,346	Tt4 = 609	Throttle position (THRO) = 30%
PT4 = 1,133	Tt5 = 483	Thrust = 8,3 kgf
PT5 = 0,248	Tt6 = 481	Fueling = 389 ml/min

Table 12: Second measurement on (30%) of test number 3.

Third measurement on (85%)		
The pression (bar)	**The temperature (°C)**	**The other Data**
PS1 = -0,028	Tt1 = 15,7	Exhaust Gas Temperature (EGT) = 704°C
PS3 = 2,468	Tt3 = 187	Revolutions of shaft (PRM) = 104.10^3 RPM
PT3 = 2,723	Tt4 = 832	Throttle position (THRO) = 30%
PT4 = 2,459	Tt5 = 664	Thrust = 19,5 kgf
PT5 = 0,530	Tt6 = 667	Fueling = 751 ml/min

Table 13: Third measurement on (85%) of test number 3.

Fourth measurement on (100%)		
The pression (bar)	**The temperature (°C)**	**The other Data**
PS1 = -0,028	Tt1 = 15,8	Exhaust Gas Temperature (EGT) = 814°C
PS3 = 2,746	Tt3 = 208	Revolutions of shaft (PRM) = $108,5.10^{3}$RPM
PT3 = 2,947	Tt4 = 935	Throttle position (THRO) = 100%
PT4 = 2,708	Tt5 = 741	Thrust = 22,1 kgf
PT5 = 0,623	Tt6 = 734	Fueling = 87 6 ml/min

Table 14: Fourth measurement on (100%) of test number 3.

We were testing the engine at various percentages of load to get an idea of how it works at first, but after that, all calculations and results will be based on 100% load because the full load is always representative as a maximum running, and the LTO cycle has one of his measurement points at 100% load, so we thought it would be the most representative load to obtain our feeds from.

Further, these trial data are then examined, offering significant insights into the engine's efficiency, aerodynamics, and future development possibilities.

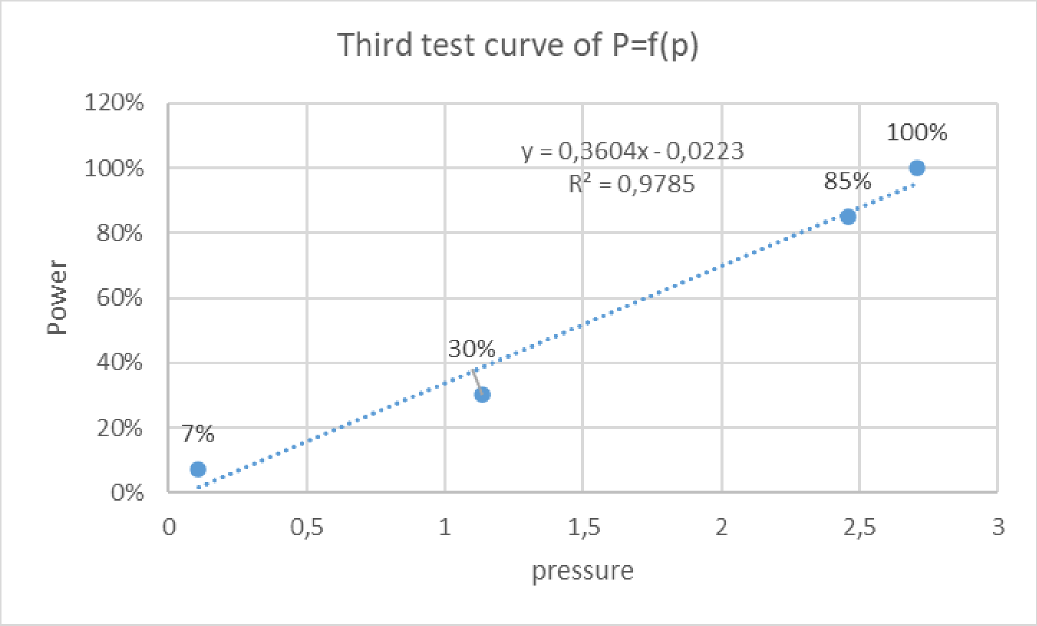

Figure 43: Third test curve of P=f(p).

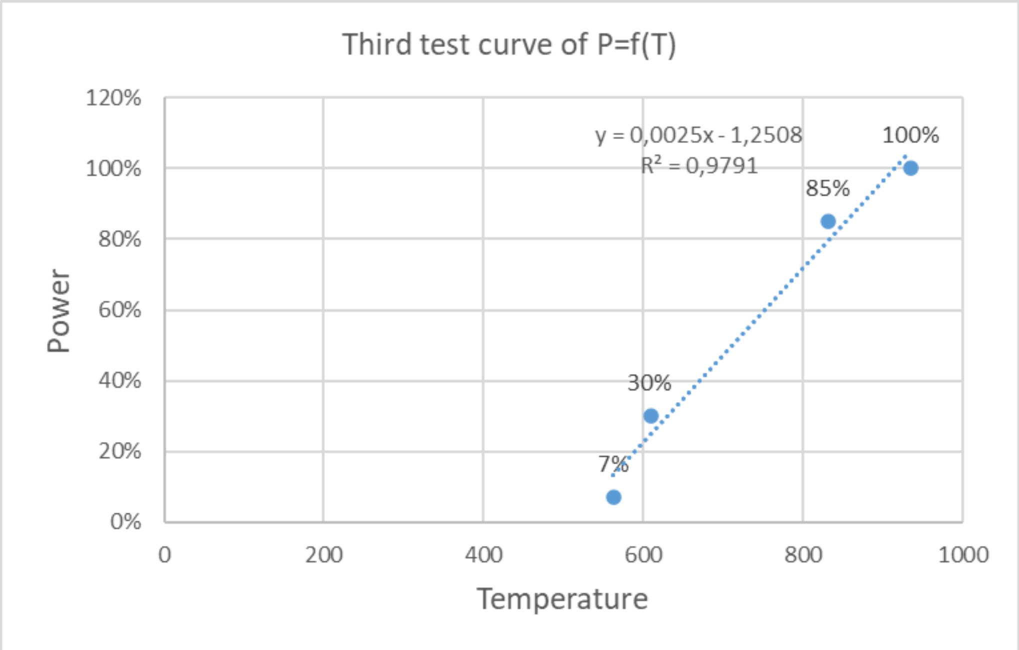

Figure 44: Third test curve of P=f(T).

If we want to have a decent curve, we need to increase the number of testing the more tests we have, the clearer curves we get.

3. Exhaust emissions experimental results:

It's important to note that exhaust emissions testing is a specialized area that often requires expertise and adherence to specific protocols and standards, also, the results can vary significantly depending on the specific engine, fuel, operating conditions, and testing methods used. We will measure exhaust emissions in the midst of the jet stream, and in order to obtain exhaust emissions experimental findings for our Olympus HP engine (see Table 15, 16 and 17), we will need to conduct experiments using specific equipment which is the ‘Testo 350 Exhaust emissions equipment’ that we talked about earlier, as it shown below the results of exhaust emissions that we obtain:

First exhaust emissions								
	O_2 (%)	CO (ppm)	NO (ppm)	NO_2 (ppm)	NO_x (ppm)	CO_2 (ppm)	HC (ppm)	H_2 (ppm)
At 0%	20,19	4857	0	1,8	1,8	20337	172	69
At 30%	20,22	2986	3	2,8	2,8	57894	553	156
At 50%	20,15	2680	7	3,8	3,8	64691	867	3

Table 15: First exhaust emissions values.

Second exhaust emissions								
	O_2 (%)	CO (ppm)	NO (ppm)	NO_2 (ppm)	NO_x (ppm)	CO_2 (ppm)	HC (ppm)	H_2 (ppm)
At 0%	16,35	3110	**0**	2,8	9,8	29203	**0**	111
At 7%	20,15	496	6	2,3	2,3	5524	14	15
At 30%	20,14	310	11	3,2	3,2	5699	53	8
At 50%	20,11	279	15	4,3	4,3	6143	20	6

Table 16: Second exhaust emissions values.

Third exhaust emissions								
	O_2 (%)	CO (ppm)	NO (ppm)	NO_2 (ppm)	NO_x (ppm)	CO_2 (ppm)	HC (ppm)	H_2 (ppm)
At 7%	17,33	2876	2	3,9	5,9	33049	235	212
At 30%	17,36	1637	6	5,3	13,3	54086	611	269
At 85%	17,09	1155	14	6,7	20,7	26223	221	113
At 100%	16,76	1300	19	5,8	24,8	28069	97	88

Table 17: Third exhaust emissions values.

As a result of these measurements, we discovered that the hydrocarbons (HC) had poor outcomes while the others performed admirably because according to the equipment, the testo devise cannot measure the fluid at a high-speed running.

4. Fuel properties experimental results:

This section of the results provides a thorough examination of the features and behaviors of the tested fuel that we have. In addition, we will provide the obtained results of our proprieties such as density, elemental analysis, and heating value, which we will begin with.

We already talked about the equipment of the density measurement, so in this section we will describes the apparatus, materials and reagents used in this experiment carried out in the laboratory, as well as the methodology followed to determine the gross calorific value of liquid and solid samples.

a. Analytical balance:

In order to measure the mass of the substances to be analyzed, measuring equipment consisting of a 31 Boeco bas 31 plus (see Figure 45) precision balance with a measuring accuracy of 0.0001g and automatic internal calibration was used.

Figure 45: Analytical balance Boeco bas 31 plus.

Before starting to use the analytical balance, it is important to make sure that it is correctly centered. To know if it is in the correct position, the balance has a guide for correct centering on the back of the balance, consisting of a spirit level.

To balance the balance (see Figure 46), the bubble must be in the set position and for this we adjust the position by means of the four adjustable feet of the analytical balance.

Figure 46: Balancing the analytical balance Boeco bas 31 plus.

As can be seen in the picture, the bubble is within the limit, so the analytical balance is well balanced.

b. Scale:

In order to weigh the amount of water that needs to be added to the tank during the process, we use a Cobos HC-K3KA Scale (see Figure 47) with an accuracy of 1g.

The quantity established by the manufacturer is 1 kg of water.

Figure 47: Cobos HC-K3KA Scale.

c. Auxiliary oxygen pressure equipment:

In order for complete combustion to take place inside the oxygen combustion vessel (1110), the necessary oxygen must be present for this reaction to take place. For this reason, we supply oxygen. Air liquid oxygen has been used (see Figure 48), supplying a quantity of 3000 kPa, which is the pressure established by the manufacturer of the calorimetric pump.

Figure 48: Auxiliary oxygen pressure equipment.

And now we'll go over the supplies we used, as well as methodology of work:

d. Cotton yarn:

The cotton thread is used for each analysis. This thread (see Figure 49) is placed in the ignition wire of the oxygen combustion vessel (1110). When we perform the process to obtain the calorific value, an electric current pass through the ignition wire, which generates heat, causing the ignition wire to burn and start the combustion process. The cotton wire used is Parr (845DD2), ignition thread, 4" 10g/1K.

Figure 49: Cotton yarn.

e. Distilled water:

We use distilled water to improve the accuracy of the calorimetric pump analysis results. We add 1ml of distilled water inside the cylinder of the oxygen combustion vessel (1110).

We needed some interventions to get better results, so we'll use one of the reagents, which are substances or compounds that are specifically chosen and used in chemical reactions or analytical procedures to facilitate or induce a desired chemical change or to detect the presence of certain compounds. the reagent that we are going to use in our assay is the Benzoic acid.

Benzoic acid (C6H5COOOH) is an aromatic carboxylic acid (see Figure 50) that under normal conditions is a colorless solid with a slight characteristic odor, poorly soluble in cold water, but has good solubility in hot water or organic solvents.

This substance, used to calibrate the calorimetric pump, is used to establish the calorific value of the calorimetric pump in accordance with the UNE-EN 14918:2011 standard, which establishes this compound as a reference in calibrations, as its enthalpy is known and it is made up solely of C, H and O.

The superior calorific value of benzoic acid is 6318 Cal/g, it comes in the form of tablets with an approximate weight of 1g.

Figure 50: Benzoic acid canister along with the pill.

f. Methodology of work:

There are times when a sample does not burn completely or has mass losses due to high volatility of the liquid used. This can be due to a number of circumstances:

o Low heat of combustion.

o High water content.

o High volatility of the liquid used.

o Solids with small particles.

In these cases, a material is added to the sample in order to add an energy supplement to ensure complete combustion. In another case, it is used in order to avoid mass losses of the material used.

Moreover, the calorimetric bomb is used to determine the calorific value of a fuel when it is burned at constant volume, since it is based on a closed vessel where oxygen will be injected at high pressure to obtain a complete combustion, and here are the steps below which demonstrates and explains this test.

-Firstly, is the lid opening (see Figure 51).

Figure 51: Lid opening.

-Secondly, the extraction of the bowl assembly (see Figure 52).

Figure 52: Extraction of the bowl.

-Thirdly, weighing a kilogram of water (see Figure 53).

We proceed to fill the tank with tap water. This procedure can be done in two ways. Using a one-liter measuring cylinder or by weighing one kilogram of water. The most accurate procedure and the one we have used is by weighing one kilogram of water, using a one-liter beaker of water.

Figure 53: Flask with a capacity of one liter.

To carry out this process, we first weigh the cuvette and tare it, leaving the weight at 0. We add water until we reach the amount of 1 kg (see Figure 54). Once the cuvette is filled with tap water and the specified amount, we proceed to put the cuvette in the calorimetric pump assembly.

Figure 54: Placing the cuvette in the calorimetric pump assembly.

Before continuing with the procedure, we verify by means of the computer software that the temperature (Jacket Temp) must be higher than the temperature (Bucket Temp), the difference must be between (0.5-2ºC). This aspect to be taken into account is established by the manufacturer for correct operation.

-Fourthly, applying sample.

We put the cotton thread on the ignition wire (see Figure 55). The most advisable way to put the cotton thread is by applying a knot to ensure contact with the ignition wire and avoid ignition failures when the combustion process starts.

Figure 55: Placement of cotton thread.

We proceed to place the cup in the capsule holder (see Figure 56), then when we placing the cup with the fluid in the capsule holder, it is important that both ends of the cotton thread are in contact with the fluid.

Figure 56: Placement of the cotton thread in the case.

We weighed the empty case and found it weighed 13.27g, so we poured 0.6g of our fuel, oil, or a mix of both and placed it on the scale before inserting the T bottom to reset to 0.

The next step is to add 1 ml of distilled water to the cylinder of the oxygen combustion vessel assembly (1110). By performing this step, the calorimetric pump obtains a more accurate result in the measurement of the calorific value on the samples. A step from, moisten the O-ring with distilled water (see Figure 57), it is important to perform this step because it guarantees a correct sealing and will not produce pressure losses.

Figure 57: O-ring moistened with distilled water.

We carefully fit the head assembly to the cylinder (see Figure 58), then we screw in the screw cap and make sure it is properly tightened.

Figure 58: Screwing of the head assembly to the cylinder.

Using a holder (see Figure 59), we fit it over the oxygen combustion vessel (1110) and place it in the cuvette.

Figure 59: Placement of the support on the screw cap, including the oxygen combustion vessel assembly on the flask.

We connect the electrical terminals; it does not have a determined position therefore the order of connection does not matter. Additionally, we attach the quick connector of the auxiliary oxygen equipment (see Figure 60).

Figure 60: Connection of electrical terminals and the oxygen connector location.

Then we close the cover of the calorimetric pump equipment (see Figure 61).

Figure 61: Closing the cover of the calorimetric pump assembly.

Before entering the sample data into the computer system, it is important to verify that the analyses to be performed are in Determination. Then enter the name of the test in the computer software by clicking on START.

We add the name of the test in Sample ID and the weight of the sample (m) always in grams in Sample Weight. Once entered, select Done and the fuel analysis process will start (see Figure 62).

We wait the determined time until the analysis is finished. The computer system will give us the result of the gross calorific value. The Gross HOC value is the gross calorific value.

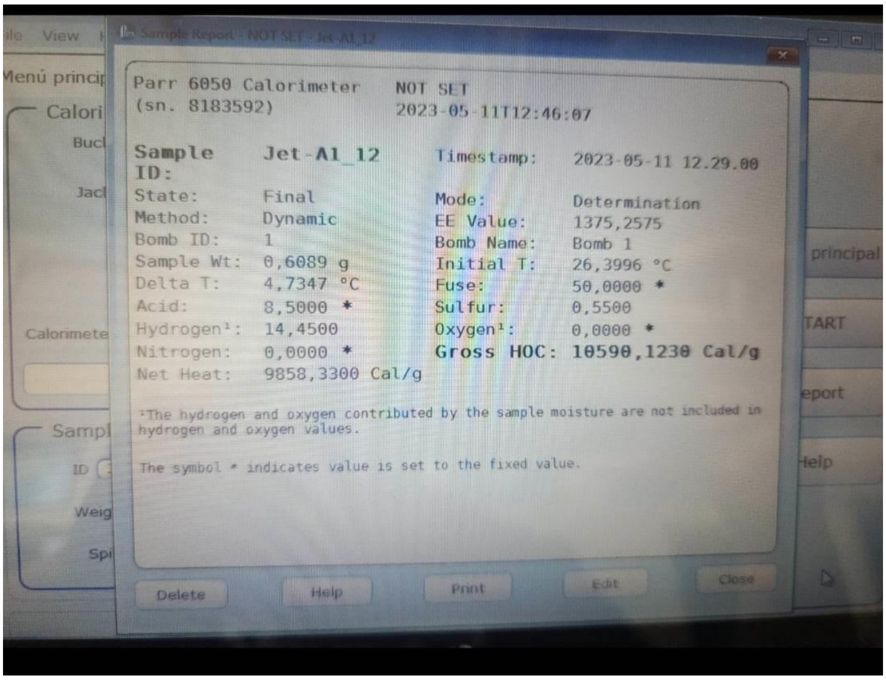

Figure 62: The gross calorific value.

Once the process is finished, we open the cover of the calorimetric pump assembly, disconnect the two electrical terminals and the quick access connector that supplies oxygen. With the support of the oxygen combustion vessel (1110) we remove the assembly (see Figure 63).

We insert the tool through the adapter and apply force to release the pressure.

Figure 63: Placement of the tool and removal of the internal pressure.

Unscrew the screw cap and proceed to separate the cylinder from the head (see Figure 64).

Figure 64: Spacing of the head.

We clean the bowl. After performing the analysis in the combustion process, there are usually some slight traces of carbon deposits (see Figure 65). It is important to clean and dry the humidity of the ignition wire, the interior of the head and the cylinder.

Figure 65: Charcoal resulting after the process.

Finally, the results of this practical test of the gross calorific value of the combination of the 95,5% Jet-A1 + 4,5% Jet cat oil are as follows and which we obtained straight from the calorimetric bomb:

Essay 1:

PCS_1 = 10852,429 Cal/g → 45363,153 kJ/kg

Essay 2:

PCS_2 = 10651,41 Cal/g → 44522,893 kJ/kg

With: 1KCAL= 4,184KJ

Essay 3:

PCS_3 = 10681,165 Cal/g → 44647,269 kJ/kg

So, the final gross calorific value of our combination is:

$$PCS = \frac{45363,153+44522,893+44647,269}{3}$$

$$= 44844,43833 \text{ kJ/kg}$$

To know the value of the lower calorific value, I have used the approximation formula below:

$$PCI = PCS - 5400 * H$$

with:

H: is the value of hydrogen that we took it from the elemental analysis results: H= 0,1445

5400: is a value coming from how much energy is needed to evacuate water from liquid to vapor.

So, for each essay the lower calorific values are:

PCI_1= 45363,153-5400*0,1445= 44582,853 kJ/kg

PCI_2= 44522,893-5400*0,1445= 43742,593 kJ/kg

PCI_3= 44647,269-5400*0,1445= 43866,969 kJ/kg

Which give us: PCI = 44844,43833-5400*0,1445

= 44064,138 kJ/kg

Moving on to the elemental analysis results, which provide useful insights into the composition and relative abundance of various elements within a sample.

The elemental analysis shows the presence and quantification of components such as carbon, hydrogen, nitrogen, oxygen, and several other trace elements through diligent experimentation and advanced analytical procedures.

These findings provide a context for understanding the chemical composition and characteristics of the sample under consideration which led to a better knowledge of matter's fundamental properties and interactions, allowing for advances in a variety of scientific domains ranging from materials science to environmental research.

Here are the elements we'll be testing: Jet A1, Jet Cat Oil, and the Blend (see Figure 66).

Figure 66: Elements of Jet A1, Jet Cat Oil and the blend.

Several samples of the standard are analyzed at the beginning of each session, and spot-check measurements are made at the end of the session. The theoretical values (in green background) relate to the percentage of Nitrogen, Carbon, Hydrogen, and Sulfur data that are semi-quantitative, which is a combination of quantitative and qualitative of the standard used to verify and rectify the equipment's drift on a daily basis. And here attached below, the results used of **Jet A1, Jet Oil and the Blend** (see Table 18), along with an explanation diagram (see Figure 67, 68 and 69):

Name	N %	C %	H %	S %	
J100(pure or net je	0,02	84,70	15,39	0,98	
J100	0,02	85,38	14,99	0,92	
JETOIL(pure or net	0,04	85,09	14,09	0,44	
JETOIL	0,02	85,21	14,09	0,26	
JOIL4-5(The blend	0,03	84,51	13,98	0,56	
JOIL4-5	0,03	84,99	14,16	0,14	
Average values	N %	C %	H %	S %	
J100(the mean valu	0,02	85,04	15,19	0,95	
JETOIL(the mean v	0,03	85,15	14,09	0,35	
JOIL4-5(the mean	0,03	84,75	14,07	0,35	
4.5% BLEND OF JETCAT OIL IN 95.5% JET-A1, CALCULATED FROM PURE COMPONENTS					
	N %	C %	H %	S %	
	0,02	84,98	14,45	0,55	Total=100

Table 18: Elemental analysis results.

The amount of oxygen in this test is zero (O=0) because it is renewable and natural source, so the primary goal is to ensure that all the concentration contents are equal to 100%.

For the Nitrogen: $N = \frac{0,02+0,03+0,03}{3} = 0,02\%$

For the carbon: $C = \frac{85,04+85,15+84,15}{3} = 84,98\%$

For the Hydrogen: $H = \frac{15,19+14,09+14,07}{3} = 14,45\%$

For the Sulfur: $S = \frac{0,95+0,35+0,35}{3} = 0,55\ \%$

Finally, we calculated the mean value from these pure components:

Mean value = 0,02 + 84,98 + 14,45 + 0,55 =100%

Here is a schematic of each test that explains the differences in sulfur properties in two colors: the black curve is a reference that corresponds to the concentration that the equipment already knows, and the red curve is the result of how much sulfur each one has. This first one, is the outcome of the JET-A1 fuel token from the Repsol 200 l drum and which ne named J100.

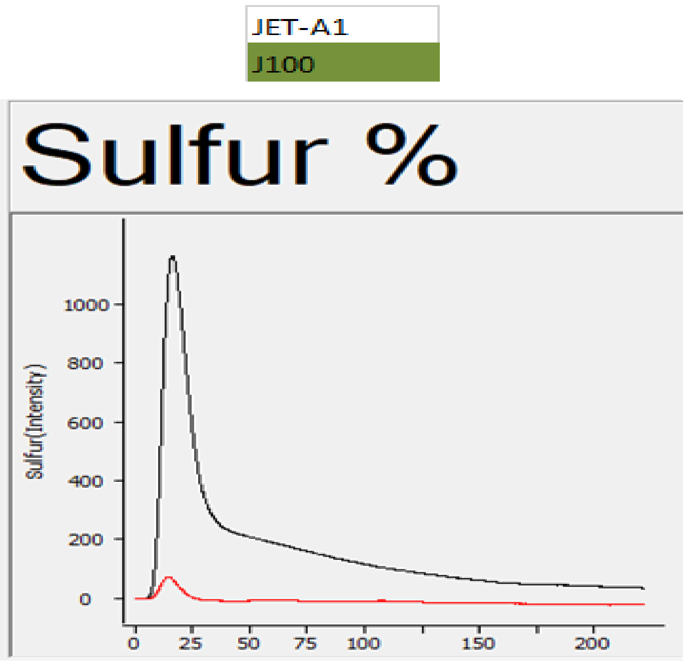

Figure 67: JET-A1 result.

This second, is the outcome of the JETCAT TURBINE OIL, which we referred to as the JETOIL.

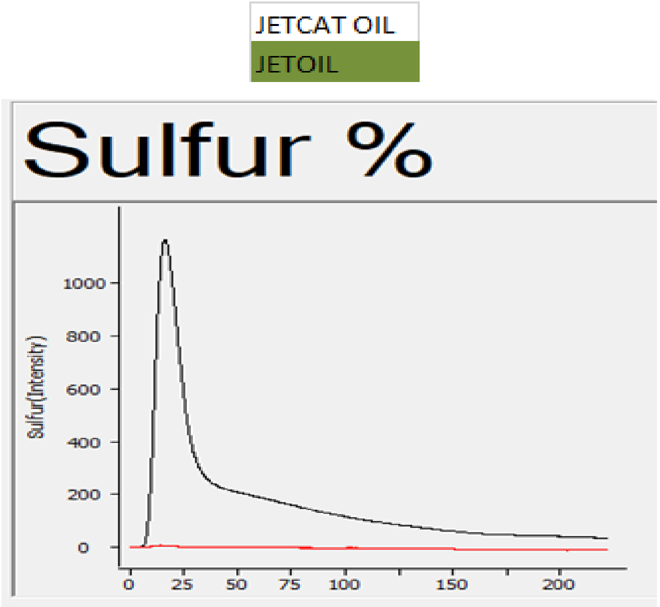

Figure 68: JETCAT TURBINE OIL result.

This final one is the outcome of blending fuel and oil, which we referred to JOIL4-5.

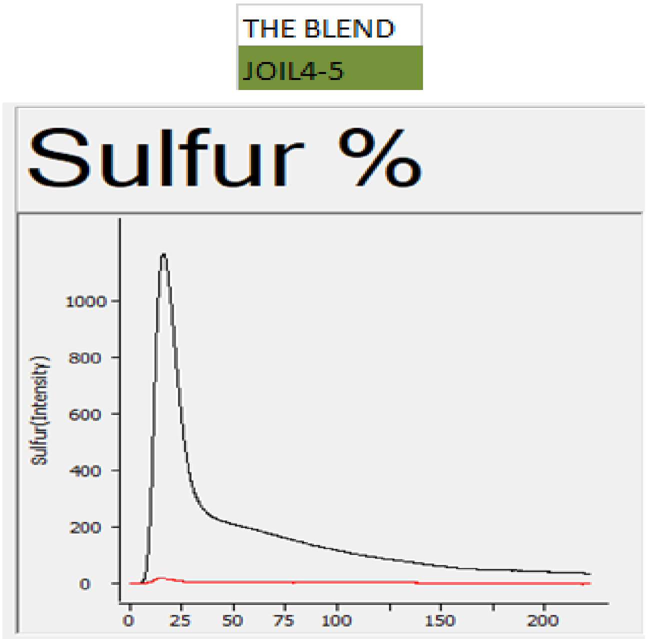

Figure 69: THE BLEND result.

When we estimated the lower calorific value in advance, we utilized this value of hydrogen, H=14,45%, which we obtained from the average values of our fuel combination of the pure JETA1, the net JET CAT oil and the blend of both.

So, we get:

$$H = \frac{15,19+14,09+14,07}{3} = 14,45\% \rightarrow \boxed{H= 0,1445}$$

Going forward to results of density measurements which provide valuable information about the mass per unit volume of the substance, offering insights into its physical properties and behavior of Jet A1, Jet Cat Oil, and the Blend (see Figure 70).

Figure 70: The samples of Jet A1, Jet Cat Oil, and the Blend.

The way of working on the Mettler Toledo D4 density meter's equipment is not complex and is reflected in this essential process. As we previously discussed, it consists of a few basic steps, which are as follows:

- To begin, a tiny amount of the sample is injected into the syringe (see Figure 71) when everything is already in order and clear to get a suitable result.

Figure 71: Injection of the sample into the equipment.

- Next, checking the density meter screen to ensure that the tube inside is completely injected by the sample and that there are no air bubbles could after affect our value results (see Figure 72).

Figure 72: Tube checking.

- The final step is to check out the results on the equipment's screen (see Figure 73) and record them one by one until it reaches the desired level of temperature.

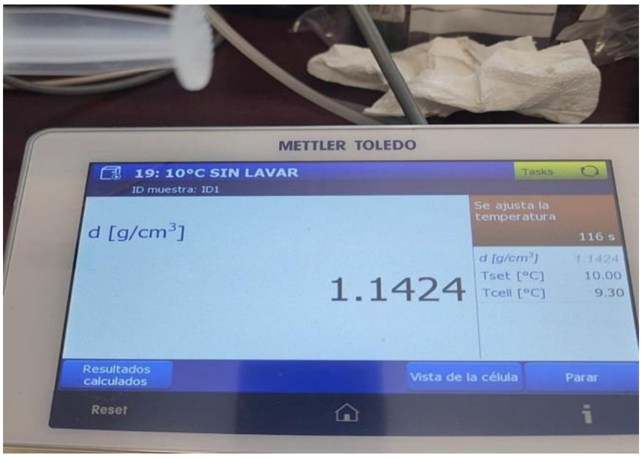

Figure 73: The obtained results.

The density of our sample can be determined through precise measurements and calculations, assisting in the characterization and identification of materials, and changes in density can indicate variations in composition, purity, or the presence of impurities within a sample.

According to the specifications provided by the company that sells us everything, and according to the documentation that they supply, 95.5% of JETA1 must be blended with 4.5% of JETCAL OIL, which is intended for lubrication. So, the results of our equipment are presented below (see Table 19), and we saw that he provides a repeating values of density for each temperature level, and since it demonstrates the changes by number by number.

Turbine sample	Nomenclature
JET-A1 fuel from Repsol 200 l drum	J100
Jetcat turbine oil	JETOIL
JET-A1+4,5%JetCat oil blend	JOIL4,5
Temperature (ºC)	**Density (g/c**
0	0,8061
0	0,8061
0	0,8061
5	0,8025
5	0,8025
5	0,8025
10	0,7988
10	0,7988
10	0,7988
15	0,7951
15	0,7951
15	0,7951
20	0,7914
20	0,7914
20	0,7914
25	0,7877
25	0,7877
25	0,7877
30	0,784
30	0,784
30	0,784
35	0,7803
35	0,7803
35	0,7803
40	0,7766
40	0,7766
40	0,7766
40	0,7729
40	0,7729
40	0,7729
40	0,7692
40	0,7692
40	0,7692
40	0,7654
40	0,7654
40	0,7654
40	0,7617
40	0,7617
40	0,7617
40	0,7579
40	0,7579
40	0,7579
40	0,7541
40	0,7541
40	0,7541
40	0,7504
75	0,7504
75	0,7504

Table 19: The values that are current under the test.

Here is the final table of these results (see Figure 74), linked by a diagram of the values obtained, from which we shall obtain a linear curve indicated by its equation:

Operator	Ilhem
Date	09/05/2023
Mean values	
Temperature	**Density (g/cr**
0	0,8061
5	0,8025
10	0,7988
15	0,7951
20	0,7914
25	0,7877
30	0,784
35	0,7803
40	0,7766
45	0,7729
50	0,7692
55	0,7654
60	0,7617
65	0,7579
70	0,7541
75	0,7504

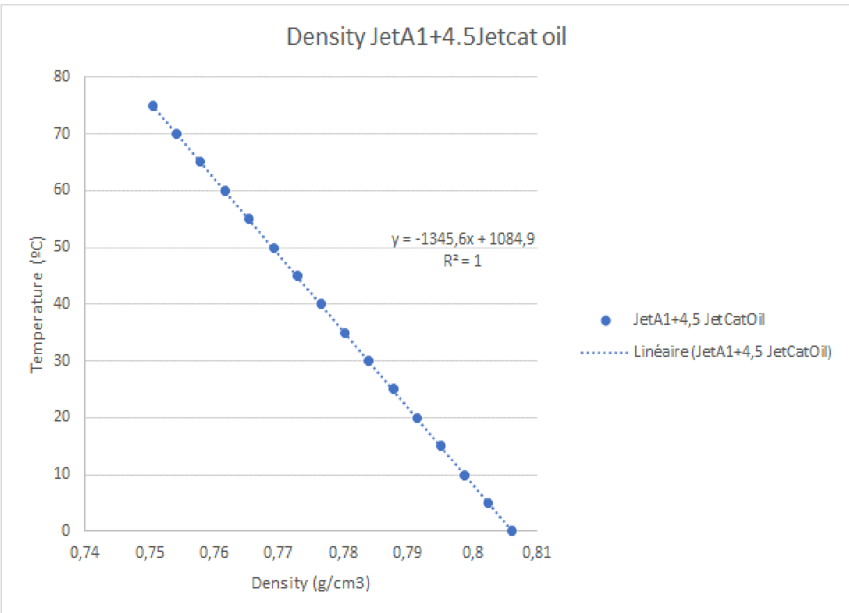

Figure 74: The final results with the impression of the diagram.

We want the density value because the fuel flow in the test equipment was volumetric, but we require mass flow, therefore density is required to convert the total fuel volumetric flow to the total air mass flow.

The fuel volumetric flow find was computed and obtained from a professor who works in the engineering department of thermal machines and motors and is in charge of various calculations and values such as density, thus he provided us the fuel volumetric flow value = 0.876 l/min

From the density table that we obtained; we choose:

$$\rho = 0{,}795\ g/cm^3$$

$$= 795\ g/l \qquad \text{with: } 1\ g/cm^3 = 10^3\ g/l$$

Then, to calculate the mass air flow:

$$MAF = 0{,}876 \times 795 = 696{,}42\ g/min$$

$$= 0{,}011607\ kg/s$$

5. Analysis of the thermodynamic cycle:

The analyzed thermodynamic cycle, a major component in energy conversion processes, demonstrates notable efficiency in harnessing energy. The cycle's efficiency, an essential measure of its performance, corresponds well with theoretical standards.

Throughout the cycle, heat exchanges and work interactions play critical roles in energy transformation. Temperature and pressure fluctuations at critical points signify phase transitions and system behavior.

These findings provide insights into cycle optimization and potential applications across power generation and industrial operations, promoting energy efficiency.

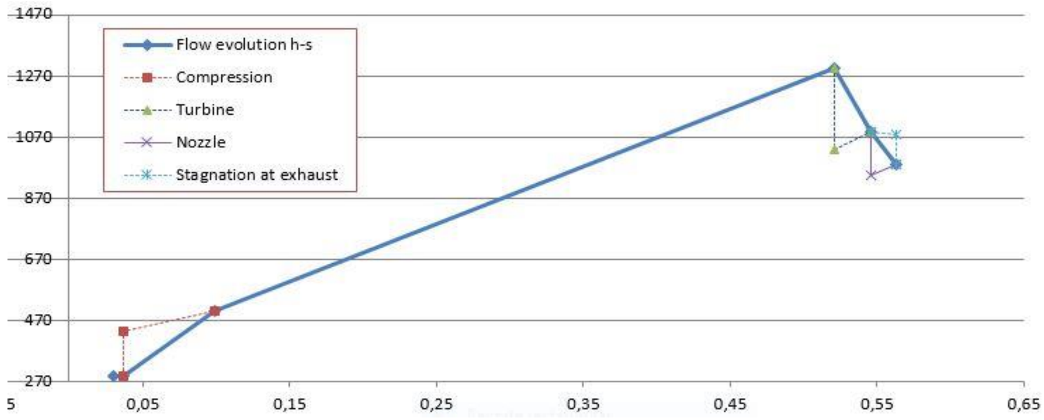

Figure 75: Olympus-HP thermodynamic cycle.

The accompanying diagram visually summarizes the outcomes of our thermodynamic cycle analysis. Through this curve, we explain the complicated interplay of various parameters across the cycle's stages. The graph serves as a full overview of the system's energy transformations, heat exchanges, and work interactions unfold within the system. By examining the trends displayed in the figure (See Figure 75), We may gain significant valuable insights into the cycle's efficiency, performance characteristics, and potential areas for optimization.

This is only a basic understanding of the thermodynamic cycle and to see how it works theoretically, and as previously stated, some of the results were done with an excel sheet where all of the calculations we need are already done and developed by a professor who belongs to the engineering department of thermal machines and motors, and one of these calculations that he made according to the experimental results that I gave him from the test bench, he was able to provide this thermodynamic cycle diagram of our Olympus-HP engine.

From the calculations that we performed, we were able to acquire the essential results that we need to know about the engine, as well as the parameters of the inputs and outputs that we need to accomplish the following part which is the simulation section and precisely through the combustion chamber.

As a result, we achieved the mechanical efficiency of the engine which is:

$$\eta = 0{,}98\%$$

The exhaust gas temperature was:

$$EGT = 502{,}85°C$$

$$= 502{,}85 + 273{,}15 = 776 \text{ k}$$

with: 0 °C + 273,15 = 273,15 K

The ambient pressure:

$$P_a = 0{,}962 \text{ bar}$$

$$= 0{,}962.10^5 \text{ pa}$$

The ambient temperature:

$$T_a = 16,1°C$$

$$= 16,1+273,15 = 289,25 \text{ k}$$

The revolutions of shaft:

$$PRM= 108,5.10^3 \text{ rpm}$$

The engine thrust:

$$T= 22,1\text{kfg}$$

$$=22,1x9,807 =216,58 \text{ N} \qquad \text{with: } 1\text{kgf} =9,807\text{N}$$

The engine pressure ratio:

$$P_R = \frac{P\ outlet}{P\ inlet}$$

$$= \frac{3,475}{3,8737} = 0,897 \text{ bar} =0,897.10^5 \text{ pa}$$

As a result, through the combustion chamber, we achieved the boundary conditions:

- The inputs are:

  C_{inlet}= 45,9m/s

  P_{inlet}(static)= 3,8737 bar =3,8737.10^5 pa

  T_{inlet}(static)= 497,46 bar

- The outputs are:

  C_{outlet}=196,55m/s

  P_{outlet}(static)= 3,475 bar =3,475.10^5 pa

  T_{outlet}(static)= 1234,59 bar

We need the value of the compressor's output during the computation so that we may have the input of the combustion chamber, and to get these values we utilized certain references and a compressor map, as shown at the conclusion of the report (see annex).

All of these results were performed with the engine at 100% load. We chose this load because the full load is always representative as a maximum running, and the LTO cycle has one of his measurement points at 100% load, so we believed it would be the best load to obtain our feeds from.

The interesting points are the points who corresponds to the standard LTO cycle, so these were some geometrical data as the inlet and outlet required through the combustion chamber where are we going to do our numerical study.

Conclusion:

Concluding our experimental results chapter requires a careful synthesis of findings and a clear reflection on the research objectives. This section serves as a culmination of the data analysis and provides meaningful insights derived from the conducted experiments and these data are required as data for the evaluation of the thermodynamic cycle using the excel file.

Further, all results of the experiments performed in the fuel are required in the excel file and in In the next chapter, we will use all of the gathered findings to conduct a simulation analysis of our engine and attempt to compare and analyze the results.

Chapter5: Numerical study

Introduction:

The analyses of the Olympus-HP engine used the computational software ANSYS Fluent to predict and study the flow behavior of the fluid that passes through his shapes in particular, as it passes through the combustion chamber, its response under numerous conditions in the frequency domain.

This chapter provides the implemented analysis interested in the numerical simulation software, with a detailed material assumptions and boundary conditions are described.

1. Geometrical characterization of the jet engine:

1.1. what's a CATIA?

CATIA (an acronym of computer-aided three-dimensional interactive application) (see Figure 76) is a multi-platform software suite for computer-aided design (CAD), computer-aided manufacturing (CAM), computer-aided engineering (CAE), PLM and 3D, developed by the French company Dassault System's [35].

Figure 76: CATIA Logo.

CATIA enables the creation of 3D parts, from 2D sketches, sheet metal, composites, molded, forged or tooling parts up to the definition of mechanical assemblies. In the case of Aerospace engineering an additional module named the aerospace sheet metal design offers the user combine the capabilities of generative sheet metal design and generative surface design [36].

In addition to 3D modeling and assembly design, CATIA offers specialized modules for various engineering tasks. These modules include functionalities such as sheet metal design, electrical and wiring harness design, composites design, finite element analysis (FEA), and more. These tools allow engineers to simulate and analyze product performance, ensuring that designs meet specified requirements and perform optimally [37].

Overall, for our study we are going to use the CATIA V5 version, which is a comprehensive and feature-rich software suite widely used in the industry for product design and development. Its extensive capabilities, from 3D modeling to simulation and manufacturing planning, make it an essential tool for companies aiming to create innovative and high-quality products.

According to our study, we will discuss about the file that we acquired from the manufacture of the Olympus-HP engine parts assembly (see Figure 77), and we can see that he is identifiable with various items such as the support, valves, and fixing screws.

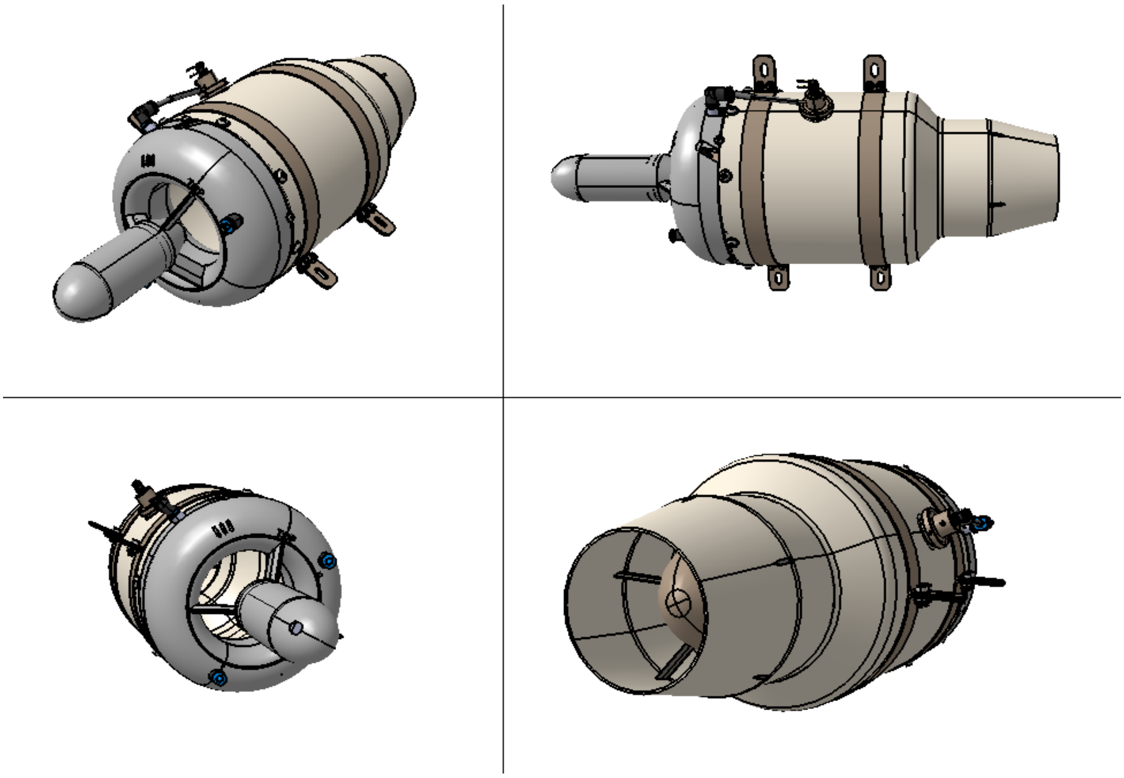

Figure 77: Olympus-HP engine Catia parts assembly.

Moreover, they sent us a cut-out of the engine (see the technical file), so we could see how it appears from the inside and gain how it operates when he is being tested (see Figure 78).

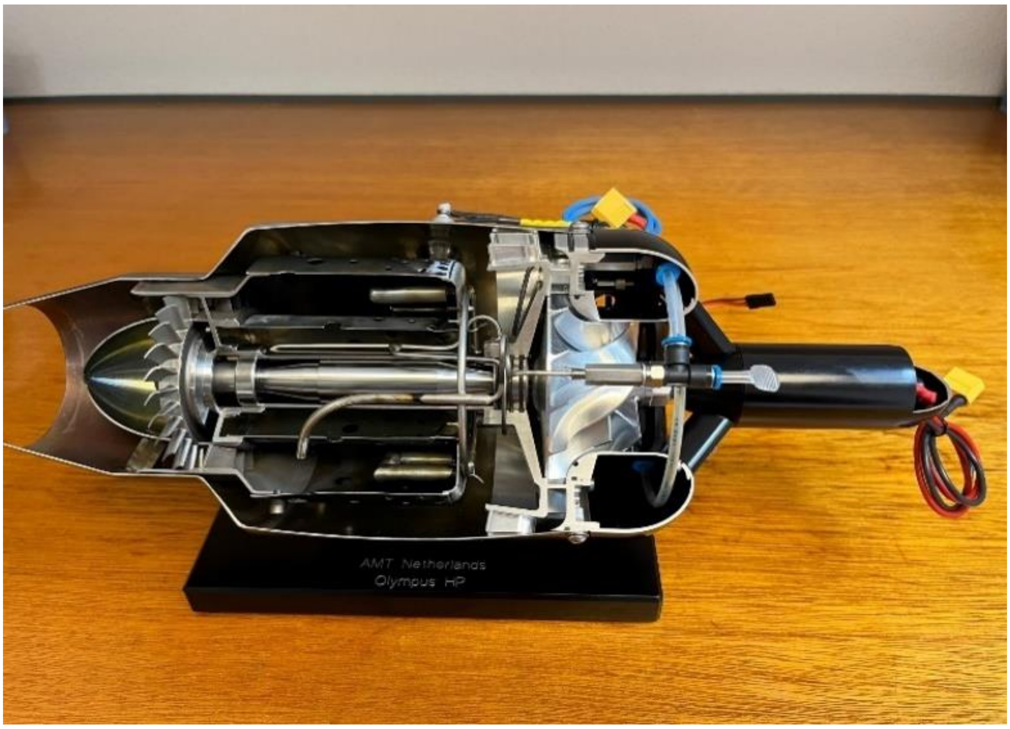

Figure 78: Cut-out of the Olympus-HP.

In my study of the geometrical characterization of this jet engine, I analyzed his various components and their spatial arrangement. The engine begins with the inlet, a large circular opening designed to efficiently capture air. Moving forward, the compressor, shaped as a cylindrical or conical structure, consists of multiple stages comprising rows of stationary and rotating blades. These blades compress the incoming air, preparing it for combustion. The combustion chamber, located after the compressor, is where fuel is mixed with the compressed air. This chamber typically exhibits a cylindrical shape and is designed to withstand high temperatures and pressures.

1.2. Engine scanner:

At the rear of the engine, the exhaust nozzle plays a crucial role in directing the flow of exhaust gases and converting thermal energy into forward thrust. Its geometry can vary, ranging from convergent-divergent shapes to adjustable nozzle designs for optimal performance across different flight regimes. Overall, the geometrical characterization of a jet engine encompasses a combination of circular, cylindrical, and conical shapes, all strategically arranged to ensure efficient air compression, fuel combustion, and propulsion.

As we previously stated, the purpose of this project is to study the behavior of the fluid that flows through this jet engine, particularly when it goes into the combustion chamber. However, other pieces were not included in the file, such as the combustion chamber which is the most important and necessary part in our study.

As a result, I attempted to create these missing elements so that we could examine the variation of the flow inside this engine. In addition, several dimensions were challenging to achieve, particularly in the combustion chamber, which includes many various diameters holes.

To obtain these measurements, I attempted two different methods, the first was by using the EinScan-SP (see Figure 79), which is an advanced desktop 3D scanner capable of capturing the geometry of small to medium-size items in three dimensions.

It is a very specific device consists principally of a scanner head, a timetable, scanner stand, scanner bracket, calibration board, calibration board holder, power cord, power adapter, USB cables, tripod, and reference points.

As we seen in the image below, we tried to set the engine on this scanner in both horizontal and vertical orientations to ensure exact measurements.

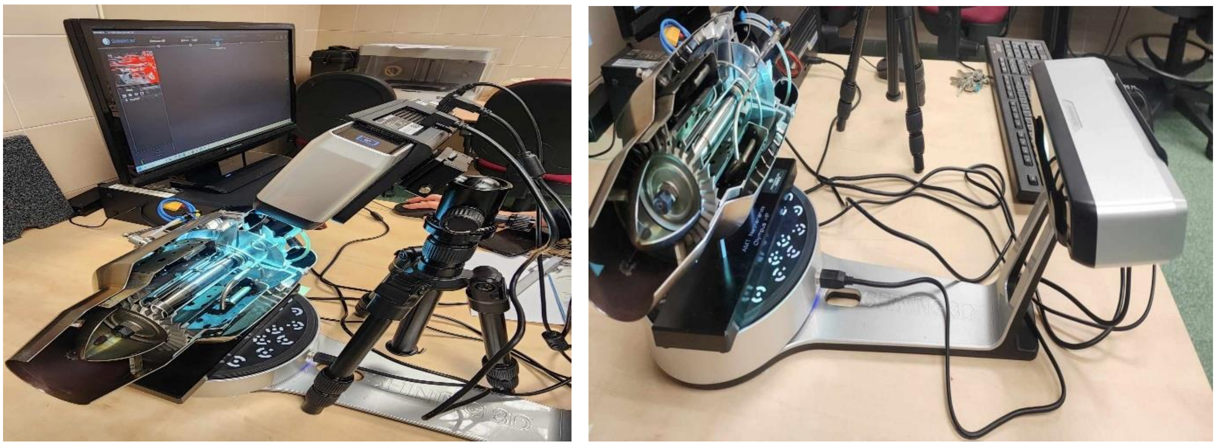

Figure 79: Engine scanner setting.

Nevertheless, even with this scanner, not all measurements were displayed on the software since the turbine was too bright and represented as a reflecting object, making scanning problematic, so estimating for getting these missing dimensions we moved on to the second way of measuring, which is an elementary method based mostly on the printing of the essential part using a paper tape, a sheet of paper and a flexible clay (see Figure 80) which is a special air-drying clay that is easy to use and mold while remaining flexible and no crack when it dries.

It's, great for sculpting delicate details, which is why we used it specifically on the combustion chamber to achieve the same hole shapes.

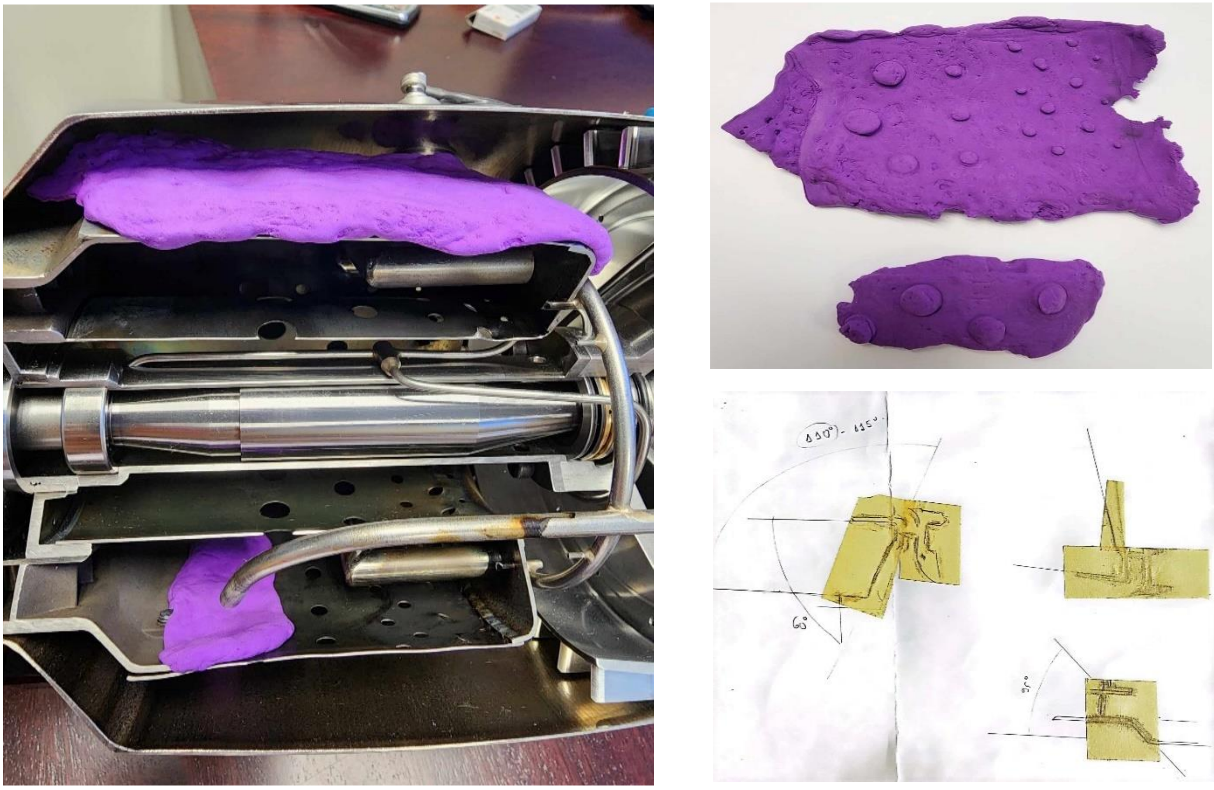

Figure 80: Obtained dimensions.

As we said in the previous chapter, digital software can simulate the problem to give an adequate solution close to reality.

In this part, I draw a real model of the combustion chamber system under study related to the center tube where the combustion chamber is attached as well as the exterior engine structure (see the technical file), using the features of CATIA V5 software producing 3D models with accurate dimensions and specific details that we previously achieved.

Here is my assembly concept depicted below, and it is complemented with a cut figure (see Figure 81).

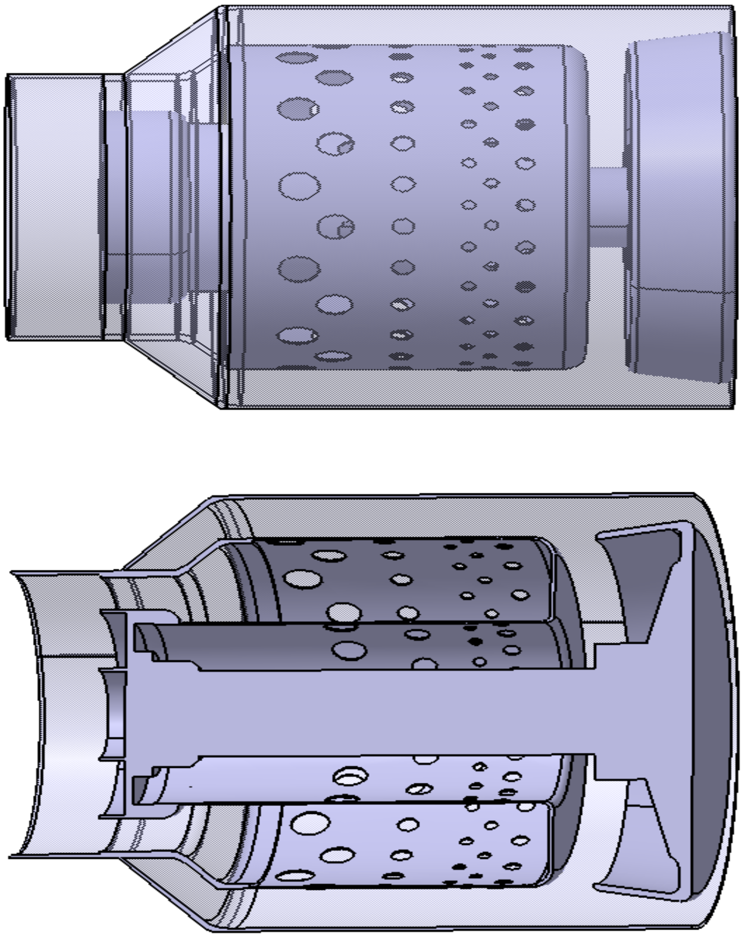

Figure 82: The additional engine parts comes with a cut-out design.

To develop relations between these three parts, I used parametric modeling approaches, which are assembly design tools that allow for the simulation of part interactions and flow, and this is exactly what we searching for in the next part to have the capability of getting a numerical simulation of the flow through the combustion chamber.

2. Numerical simulation of the flow through the combustion chamber:

2.1. Numerical Modeling:

a. Computational Fluid Dynamics Definition:

Computational fluid dynamics (CFD) is a branch of fluid mechanics that uses numerical analysis and data structures to analyze and solve problems that involve fluid flows [38]. Computers are used to perform the calculations required to simulate the free-stream flow of the fluid, and the interaction of the fluid (liquids and gases) with surfaces defined by boundary conditions. With high-speed supercomputers, better solutions can be achieved, and are often required to solve the largest and most complex problems [39].

CFD finds applications in various fields, including aerospace, which is used to optimize designs, improve efficiency, and understand complex fluid phenomena that may be difficult or expensive to study experimentally.

b. Computational Fluid Dynamics Principle of Operation:

The increase in computer speed and memory availability made is possible to obtain solutions to many flow problems.

A variety of reasons can be mentioned for the increased importance of CFD simulation techniques in recent years:

- The need to forecast performance
- The wish to prevent costly or impossible experiments
- The desire for increased insight

There are essentially three elements to every CFD simulation process:

- pre-processing
- Numerical solving
- post-processing

Before beginning to define these elements, let us present the software, ANSYS, used to make all the computations.

2.2. Description of ANSYS Software:

ANSYS CFD simulation software (see Figure 83) is one of the most used commercial programs in the industries, to calculate the aerodynamics characteristics of aircraft and many other fluid mechanics and dynamics problems of a comprehensive suite of products that allows us to predict, with confidence, the impact of fluid flows on our product throughout design and manufacturing as well as during end-use [40]. It can be used to solve laminar or turbulent cases, using different turbulence models.

The main problems that the user can face are the limited element number for the memory needed when the computation is too large and the mesh requires too many elements that the standard computer cannot satisfy.

Figure 83: Ansys Logo.

2.3. Pre-Processing:

This is the first step in building and analyzing a flow model. It includes building the model within a computer aided design (CAD) package (the domain), creating and applying a suitable

computational mesh or grid, selection of fluid properties and phenomena that need to be modelled and entering the flow boundary conditions. The accuracy of the solution is defined by the number of cells in the grid (mesh). The larger the number of cells the better the accuracy

but also, the higher the necessary amount of calculation time [41]. Optimal grids are therefore non uniform: finer at points of interest of in situations where large variations are expected There are large numbers of commercial CAD packages for creating complex 3D geometries.

a. Geometry Generation:

The first step of the CFD modelling process is to define the geometry of the problem to be solved which generally comes from a CAD model or a simplified representation. The geometry can be included in a computational domain.

The computational domain is the portion of space where the solution is required [42]. In external flow problems, the computational domain is typically a volume around the geometry of interest which should have adequate dimensions.

b. Mesh Generation:

Mesh generation (see Figure 84) is the practice of creating a mesh, a subdivision of a continuous geometric space into discrete geometric and topological cells. Often these cells form a simplicial complex. Usually, the cells partition the geometric input domain. Mesh cells are used as discrete local approximations of the larger domain. Meshes are created by computer algorithms, often with human guidance through a GUI, depending on the complexity of the domain and the type of mesh desired. The goal is to create a mesh that accurately captures the input domain geometry, with high-quality (well-shaped) cells, and without so many cells as to make subsequent calculations intractable [43]. The mesh should also be fine (have small elements) in areas that are important for the subsequent calculations.

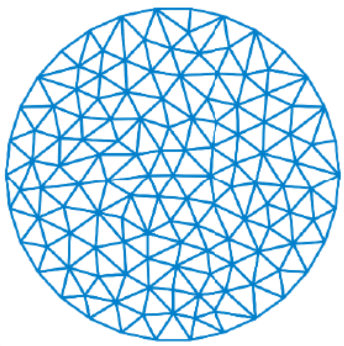

Figure 84: Example of Mesh.

A mesh size is defined by:

- His landmark;
- Points the constituent, characterized by their co-ordinates;
- Cells, constituting polytopes linking up n of these points;

And is possible be notably characterized by:

- His dimension: typically, 2D or 3D.
- Her volume (covered complete dimension).
- His delicacy: surface or medium volume of cells composing mesh size.
- The geometry of cells: triangles, quadrilaterals (parallelograms, rectangles, squares). polygons, tetrahedrons, prisms, hexahedra (parallelepipeds, cubes), polyhedrons.
- The degree of the element: it is the degree of the polynomial serving for describing sides or bones of elements, an element of degree 1 has sides or straight bones; in the case of the finished elements, it is also the degree of polynomials of interpolation.

c. Boundary Conditions:

In order to obtain a solution of the flow, a boundary condition must be assigned to the surfaces representing the computational domain and the geometry and an initial value must be assigned to the flow variables (velocity, pressure, etc.) in each mesh cell. The initial and boundary conditions are mathematical representations of the actual flow conditions present in real problem.

d. Numerical Solving:

The CFD solver does the flow calculations and produces the results by solving the discretized form of governing equation. This stage needs clear understanding of flow physics involved in the problem like phenomena related with heat transfer, mass transfer, multispecies flow, multiphase flow, reacting flow, turbulence, radiation, etc. In most of the commercial CFD packages there are different options regarding the numerical methods can be used to solve the governing equations. The final solution is achieved with an iterative process and several iterations (see Figure 79) are generally required to converge the system of equations. The solution starts from the initial conditions and evolves based on the boundary conditions, iteration by iteration.

2.4. Post-Processing:

Once the simulation is completed, the CFD solution consists of knowing the values of the flow variables, like velocity and pressure, in every node of the computational grid. The raw numbers can be difficult to interpret, therefore these results are generally post-processed to obtain integral quantities, graphs and plots that the user can easily interpret and compare.

The goal of post-processing is to make the data and flow structures interpretation intuitive for the final user [44]. The values are usually presented in a graphical form with colors varying according to user's defined settings.

3. ANSYS Analysis:

In my current analysis, I will be focusing on the combustion chamber of our Olympus jet engine, which I have already designed it on Catia (see Figure 85) which is of a micro jet engine developed by AMT Netherlands [45], a vital component where the combustion of fuel takes place. It is designed specifically for small-scale engines, which is typically compact and lightweight, optimized for efficient fuel combustion within limited space constraints.

It consists of a cylindrical or annular chamber with precise geometries and holes to promote the mixing of fuel and air, creating an ideal environment for combustion.

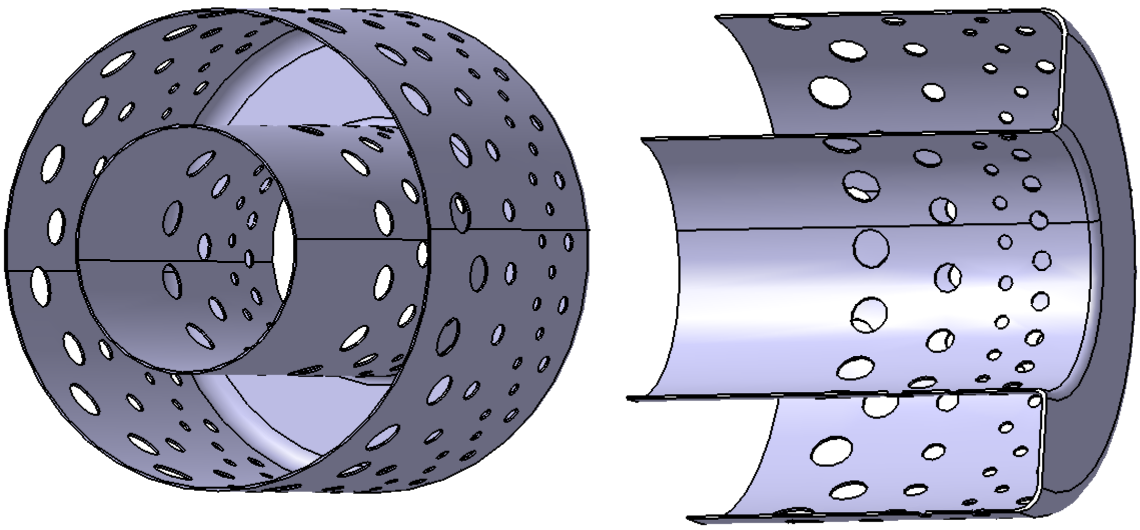

Figure 85: The Combustion Chamber accompanied with a cut-out design.

The simulation was running for a lot of days, and statistical measurements including average reaction time, throughput, and utilization of resources were recorded at regular intervals to evaluate system performance.

The ensuing figures provide a graphic representation of the results that our ANSYS simulation generated. These serval graphics represent the detailed behavior of the combustion chamber system under, transforming numerical data into an understandable manner. Each graphic explains a different aspect of the analysis, such as vectors, contours and pressures.

These below not only help us understand how the system responds when the fuel goes through the combustion chamber, but they also serve as a foundation for future research. We may discover patterns, anomalies, and important spots by diving into the data, which affect our interpretation of the simulation findings and drive future decision-making and design considerations.

As a first step, and as previously explained in the Ansys fluent procedures, we imported the Catia geometry into the Ansys CFD after changing the plan simulation scale, right after we did the Mesh generation and we used tetrahedron as a mesh type because it offers advantages in capturing complex geometries and intricate flow behaviors, then we completed the boundary conditions choosing aluminum as the material type for our parts because it is commonly utilized in aviation jet engines, and finally we concluded the simulation results.

3.1. Geometry:

These geometries serve as the digital counterparts of the physical structure of the combustion chamber system under study related to the center tube where the combustion chamber is attached as well as the exterior engine structure, enabling us to virtually interact with and analyze the behavior of the object in a controlled environment. The coordinates of these parts were imported and introduced to ANSYS from the Catia software.

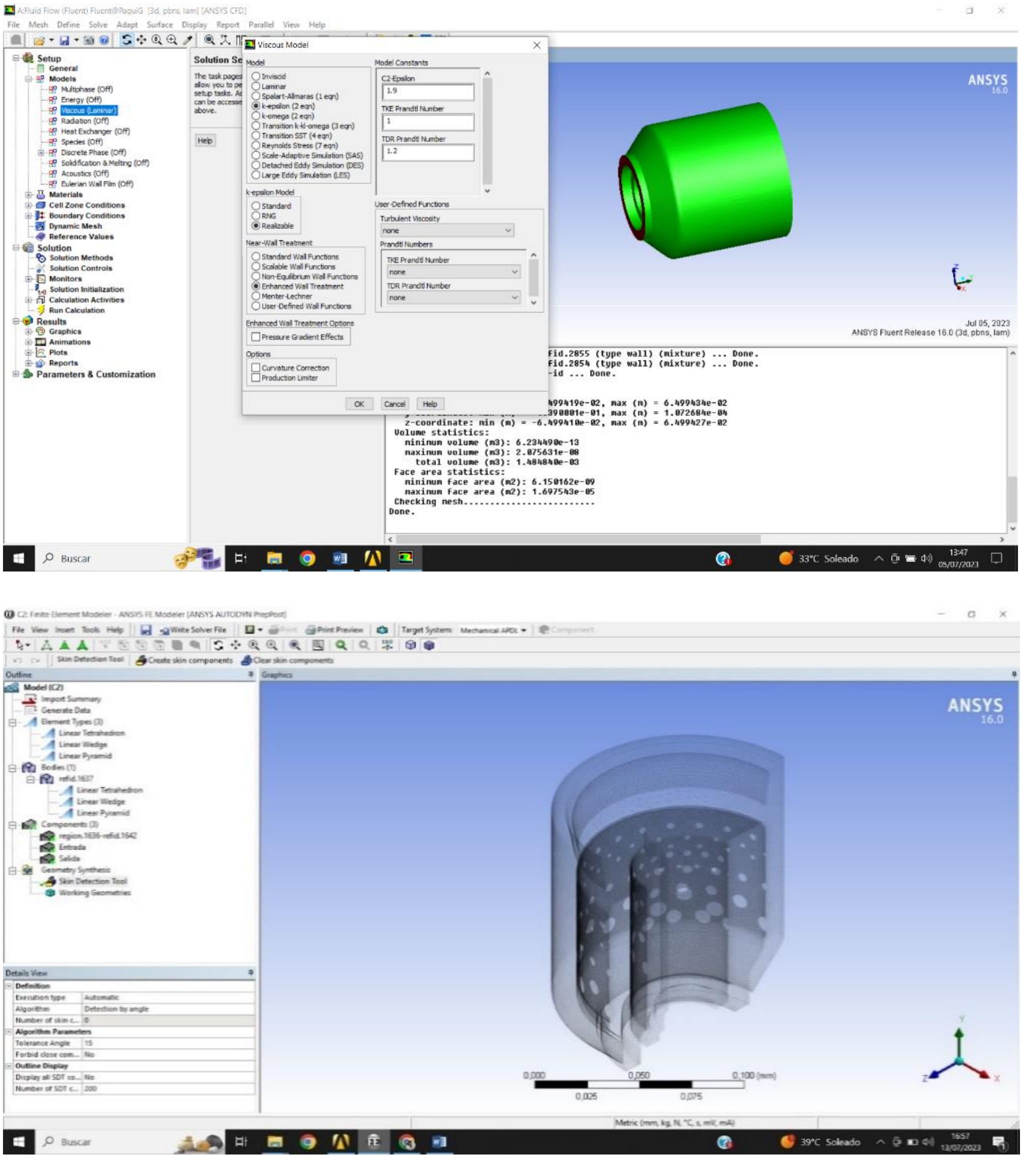

Figure 86: Combustion chamber geometry.

3.2. Mesh:

An unstructured mesh is used for the computational domain thanks to its elements flexibility in total frame capturing. As a consequence, we used mesh refinement approaches, also known as mesh controls, to improve precision in obtaining high fidelity and accuracy results.

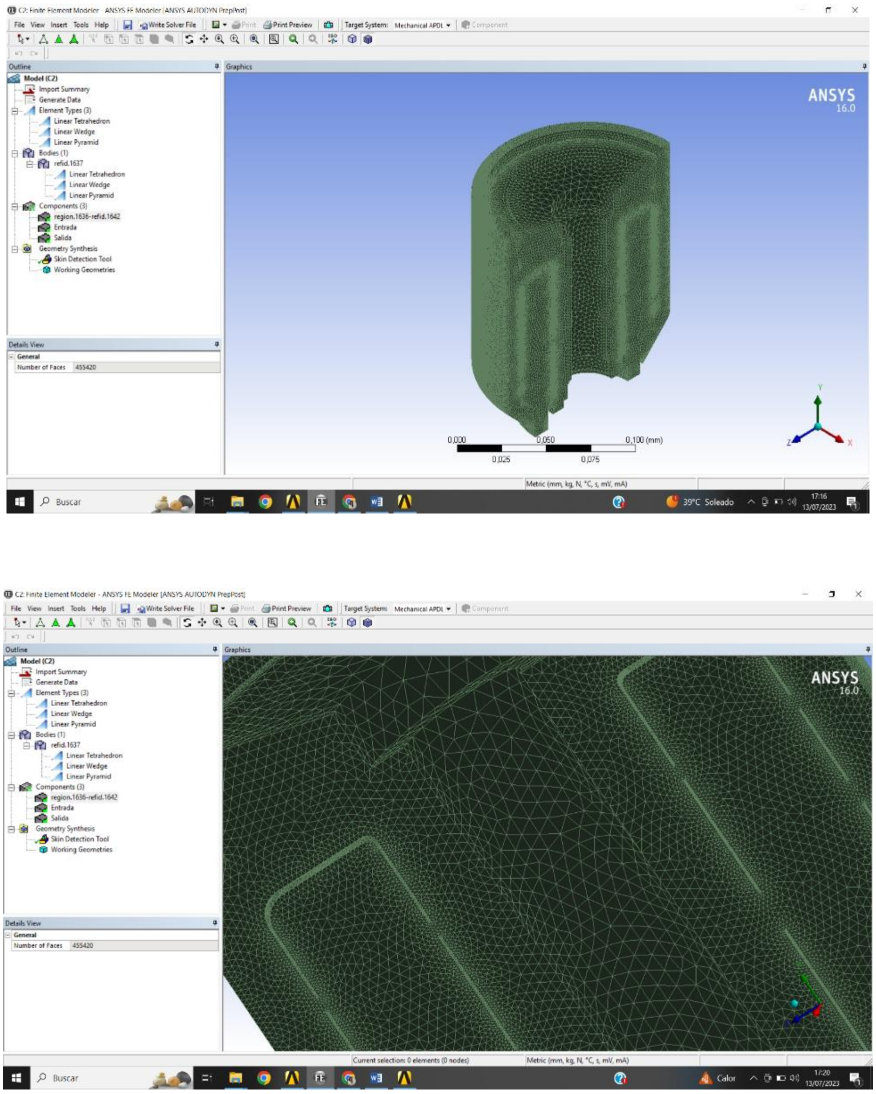

Figure 87: Combustion chamber Mesh.

We decided on a tetrahedron. Because we have a mesh issue and multiple curvatures in our combustion chamber, we can only utilize a tetrahedron mesh type in this situation because it is a crucial requirement to be more responsive to fluctuations and for obtaining precise outcomes and converging near to real-world conditions.

3.3. Boundary conditions:

The boundary conditions setting is the same used in experimentation based on the industry documentary test conditions (see Tables 20 and 21).

Fluid	**Properties**
Air	Density = 1,254kg/m3
	Viscosity= 1,7894 e-0.5(kg/ms)

Table 20: 2D Fluid characteristics.

Boundary	**Type**	**Properties**
Inlet	Velocity	u= 45,9 (m/s)
	Static pressure	Ps= 387370 pa
Outlet	Static pressure	Ps= 347500 pa

Table 21: 2D Boundary conditions features.

It was necessary to calculate the hydraulic diameter which is a characteristic length used in fluid mechanics to quantify the effective cross-sectional area through which a fluid flows in a non-circular conduit or channel, it is particularly useful when we dealing with the flow resistance and fluid dynamics, that’s why we calculated it using the formula below:

$D_h = \frac{4A}{P}$ with: Dh = hydraulic diameter (m)

A = area section of the duct or pipe (m^2)

p = "wetted" perimeter of the cylinder (m)

For the Inlet combustion chamber cylinders, we have:

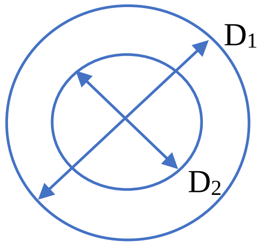

$D_1 = 2 \times 65 = 130mm \rightarrow 0{,}13m$

$D_2 = 2 \times 57{,}64 = 115{,}3mm \rightarrow 0{,}1153m$

For: $A_{in} = \frac{\pi}{4}(D_1^2 - D_2^2)$

$= 0{,}00288\ m^2$

And for: $P_{in} = \pi \times (D_1 + D_2)$

$= 0{,}77m$

Then we will find that: $Dh_{Inlet} = 0{,}015m$

Now, we doing the same approach for the Outlet combustion chamber cylinders, we have:

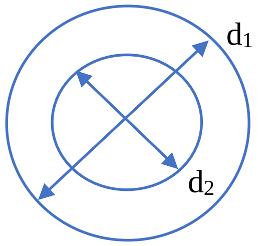

$d_1 = 2 \times 52{,}5 = 105mm \rightarrow 0{,}105m$

$d_2 = 2 \times 31{,}6 = 632mm \rightarrow 0{,}0632m$

For: $A_{out} = \frac{\pi}{4}(d_1^2 - d_2^2)$

$= 0{,}0055\ m^2$

And for: $P_{out} = \pi \times (d_1 + d_2)$

$= 0{,}53m$

Then we will find that: $Dh_{Outlet} = 0{,}042m$

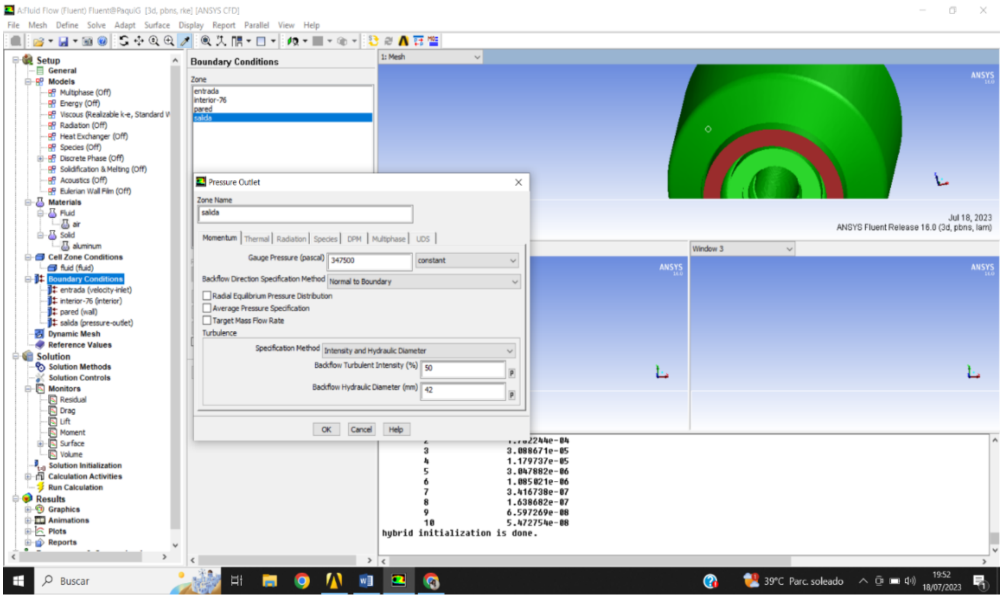

Figure 88: Outlet diameter.

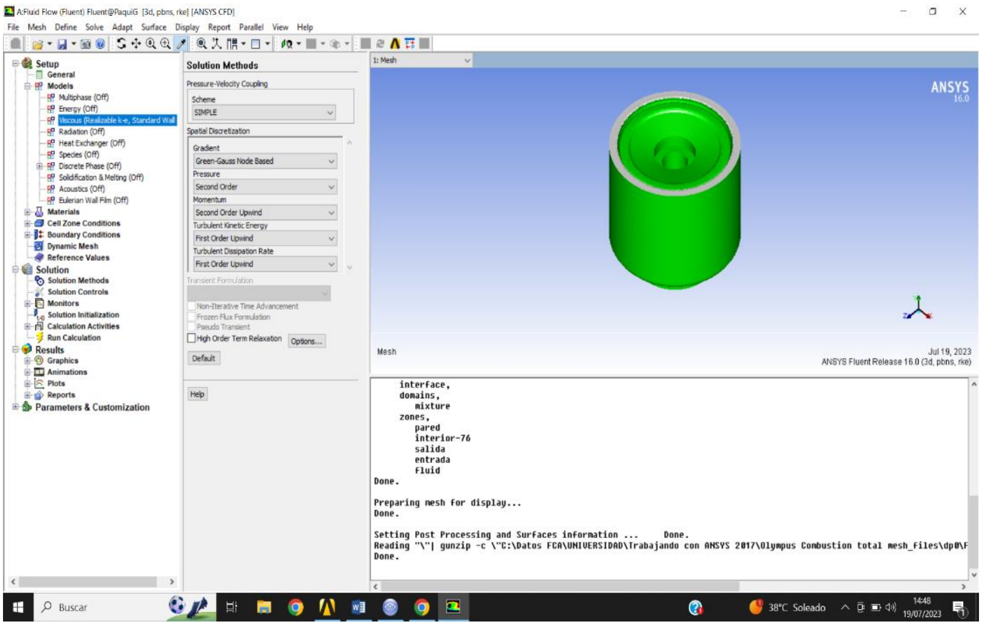

Figure 89: Inlet diameter.

Also, we get the rate of the air mass flow as well:

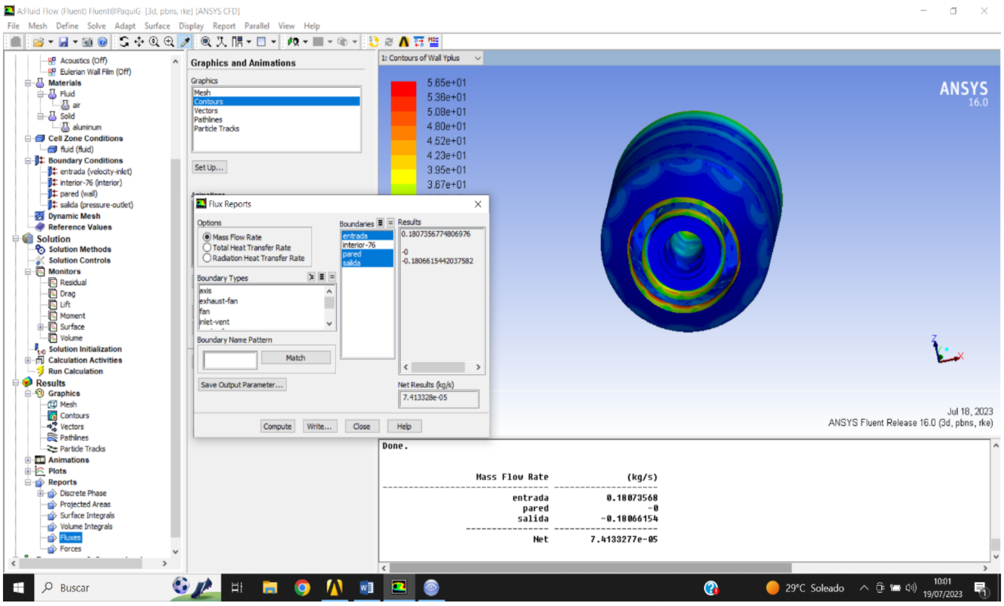

Figure 90: Air mass flow rate.

MAF_{int}= 0,180735kg/s

MAF_{out}=-0,180661 kg/s

these two values, gives us as a net air mass flow:

MAF_{net}= $7{,}413327^{-05} = 4{,}46616.10^{-5}$kg/s

This is the simulation process's residuals; the crucial thing about these residuals is that they are decreasing

The first 11 iterations:

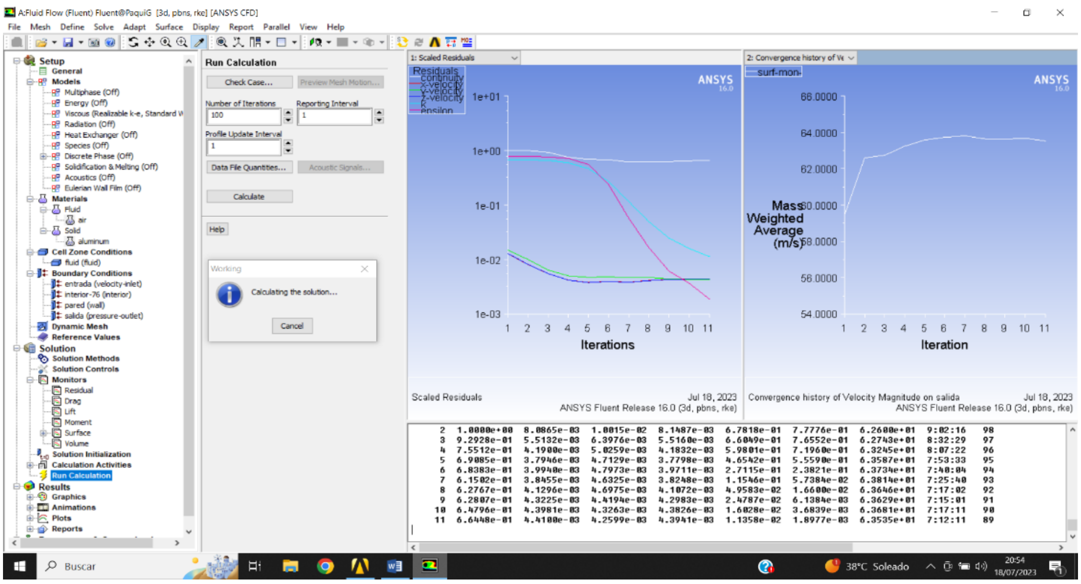

Figure 91: Run calculation of the 11 iterations.

This until 24 iterations:

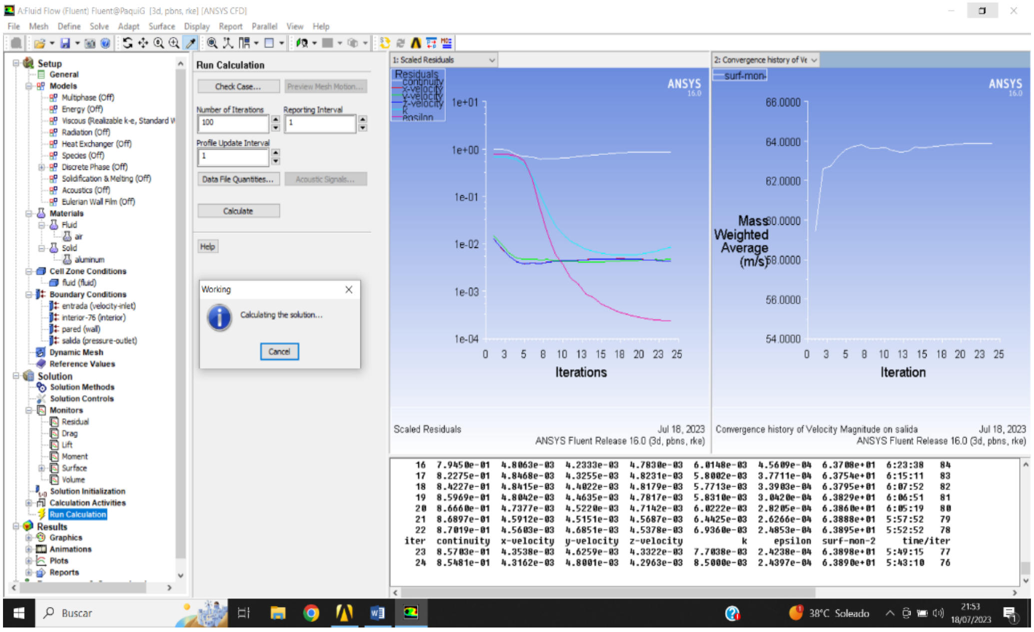

Figure 92: Run calculation of the 24 iterations.

This is until 47 iterations:

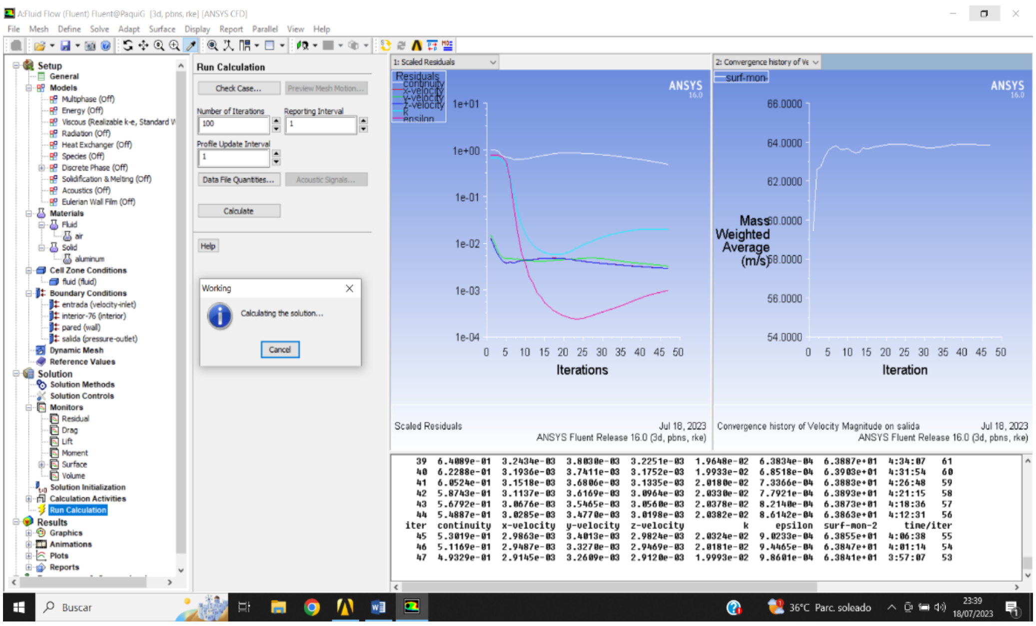

Figure 93: Run calculation of the 47 iterations.

This is until 100 iterations:

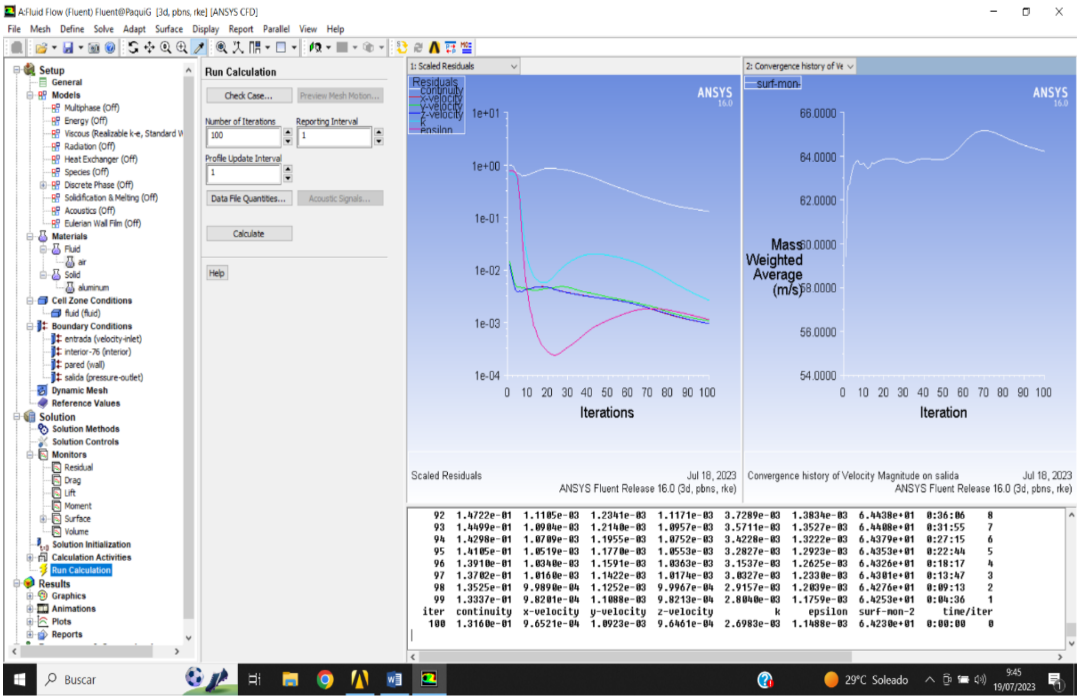

Figure 94: Run calculation of the 100 iterations.

this residual curve represents the variation of the speed according to number of iterations one notices the court passes by an unstable zone or a transitory zone then it converges towards a stable value around:

$$C_{num} = \sqrt{Xx^2 + Yy^2 + Zz^2}$$

$$= \sqrt{(9{,}6521^{-04})^2 + (1{,}0923^{-03})^2 + (9{,}6461^{-04})^2}$$

$$= 0{,}9767 \text{ m/s} \simeq 1 \text{ m/s}$$

We got 100 iterations, each of them took 5 minutes, and 12 of them took 1 hour, so we waited 8 hours in all, we wanted to include density variation, but if each iteration takes 5 minutes and the program takes into account the energy equation, each iteration will most likely take more than 10 minutes, which is a significant amount of time, so this is just a first simulation impression of which is the better way to learn about something inside the combustion chamber without the energy equation and density variation.

3.4. Pressure contours results of the combustion chamber:

The pressure contours variations are shown in these figures below:

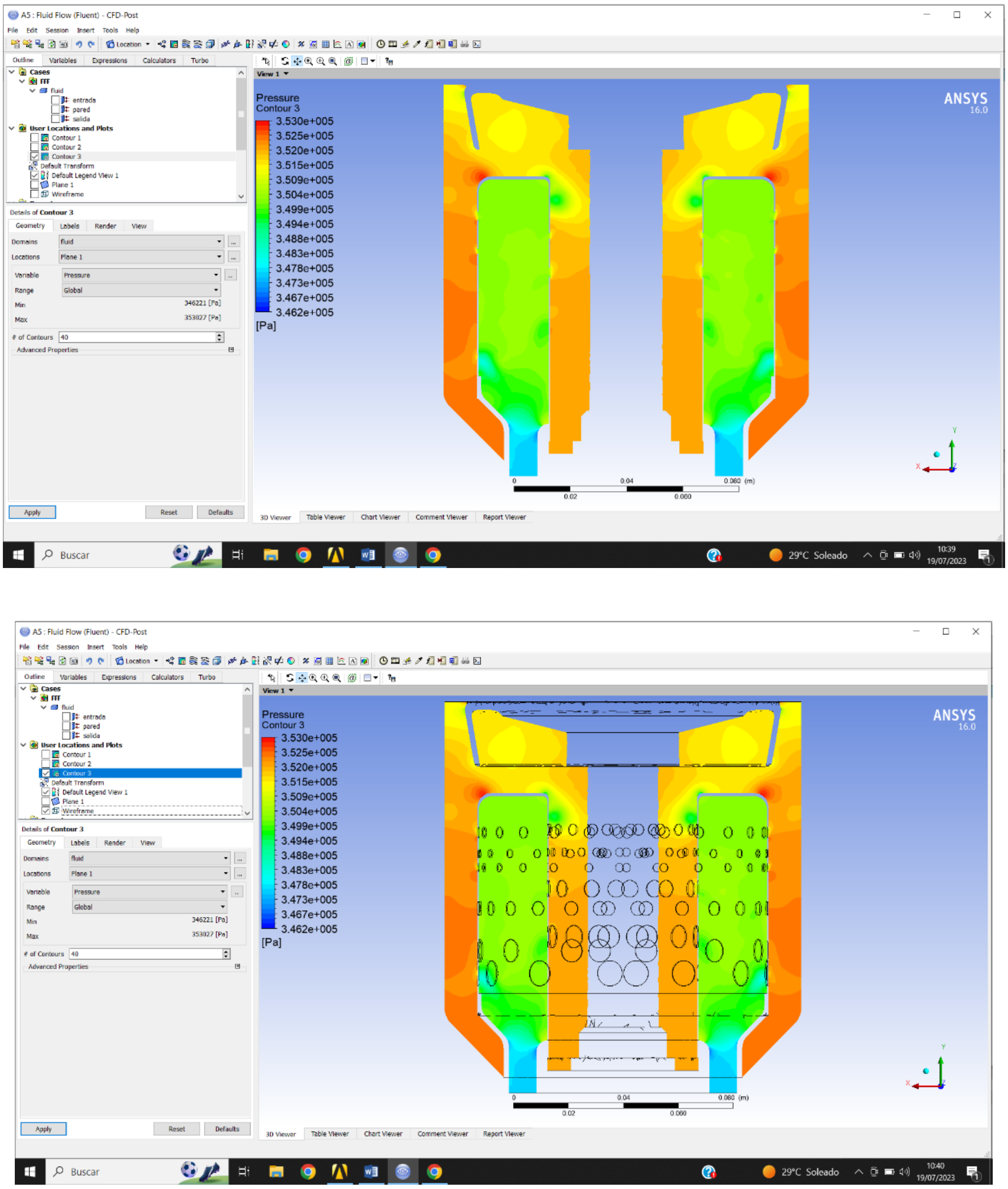

Figure 95: Pressure contour 3.

Colors on pressure contour plots in fluid simulations show the distribution of pressure values over the studied domain. Higher pressures are often represented by warm colors like red and orange, whereas lower pressures are represented by cooler colors like blue and green. This color mapping help in the identification of pressure variations, high- and low-pressure zones, and flow behavior.

To ensure the symmetry of the combustion chamber and the symmetry of the outcomes, we worked on the complete section, not just half of it, and to decrease the execution time, we can work on a quarter of our combustion chamber.

This speed data does not validate the boundary conditions established in the experimental section, and we have two red dots at the end of the combustion chamber, which is the most important zone where the speed is highest.

Also, at the level of the pressure we got:

We have as:

Maximum Pressure: P_{max}= 3,53027e^{+005}pa

Minimum Pressure: P_{min}= 3,46221^{e+005}pa

Then, we can calculate the average value of the pressure:

$$P_{num}= \frac{353027+346221}{2} = 3{,}49624.10^{5} \text{ pa}$$

And we had already got the pressure experimentally from the test and we found:

$$P_{exp} = 2{,}708.10^{5} \text{ pa}$$

So, to compare these two obtained values, we got:

$$P_{num} > P_{exp}$$

Thus, we must compute here the error estimation calculation which assessing the accuracy of numerical simulations by comparing the simulated results to known reference values or analytical solutions. This procedure aids in quantifying the difference between our simulated and experimental results.

Our error estimate is as follows:

$$\varepsilon = \left| \frac{\text{Exprimental value} - \text{Refrence value}}{\text{Exprimental value}} \right| \text{ x } 100\%$$

$$= \left| \frac{270800 - 349624}{270800} \right| = \left| -0{,}291 \right| = 0{,}291$$

$$0{,}291 \times 100 = 29{,}1\% \quad \Longrightarrow \varepsilon \simeq 29\%$$

We did not do digital testing on the actual chemical reaction of our fluid and instead utilized air as a reference, thus this error is just computed to give the appearance that we did.

3.5. Velocity contours and streamlines results:

The visualization of velocity contours and streamlines findings in ANSYS provides a clear representation of fluid flow dynamics. Velocity contours use a color spectrum to show various flow speeds, providing an instant comprehension of locations with quick or slow movement:

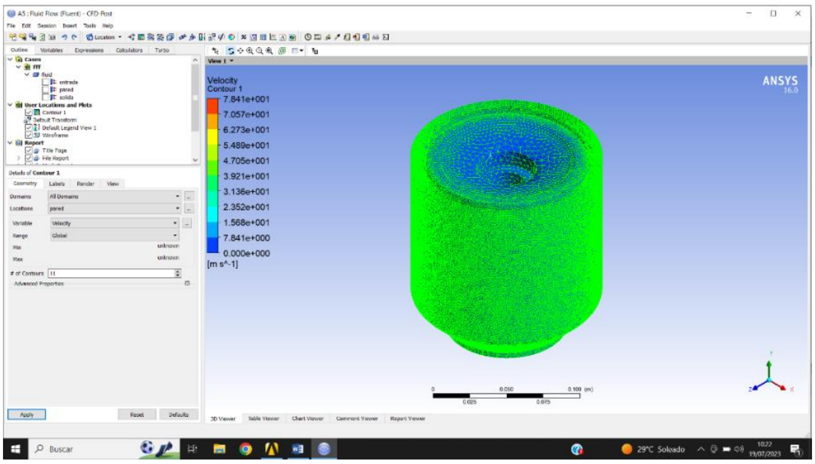

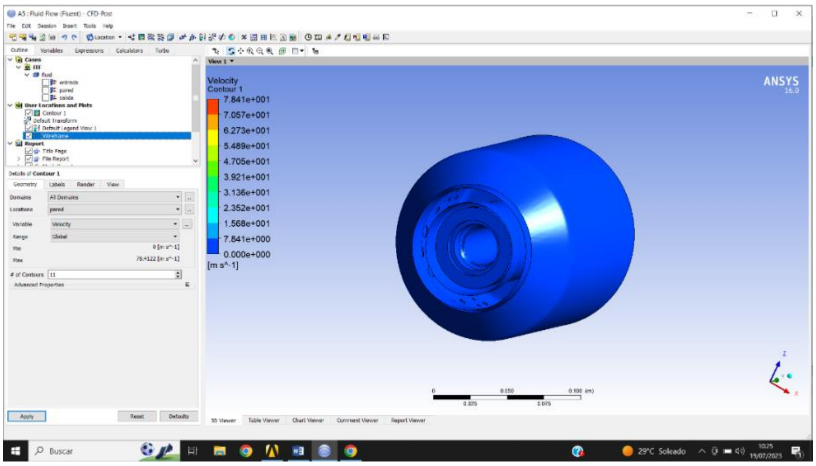

Figure 96: Velocity contours.

In addition, streamlines display fluid trajectories, detailing the pathways that particles travel inside the flow. This combined representation reveals crucial insights into the direction, turbulence, and circulation patterns of the flow, enabling an extensive knowledge of fluid dynamics within the simulated system.

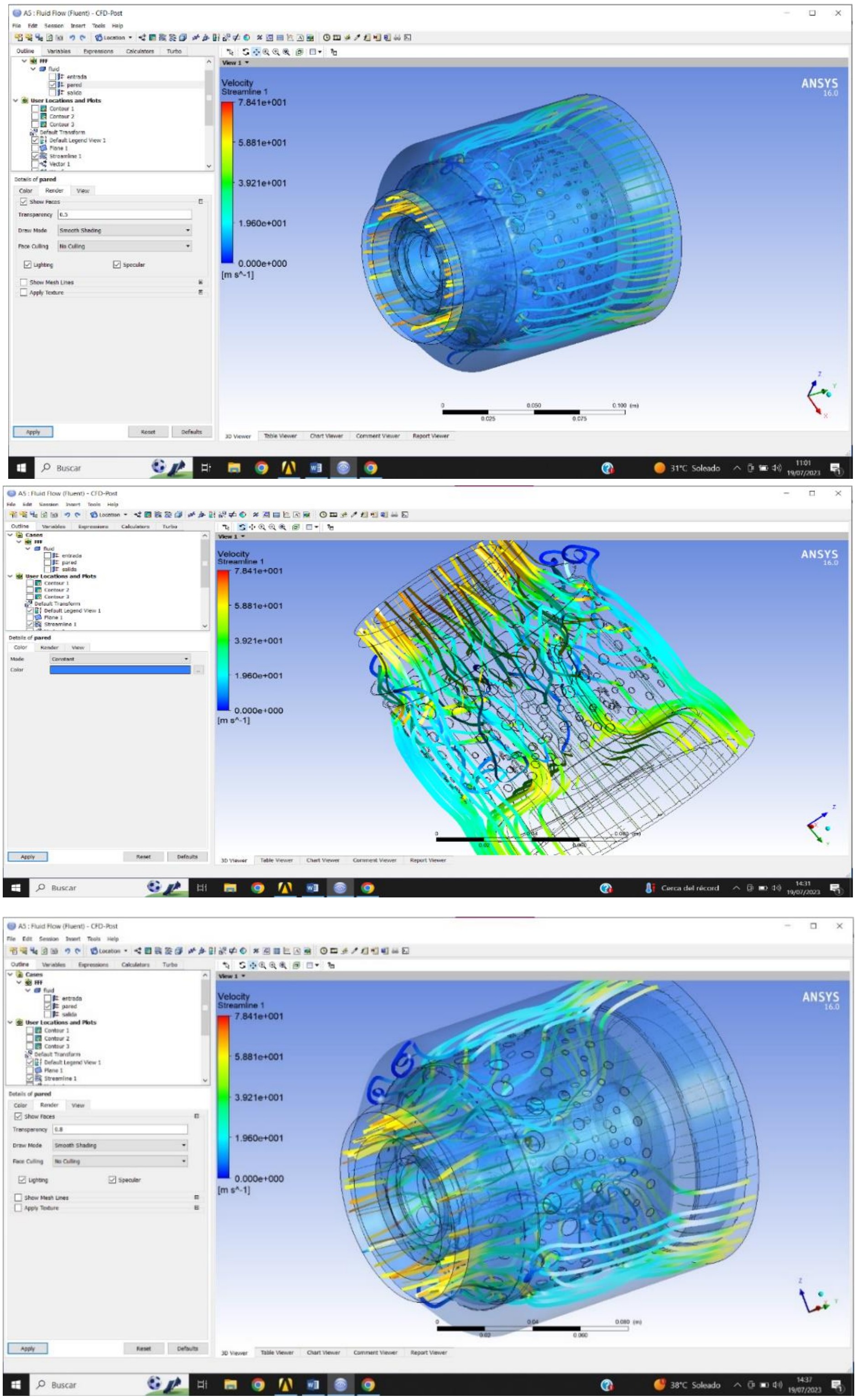

Figure 97: streamlines results.

We have some turbulences that refers to the intricate, chaotic motion of air molecules caused by complex interactions of flow. Turbulence significantly impacts fluid behavior, affecting parameters like pressure, velocity, and temperature.

This approach provides an instant understanding of important flow directions, areas of convergence or divergence, and possible locations of interest for further analysis. The visualization of velocity vectors improves knowledge about fluid dynamics, assisting in design optimization and decision-making processes:

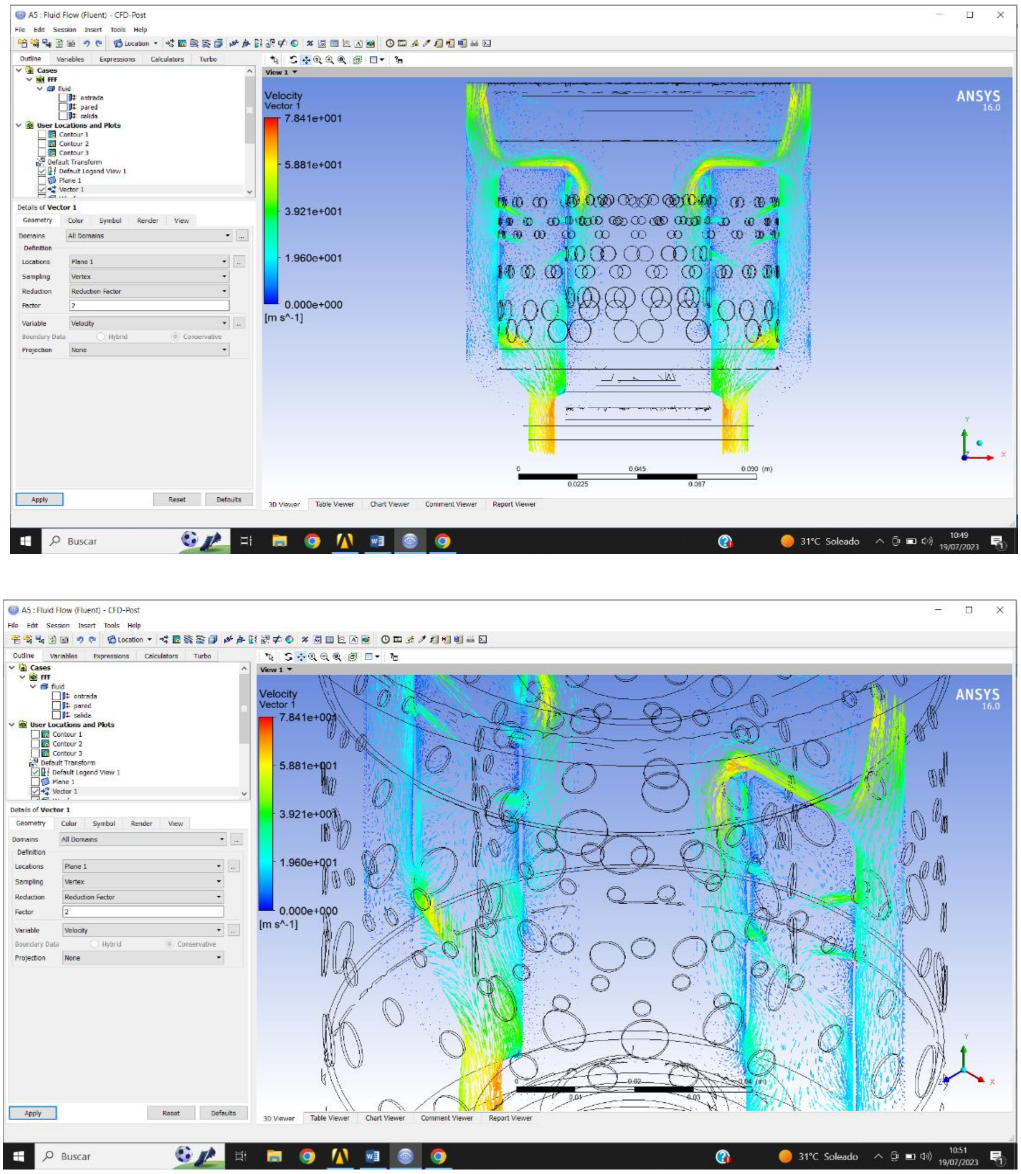

Figure 98: velocity vectors.

The velocity streamlines demonstrate what was explained in the velocity contour by showing the vortices created by the vortex generators around the old stall region and the tendency of the flow to adhere to the surface of the blade.

Numerical simulation is used to validate the experimental values, and the simulation described here is exclusively concerned with the physics of the system, with no regard for the complexities of chemical reactions. As a result, certain parts of the simulation's output are expected to line up with real-world data, while others are likely different due to the absence of chemical interactions. This shows only the necessity of understanding the simulation's boundaries and limits, as well as interpreting its results on the basis of the simplified parameters used.

Conclusion:

the numerical study chapter has been instrumental in gaining a comprehensive understanding of the combustion chamber dynamics in a laboratory-scale jet engine. Also, it has provided valuable insights into the combustion efficiency, pollutant emissions, and the impact of various design modifications.

The findings from this chapter serve as a basis for further research and optimization of combustion chamber designs, contributing to the development of more efficient and environmentally friendly jet engines. So, in order to improve the numerical research and get closer to reality, we may try to make an experimental test that is entirely accurate to the reality by altering certain characteristics, such as the mesh type or other factors.

General Conclusion

This work, aimed to conduct a theoretical-experimental study on the combustion chamber of a laboratory-scale jet engine, provided important insights into the complex realities of combustion processes and the consequences for engine performance. This effort improved our understanding of combustion behavior by combining mathematical simulations and real-world data. It also provided practical advice to improve combustion chamber design.

Important components were studied using theoretical analysis, which offered information on their impact on combustion efficiency and pollutant emissions. The simulations not only provided a better understanding of the combustion process, but also can allowed for the future the examination of different design alterations to improve the engine performance.

The practical studies supplemented the theoretical simulations by giving real-world data and assessing the simulations correctness. Temperature, pressure, emission levels, and other parameters were all monitored and supplied essential input into the operation of the combustion chamber. Also, the findings can be used to guide future technical efforts aimed at enhancing combustion performance, lowering emissions, and increasing fuel efficiency.

Our study lays the groundwork for further exploration and improvement of combustion chamber concepts ultimately contributing to the advancement of Olympus-HP E jet engine technology and the pursuit of sustainable aviation, and possibly opening the way for more efficient and environmentally friendly aviation propulsion systems.

Future works and perspectives

- We can simulate the technical reaction inside to check how many emissions invalidated the simulation based on the experimental data.

- Because our present fuel is composed of plastic and the amount of fuel is insufficient to feed the turbine, we can try another fuel that may be better and cheaper.

- If I analyze the chemical reaction, the simulation will be very complicated, so we can try to simulate the chemical reaction of the combustion in the combustion model using Ansys-Chemkin software: https://www.ansys.com/products/fluids/ansys-chemkin-pro, and compare the data with the data obtained experimentally.

- We noticed that the hydrocarbons (HC) emissions performed poorly while the others worked excellently because the testo device cannot detect the fluid at fast speeds, thus we may enhance the established results by experimenting with other equipment.

- By undertaking such turbine installations for experimental purposes, researchers and engineers can pave the way for advancements in renewable energy and sustainable power generation.

- We can numerically model the flow through an alternate combustion chamber, and if we can increase the number of holes (more holes or larger hole size), or tweak the shape slightly to enhance the flow and go through lower pressure, the results maybe will be better.

- We can do the TAKOCHI method which presenting a novel approach to problem-solving that combines elements of Task, Operator, Object, and Context, offering a comprehensive framework for analysis and optimization, so instead of doing a certain or a million essays, and to eliminate the price of the combination essays, we can take some values and do a statical study based on a relation and gave me all the calculation and the necessary values that we need to know.

References

[1]. https://www.clearias.com/scramjet-engine/

[2]. https://mechanicalboost.com/jet-engine/

[3]. https://mechanicalboost.com/jet-engine/

[4]. https://amtjets.com/OlympusHP.php

[5]. https://www.thoughtco.com/different-types-of-jet-engines-1992017

[6]. T. Kandaramath Hari, Z. Yaakob, and N. N. Binitha, "Aviation biofuel from renewable resources: Routes, opportunities and challenges," *Renew. Sustain. Energy Rev.*, vol. 42, pp. 1234–1244, 2015.

[7]. Blakey, L. Rye, and C. W. Wilson, "Aviation gas turbine alternative fuels: A review," *Proc. Combust. Inst.*, vol. 33, no. 2, pp. 2863–2885, 2011.

[8]. B. M. of D. Standard, "DEF STAN 91-91/Issue 7 Amendment 2, 1 December, 2012 for Turbine Fuel, Kerosene Type, Jet A-1.".

[9]. A. S. for T. and Materials, "Standard specification for aviation turbine fuels, ASTM International D1655-13."

[10]. "Aviation Fuels Technical Review Table of Contents," *Rev. Lit. Arts Am.*

[11]. C. Forster, "The residence times of aircraft emissions in the stratosphere using a mean emission inventory and emissions along actual flight tracks," *J. Geophys. Res.*, vol. 108, no. x, 2003.

[12]. N. A. and S. Administration, "Aviation-Fuel Property Effects on Combustion," 1984.

[13]. G. Liu, B. Yan, and G. Chen, "Technical review on jet fuel production," *Renew. Sustain. Energy Rev.*, vol. 25, pp. 59–70, 2013.

[14]. S. Dooley, S. H. Won, M. Chaos, J. Heyne, Y. Ju, F. L. Dryer, K. Kumar, C. J. Sung, H. Wang, M. a. Oehlschlaeger, R. J. Santoro, and T. a. Litzinger, "A jet fuel surrogate formulated by real fuel properties," *Combust. Flame*, vol. 157, no. 12, pp. 2333–2339, 2010.

[15]. S. Humer, a. Frassoldati, S. Granata, T. Faravelli, E. Ranzi, R. Seiser, and K. Seshadri, “Experimental and kinetic modeling study of combustion of JP-8, its surrogates and reference components in laminar nonpremixed flows,” *Proc. Combust. Inst.*, vol. 31 I, pp. 393–400, 2007.

[16]. TFG_Juan Carlos Zamora Morales_firmado/ junio2021.

[17]. https://www.sciencedirect.com/science/article/abs/pii/S0021961422001604

[18]. https://manualzz.com/doc/11711169/omega-hhp241-series-owner-manual

[19]. https://www.pressure-transducers.net/viatran-corporation/

[20]. International Civil Aviation Organization (ICAO), “Doc 7300/9 - Convention on International Civil Aviation,” 2006.

[21]. International Civil Aviation Organization (ICAO), “Circular 134-AN/9: Control of Aircraft Engine Emissions,” 1977.

[22]. D. Wuebbles, M. Gupta, and M. Ko, “Evaluating the Impacts of Aviation on Climate Change,” *Eos, Trans. Am. Geophys. Union*, vol. 88, no. 14, p. 157, 2007.

[23]. https://www.testo.com/en-US/testo-350/p/0632-3510

[24]. https://www.muser-my.com/product/testo-malaysia-350-analysis-box-exhaust-gas-analysis-systems/

[25]. Camara merono, Alberto. diseño u puesta a punto de un protocolo para determinar el poder calorífico de sólidos. Aplicación a residuos plásticos. 2017. Tesis Doctoral.

[26]. https://www.microsoft.com/en-us/p/fuel-density-calculator/9nc7zg5dwg34

[27]. https://en.wikipedia.org/wiki/Density_meter/

[28]. https://www.ujaen.es/servicios/scai/recursos/aq07-analizador-elemental-automatico-chns-2

[29]. International Civil Aviation Organization (ICAO), “Doc 9184: Airport Planning Manual,” 2002.

[30]. International Civil Aviation Organization (ICAO), “Annex 16 Environmental Protection - Volume II: Aircraft Engine Emissions,” 2008.

[31]. International Civil Aviation Organization (ICAO), “Doc 9889: Airport air quality manual,” 2011.

[32]. J. Graichen and B. Gugele, “Greenhouse Gas Emissions from Aviation,” *ETC/ACC Tech nical Pap.*, no. December, 2006.

[33]. International Civil Aviation Organization (ICAO), “Cir 303: Operational Opportunities to Minimize Fuel Use and Reduce Emissions Cir 303,” 2003.

[34]. ICAO, Protección del medio ambiente Vol II. 2008.

[35]. https://www.studocu.com/row/document/university-of-malawi/development-economics/catia-lab-task1/2088028/

[36]. https://www.scribd.com/document/433000853/Lab-Report-Component-Design

[37]. https://www.scribd.com/document/610821810/Sample-Internship-Report/

[38]. https://en.wikipedia.org/wiki/Computational_fluid_dynamics

[39]. https://www.researchgate.net/post/What-is-computational-fluid-dynamics

[40]. https://www.cimdata.com/en/trending/item/2422-ansys-inc

[41]. https://www.ncbi.nlm.nih.gov/pmc/articles/PMC6263693/

[42]. https://www.idealsimulations.com/resources/cfd-modelling/

[43]. https://www.hellenicaworld.com/Science/Mathematics/en/MeshGeneration.html

[44]. https://www.idealsimulations.com/resources/cfd-modelling/

[45].https://www.jettech.ch/12-Triebwerke/12-2-Technische%20Beschriebe/AMT---Olympus%20manual%202.17.pdf

Annexes

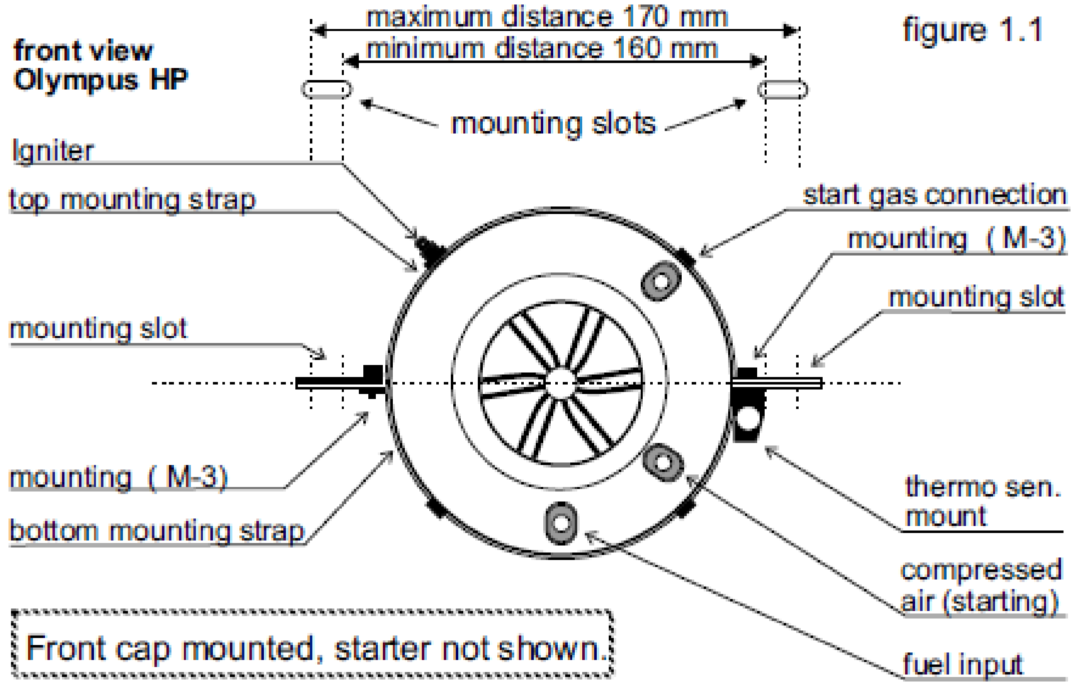

front view
Olympus HP
maximum distance 170 mm
minimum distance 160 mm
figure 1.1
mounting slots
Igniter
top mounting strap
start gas connection
mounting (M-3)
mounting slot
mounting slot
mounting (M-3)
bottom mounting strap
thermo sen. mount
compressed air (starting)
fuel input
Front cap mounted, starter not shown.

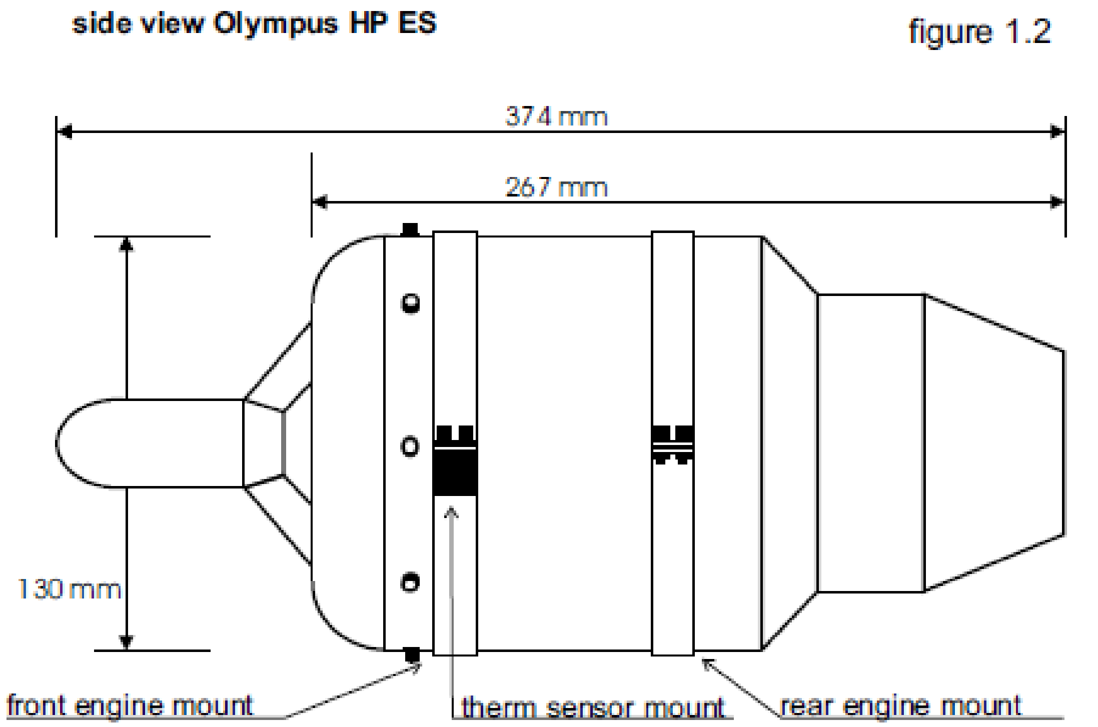

side view Olympus HP ES
figure 1.2
374 mm
267 mm
130 mm
front engine mount
therm sensor mount
rear engine mount

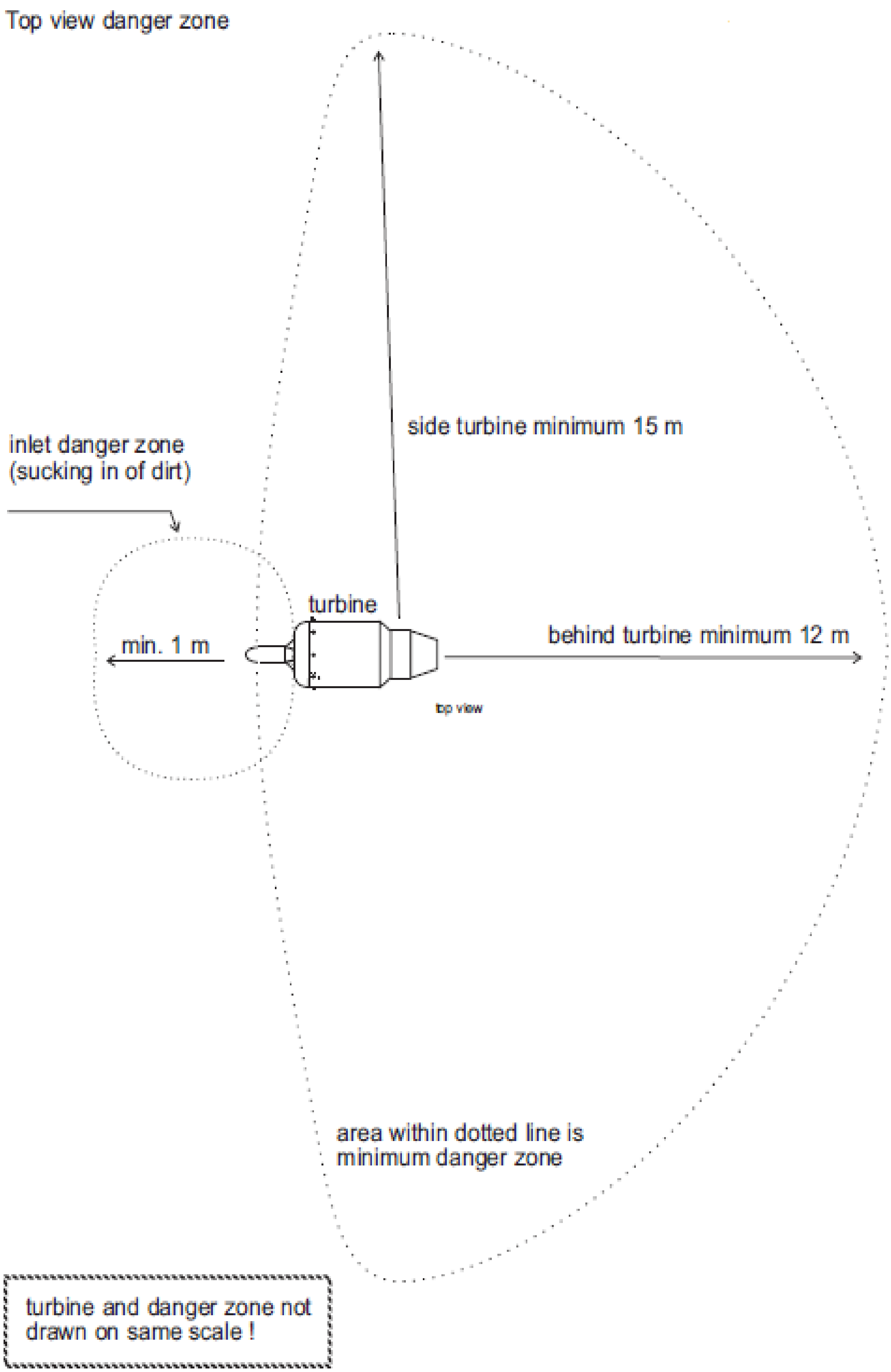
Top view danger zone
side turbine minimum 15 m
inlet danger zone
(sucking in of dirt)
turbine
min. 1 m
behind turbine minimum 12 m
top view
area within dotted line is
minimum danger zone
turbine and danger zone not
drawn on same scale !

side view Olympus HP ES

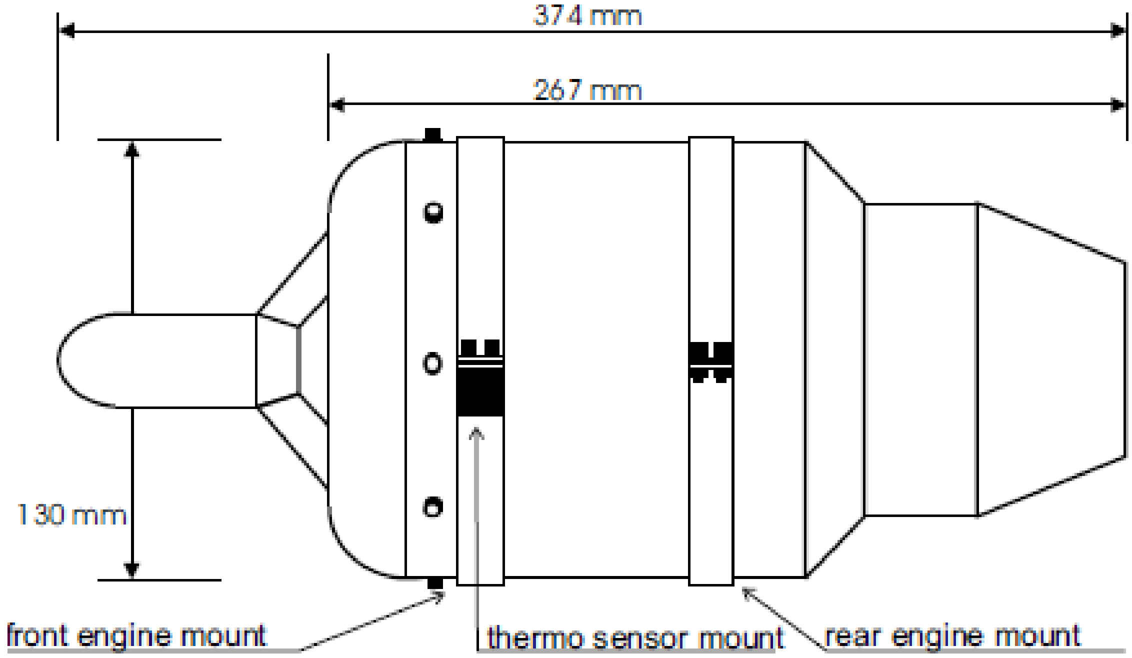

inlet shape

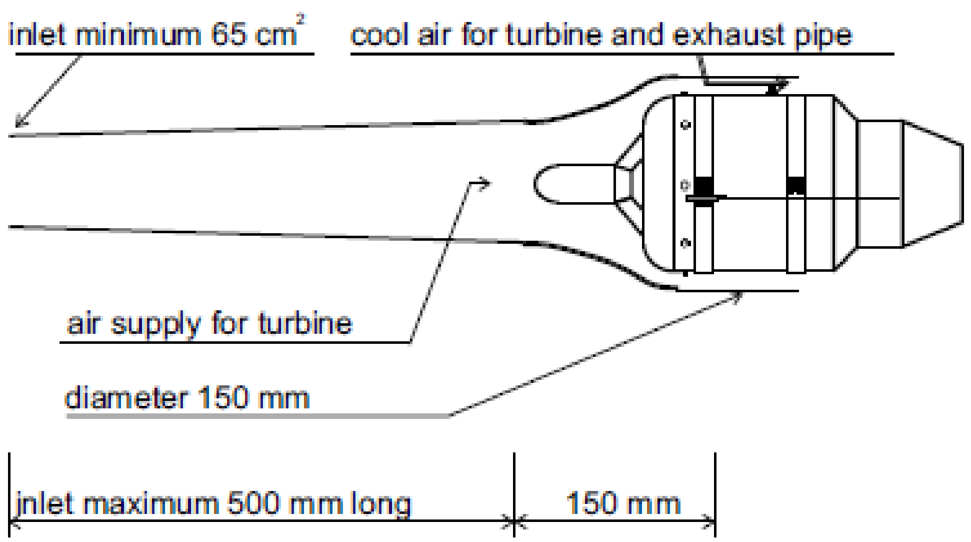

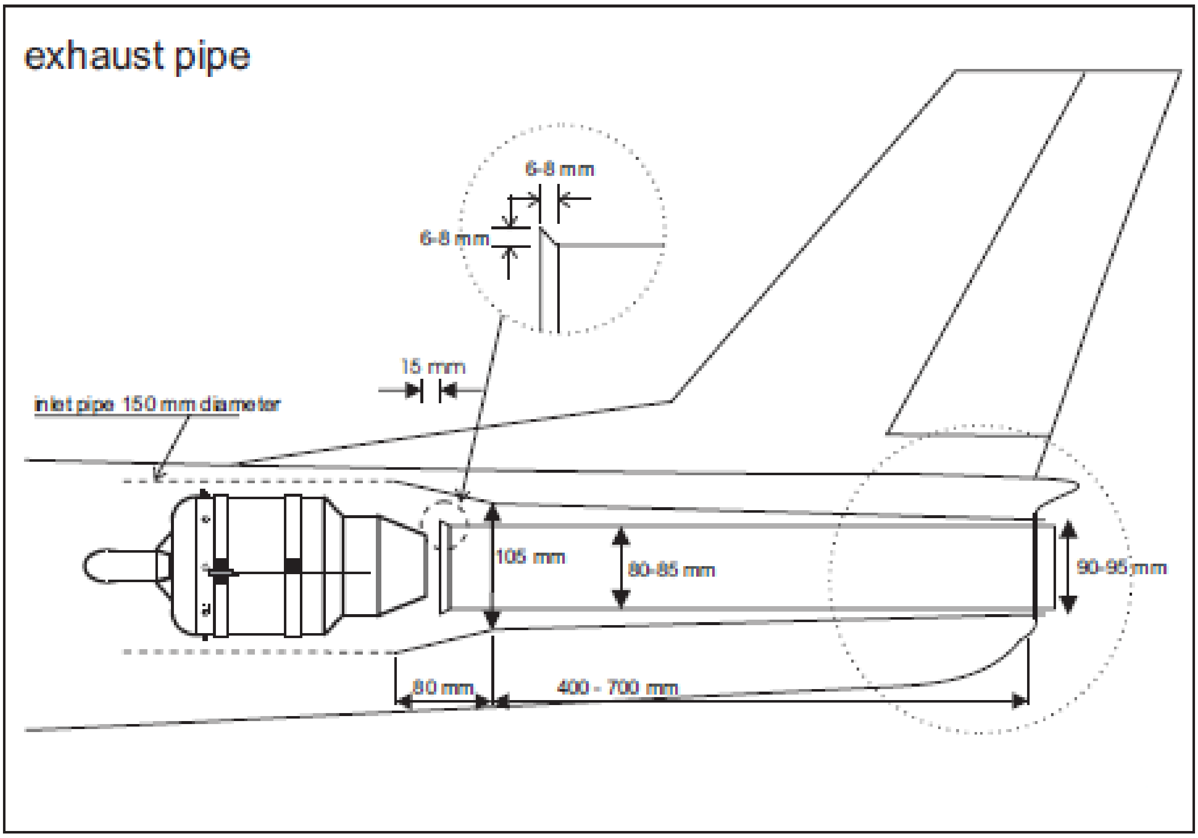
exhaust pipe
6-8 mm
6-8 mm
15 mm
inlet pipe 150 mm diameter
105 mm
80-85 mm
90-95 mm
80 mm
400 - 700 mm

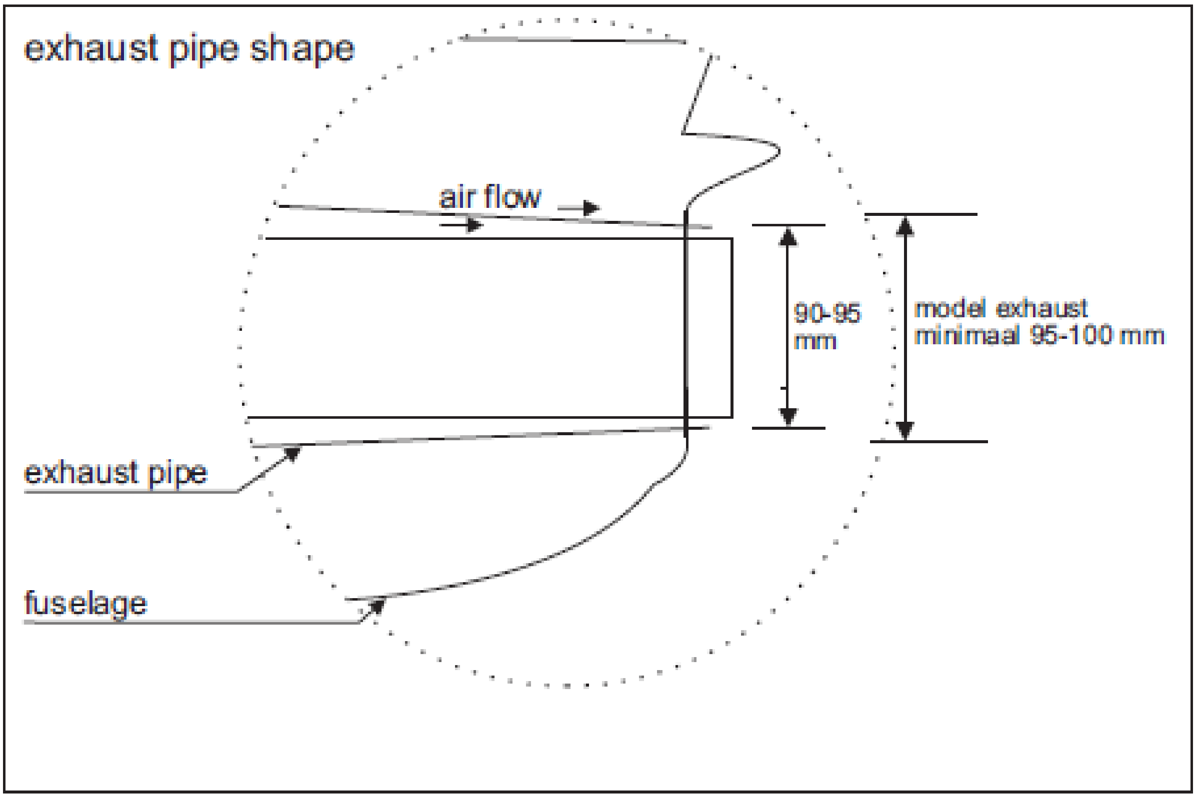
exhaust pipe shape
air flow
90-95 mm
model exhaust minimaal 95-100 mm
exhaust pipe
fuselage

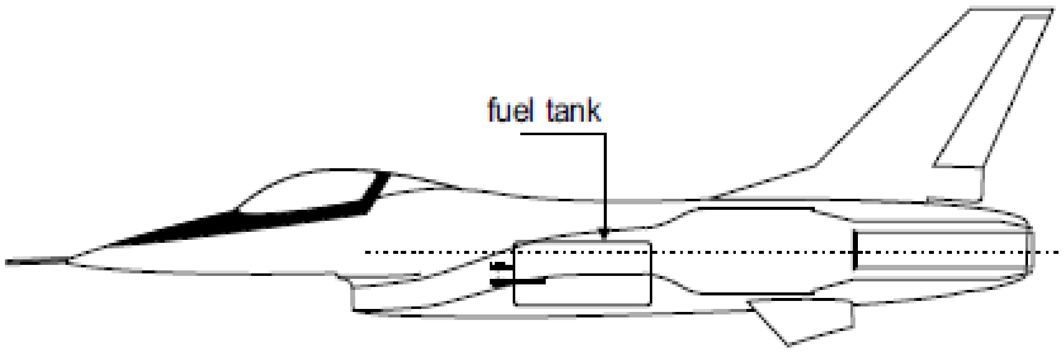

In this example of an F16, 2 fuel tanks are placed left and right of the air inlet duct.

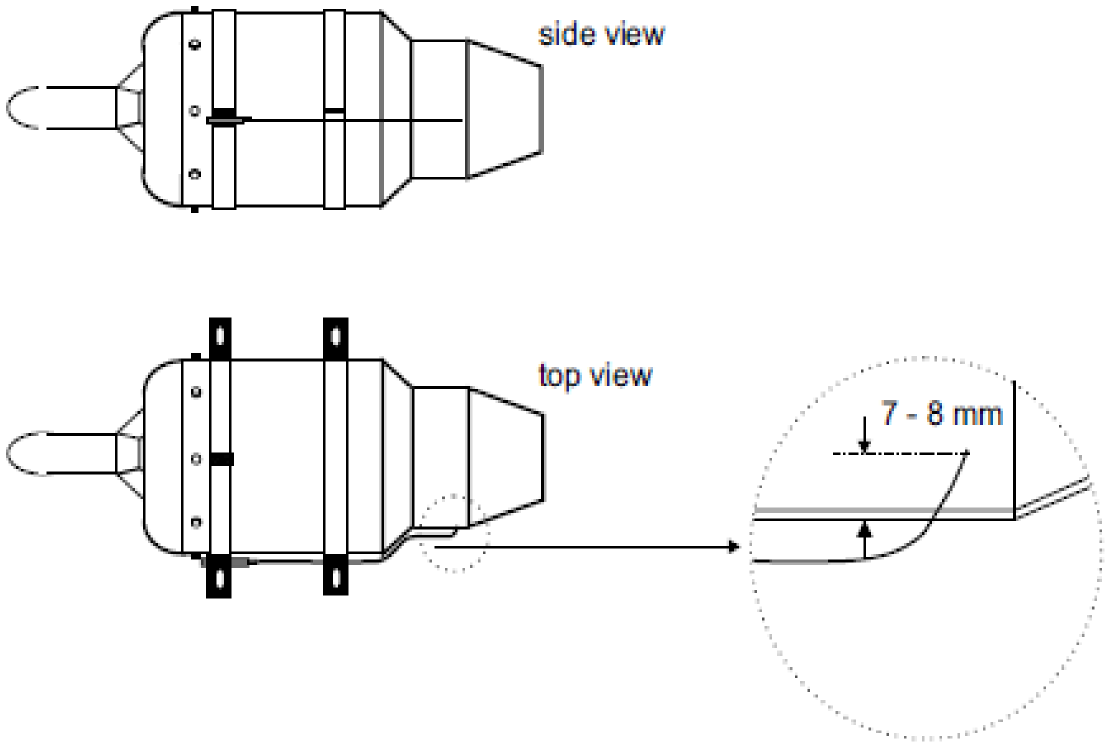

Note: put thermo couple
7 - 8 mm inside exhaust.

AMT Netherlands b.v.
Spaarpot 34
NL-5667 KX Geldrop
Netherlands/Holland

Tel: int+31 40 7873130
Fax: int+31 40 7873139
Email: email@amtjets.com
website: www.amtjets.com

Description of the AMT Netherlands Olympus HP gas turbine.

January 2019

The original Olympus design was redesigned in 2004 to the HP version, in 2010 the engine is converted to a direct kerosene starting system.
The engine is highly used in the "model jet scene" but also professionals are using the Olympus HP. A spinoff of the Olympus HP is being certified by EASA for the use as a "bringing home device" for a full size glider.
For universities a "special" layout is available with measuring points.

Pricing : http://www.amtjets.com/form_pricelist.php

Specifications

All data at STP +/- 2%

Engine diameter	130 mm	/	5.1 Inch
Engine length	374 mm	/	14.7 Inch
Engine weight	2900 gram	/	6.4 Lbs
System airborne weight *	3845 gram	/	8,5 Lbs
Thrust at S.T.P. **	230 N	/	51.7 Lbf
Maximum RPM	108.500	/	108.500
Thrust at Idle RPM	13 N	/	2.9 Lbf
Pressure ratio	3.5:1	/	3.5:1
Mass flow	450 Gr/sec	/	0.99 Lb/Sec
Max continues EGT	750 Deg C	/	1380 Deg F
Fuel consumption	640 Gr/min	/	22,5 oz/min
Specific fuel consumption	46,4 gr/(Kn*sec)	/	1,64 lb/(lbf*hr)
Starting method	Direct kerosene starting gas turbine, on request propane start.		

* Total weight of; Engine,ECU,pump,battery,thermosensor, valves, mounting straps.
** On request the RPM can be raised to 110.000 RPM giving 10 Newton additional thrust.

Operating conditions

Min operation temperature *	- 35 Deg. Celsius	/	-31 Deg F
Maximum operating temperature	+ 50 Deg. Celsius	/	+122 Deg F
Maximum operating altitude	8000 Meter	/	26250 feet
Maximum operating speed	1000 Km / hour	/	620 Mile / hour

* With the use of LiPo batteries the minimum operation temperature is limited to -10 Deg Celsius.

Engine control possibilities

1 x RS232	Throttle and switch settings including special functions *	
2 x PWM between 1-2 milliseconds **	Throttle and switch settings.	(special functions * with push button)
2 x Analog inputs 0-5 volt DC **	Throttle and switch settings.	(special functions * with push button)

* Activation of prime function, igniter function, starter function, speed cool.
** Specify ECU at ordering with PWM inputs or Analog inputs.

All specifications are subject to change without notice. S.T.P. : 15 Degrees Celsius / 59 Degrees Fahrenheit, Pressure : 1013 Mbar / 29.91 in

Illem jebrt

<u>**Olympus HP E-start data as graphical information**</u>

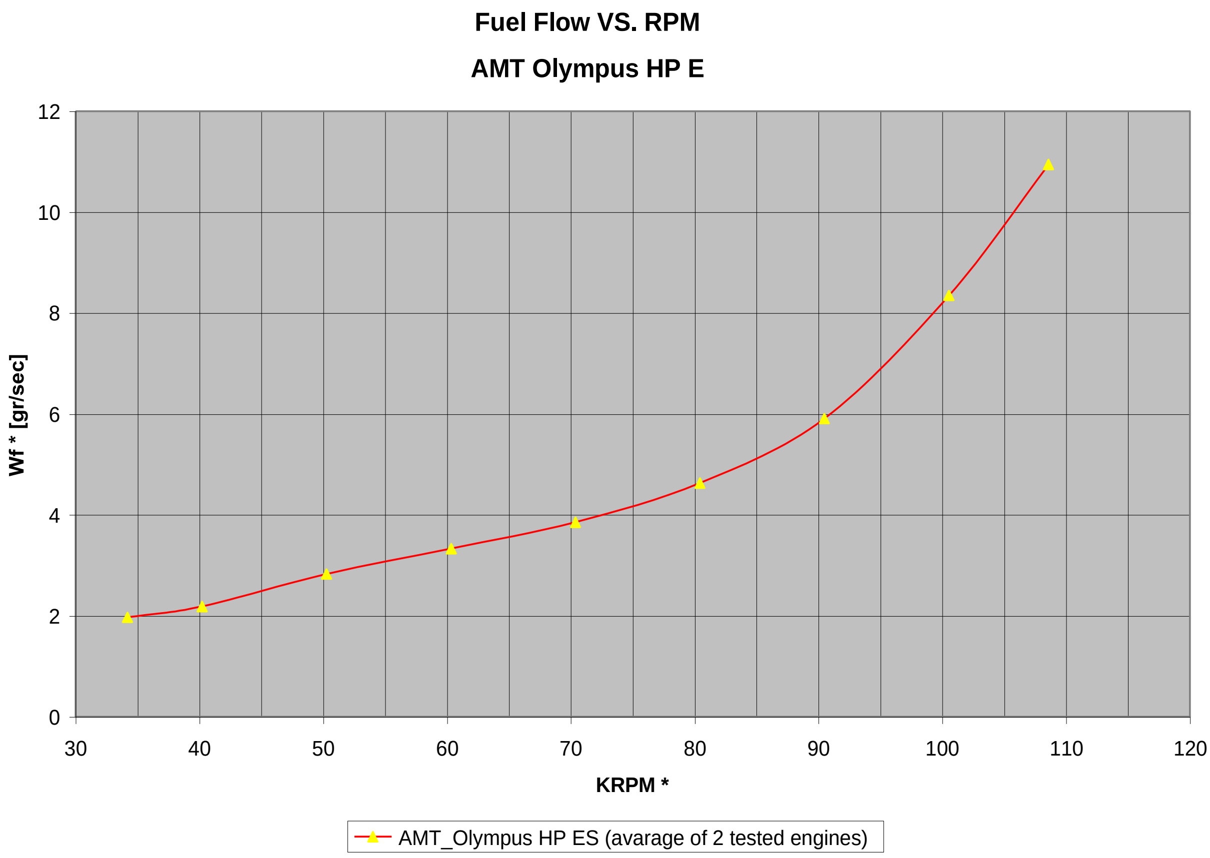

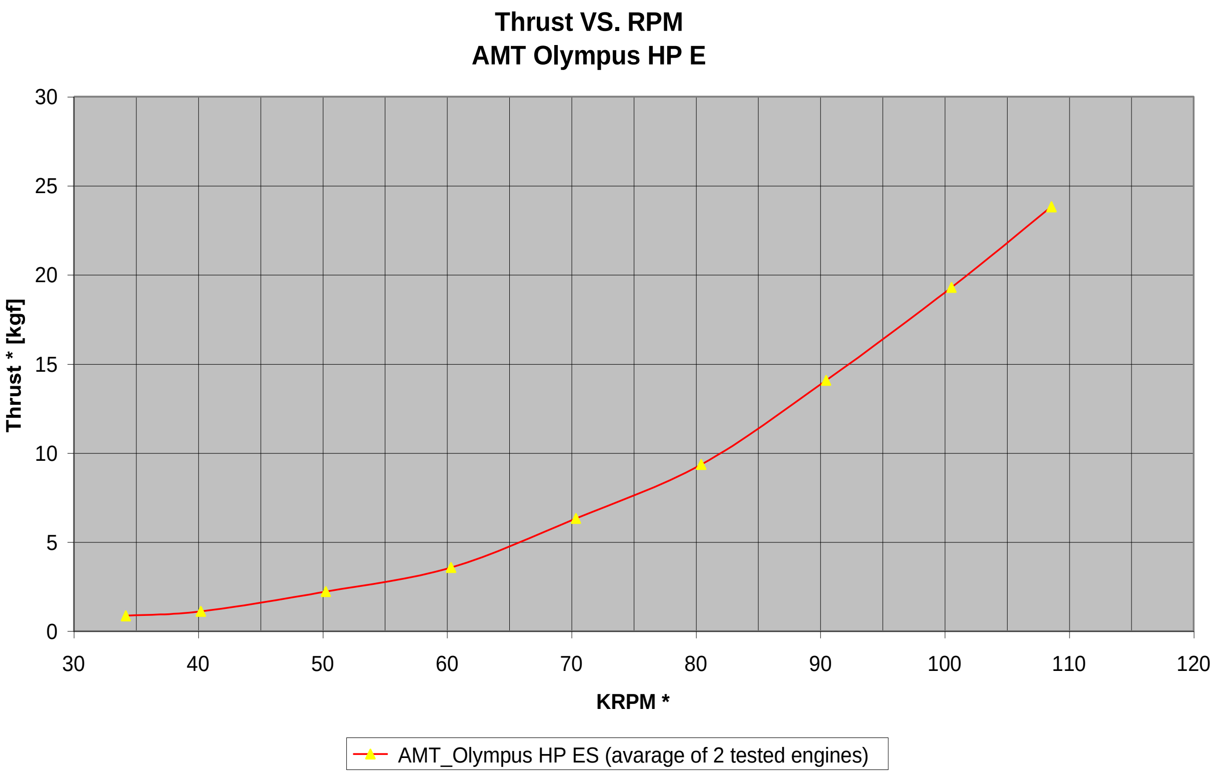

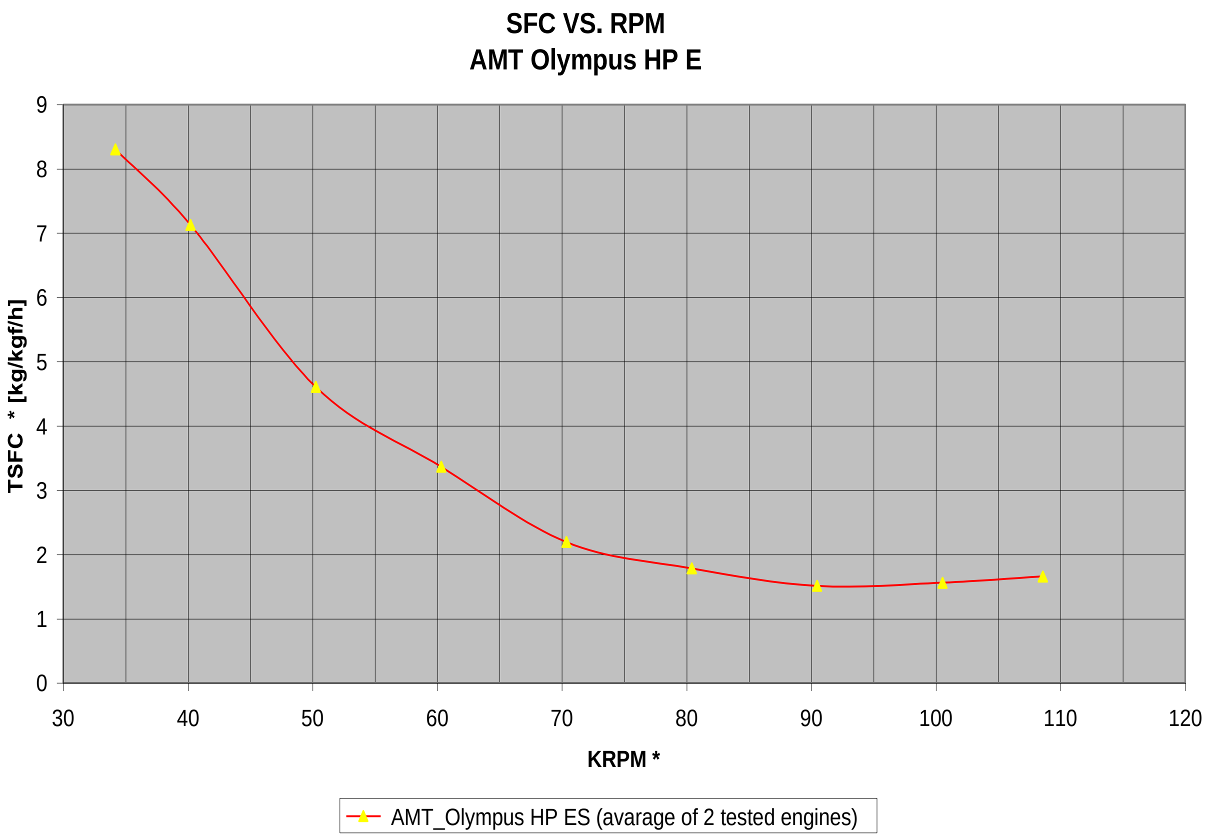
SFC VS. RPM
AMT Olympus HP E
TSFC * [kg/kgf/h]
9
8
7
6
5
4
3
2
1
0
30
40
50
60
70
80
90
100
110
120
KRPM *
AMT_Olympus HP ES (avarage of 2 tested engines)

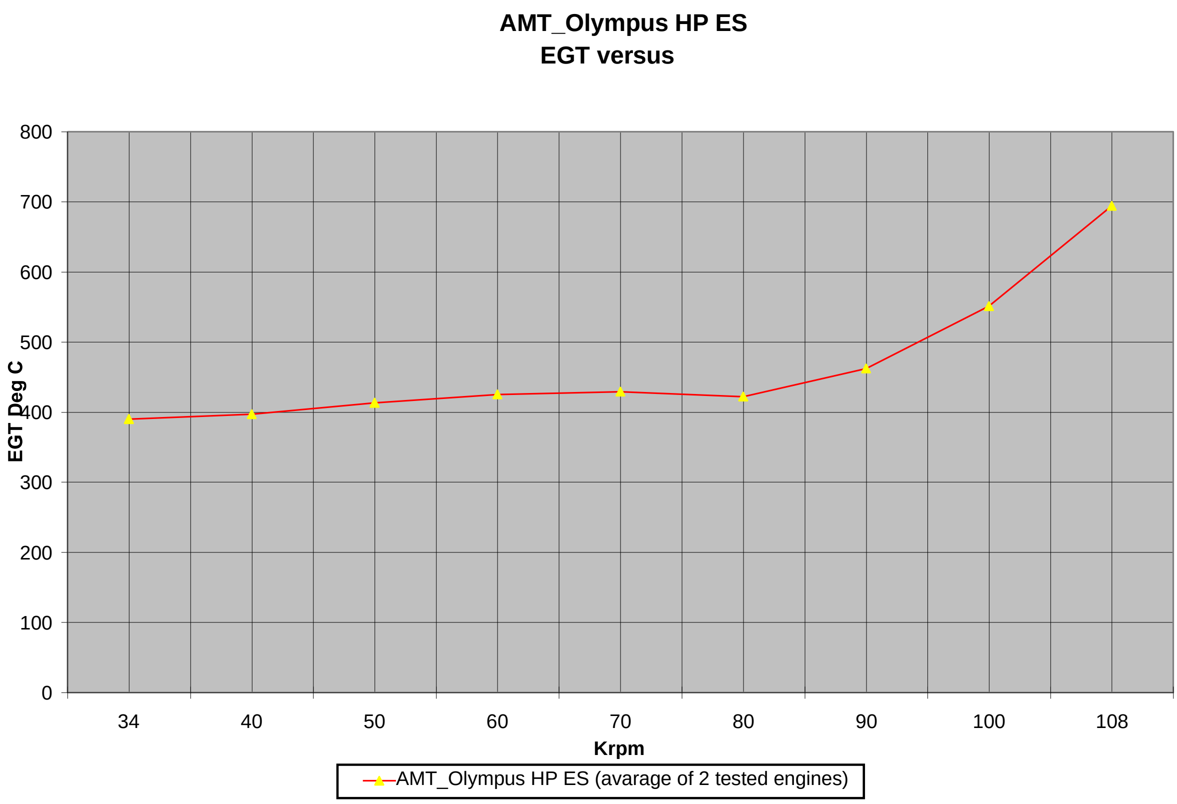
AMT_Olympus HP ES
EGT versus
EGT Deg C
800
700
600
500
400
300
200
100
0
34
40
50
60
70
80
90
100
108
Krpm
AMT_Olympus HP ES (avarage of 2 tested engines)

Olympus HP "Air mass flow" measurments

Ambient conditions: 26 Deg C 1020 mBar

Measurement 1

RPM		Air mass flow
rpm/min	Pressure	
1000/min	mm water	(kg/s)
36,5	5,0	0,1157
50,0	24,0	0,1678
62,5	44,5	0,2283
71,5	68,0	0,2755
80,5	94,0	0,3289
90,0	130,0	0,3974
100,5	178,0	0,4520
105,0	197,0	0,4704
108,5	211,5	0,4813

Measurement 2

RPM		Air mass flow
rpm/min	Pressure	
1000/min	mm water	(kg/s)
36,5	5,0	0,1157
49,5	22,5	0,1678
60,5	41,0	0,2214
65,0	51,5	0,2384
70,0	60,5	0,2667
75,5	78,0	0,3010
81,0	95,0	0,3390
85,5	113,5	0,3688
90,0	131,5	0,3959
95,0	152,0	0,4255
99,5	171,0	0,4480
105,5	198,5	0,4718
108,5	211,5	0,4813

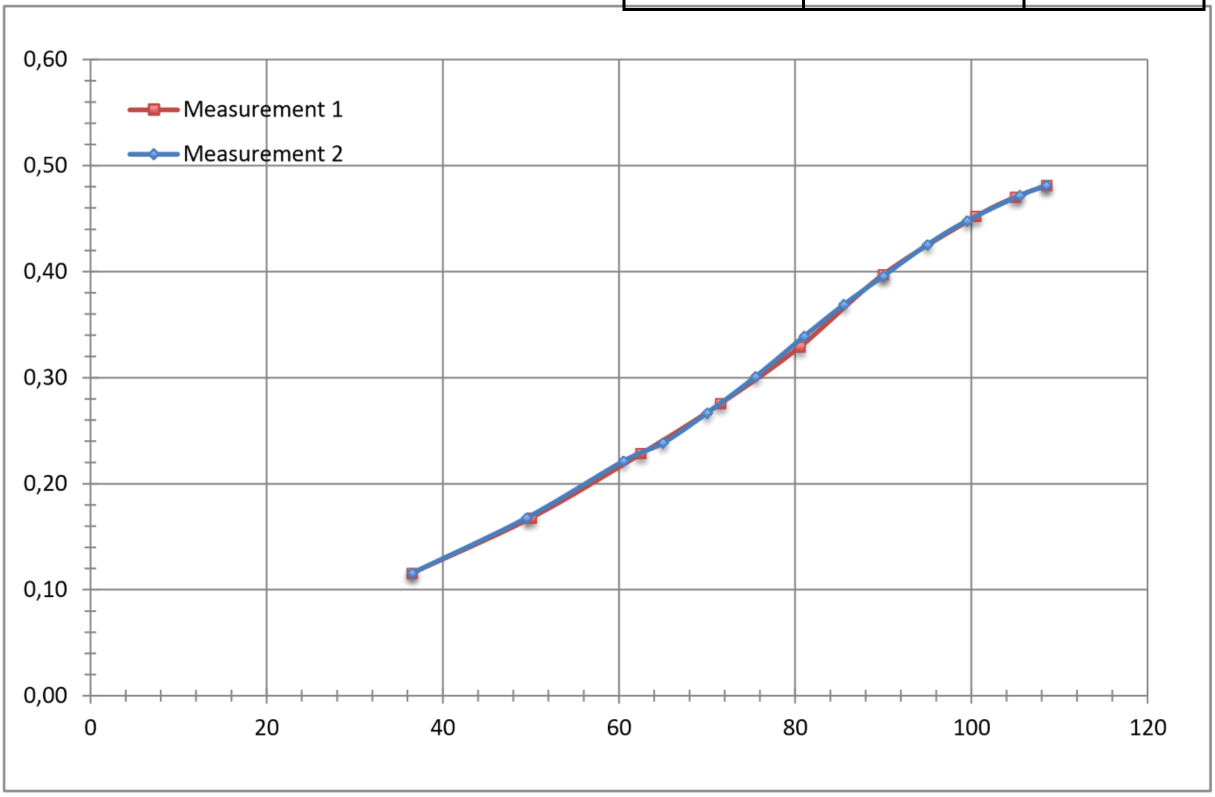

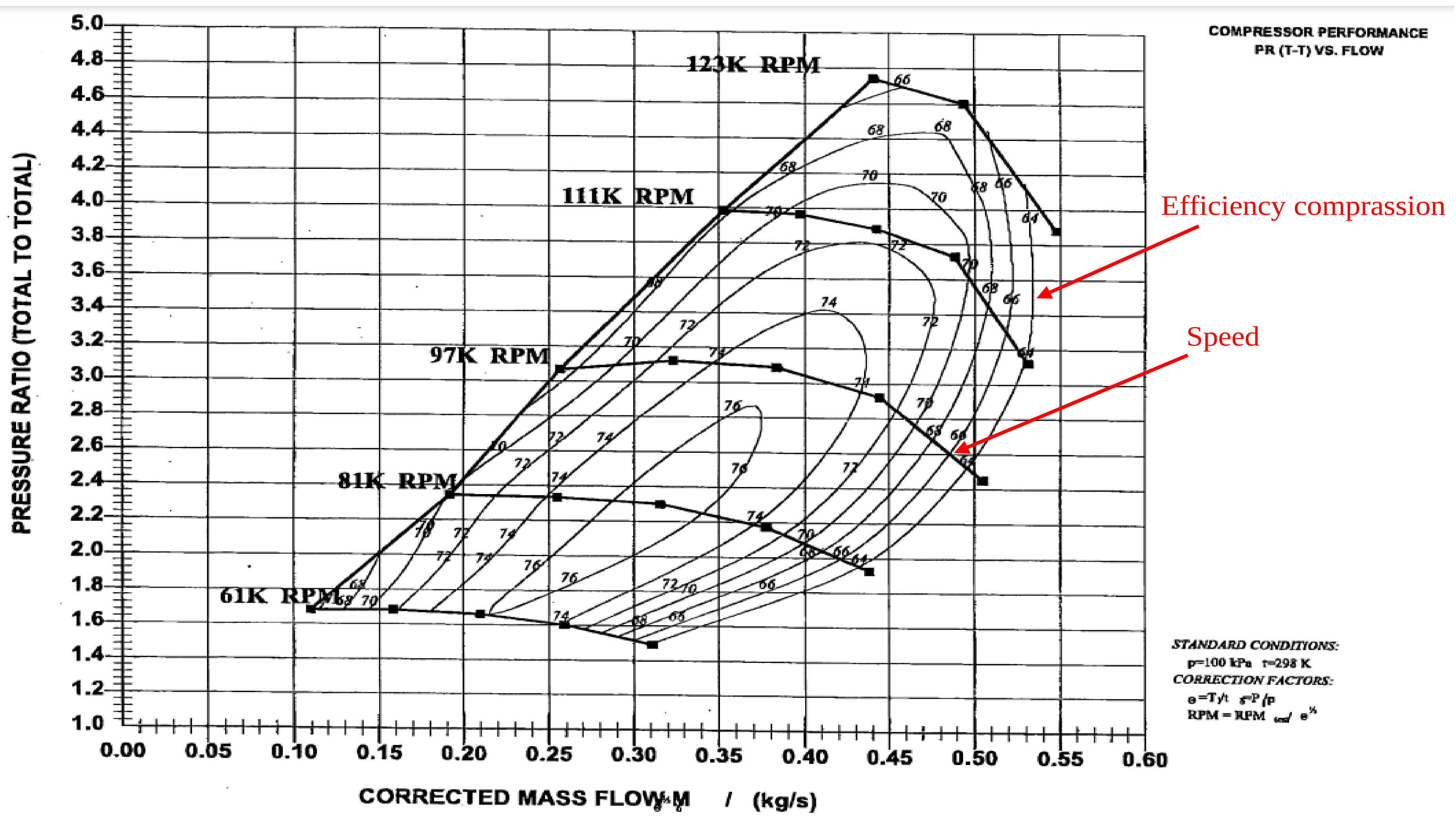

- Air mass flow and speed → the inputs
- Pressure ratio and efficiency → the outputs

The above system provides pressure data from Ps1, Ps3, Pt3, Pt4, Pt5 and temperature data from Tt1, Tt3, Tt4, Tt5, Tt6, and here is the cut out of our Olympus-HP E engine to know exactly the positions of each point.

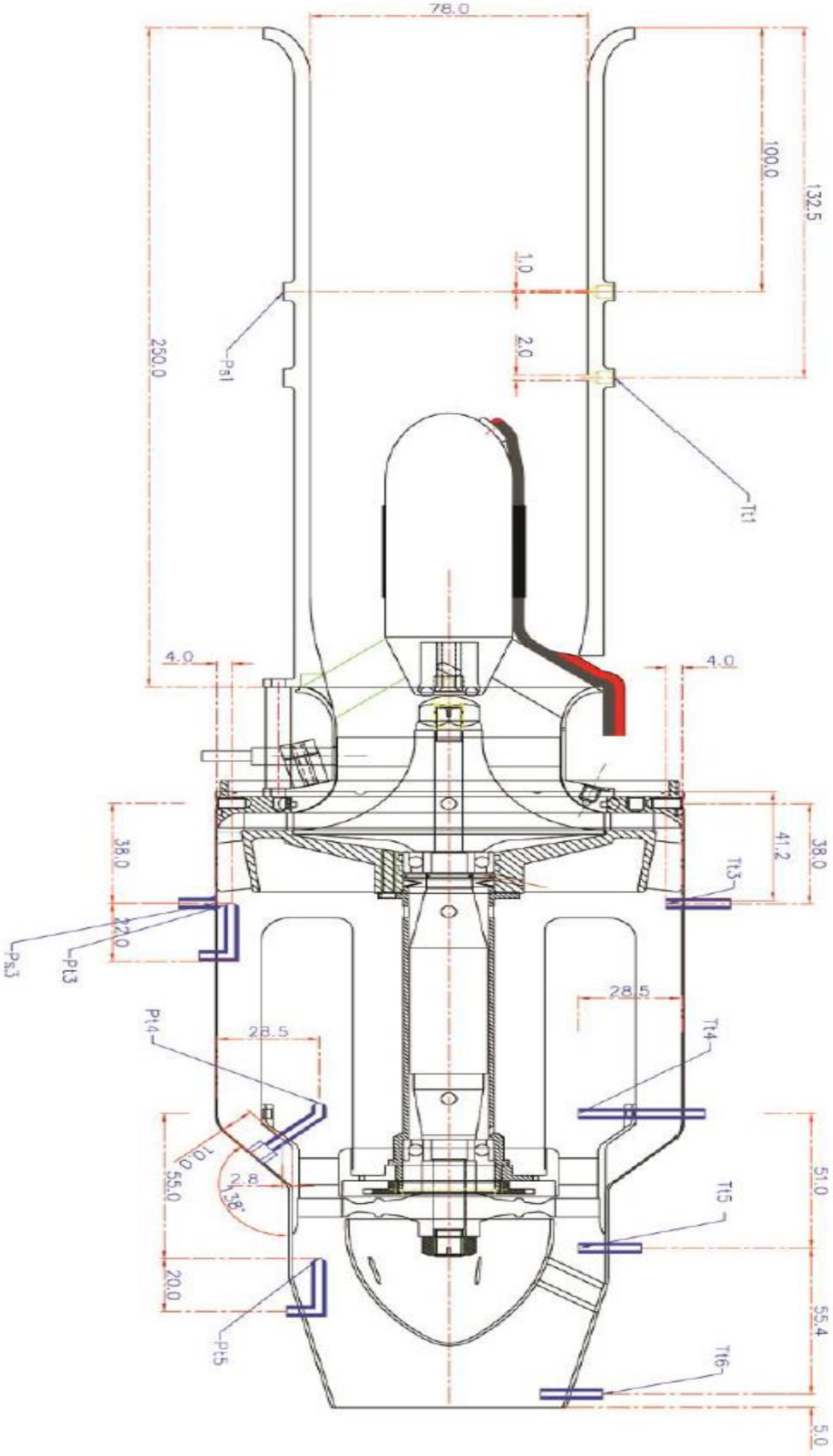

Abstract

The objective of this work is to experimentally and numerically characterize the behavior of the fluid that passes through a jet engine which is the Olympus-HP E type and in particular as it passes through the combustion chamber. This experimental and numerical study is split into two major sections: The first is to do a general inspection of our engine and discuss the essential instruments that we will need in our engine tests to obtain parameter values such as temperature, pressure, and exhaust emissions. The second is to check calculation findings with experimental measures and investigate numerical outcomes. Finally, this study effort bridges the theoretical knowledge and actual application gap inside jet engine combustion chambers. A full image of the Olympus-HP E jet engine's behavior is produced by unraveling the nuances flow of fluid dynamics through testing and numerical modeling. This research, as a monument to innovation, influences the future trajectory of aviation technology, ushering in a decade of productivity, reliability, and environmental awareness.

Keywords: Jet engine, thermodynamic cycle, Exhaust emissions, Combustion chamber, Mesh, CFD, Fluent.

Résumé

L'objectif de ce travail est de caractériser expérimentalement et numériquement le comportement du fluide qui traverse un moteur à réaction ce qui est le type Olympus-HP E et en particulier lorsqu'il traverse la chambre de combustion. Cette étude expérimentale et numérique est divisée en deux sections principales: La première consiste à effectuer une inspection générale de notre moteur et à discuter des instruments essentiels dont nous aurons besoin pour obtenir les valeurs des paramètres tels que la température, la pression et les émissions de gaz d'échappement. La seconde consiste à vérifier les résultats des calculs avec les mesures expérimentales et à étudier les résultats numériques. Cette étude comble le fossé entre les connaissances théoriques et les applications réelles dans les chambres de combustion des moteurs à réaction. Une image complète du comportement du moteur à réaction Olympus-HP E est produite en démêlant le flux des nuances de la dynamique des fluides par des essais et une modélisation numérique. Cette recherche, monument de l'innovation, influence la trajectoire future de la technologie de l'aviation, inaugurant une décennie de productivité, de fiabilité et de sensibilisation à l'environnement.

Mots-clés : Moteur à réaction, Cycle thermodynamique, Émissions de gaz d'échappement, Chambre de combustion, Maillage, CFD, Fluent.

Technical file

The technical file shown below is the result of different efforts made throughout the End-of-Study Project internship. Its goal is to supply the firm and its industrial customers with a file that meets current visual representation standards for mechanical design. This is with a view to subsequent product operation, consumption, maintenance, and modification, since:

« A good drawing is worth more than a long speech »

At this level, the dossier is frequently coupled with manufacturing-related professional know-how. To that goal, the dossier is separated into two major sections, which are listed below in this order:

- The Ensemble Drawings:

Which enables us to depict all or part of the proposal or object in detail, while also being supported by a nomenclature that describes the numerous standard sections and components.

- The Definition Drawings:

In this manner, we describe the numerous pieces to be machined while specifying all of the necessary dimensions and technological limits, and, of course, while adhering to all applicable standards.

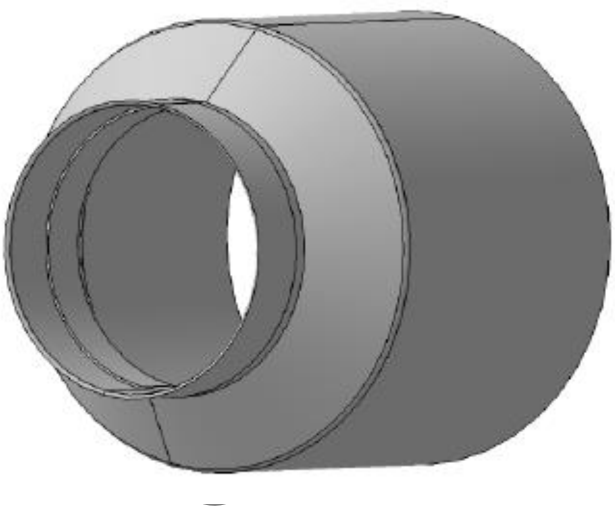

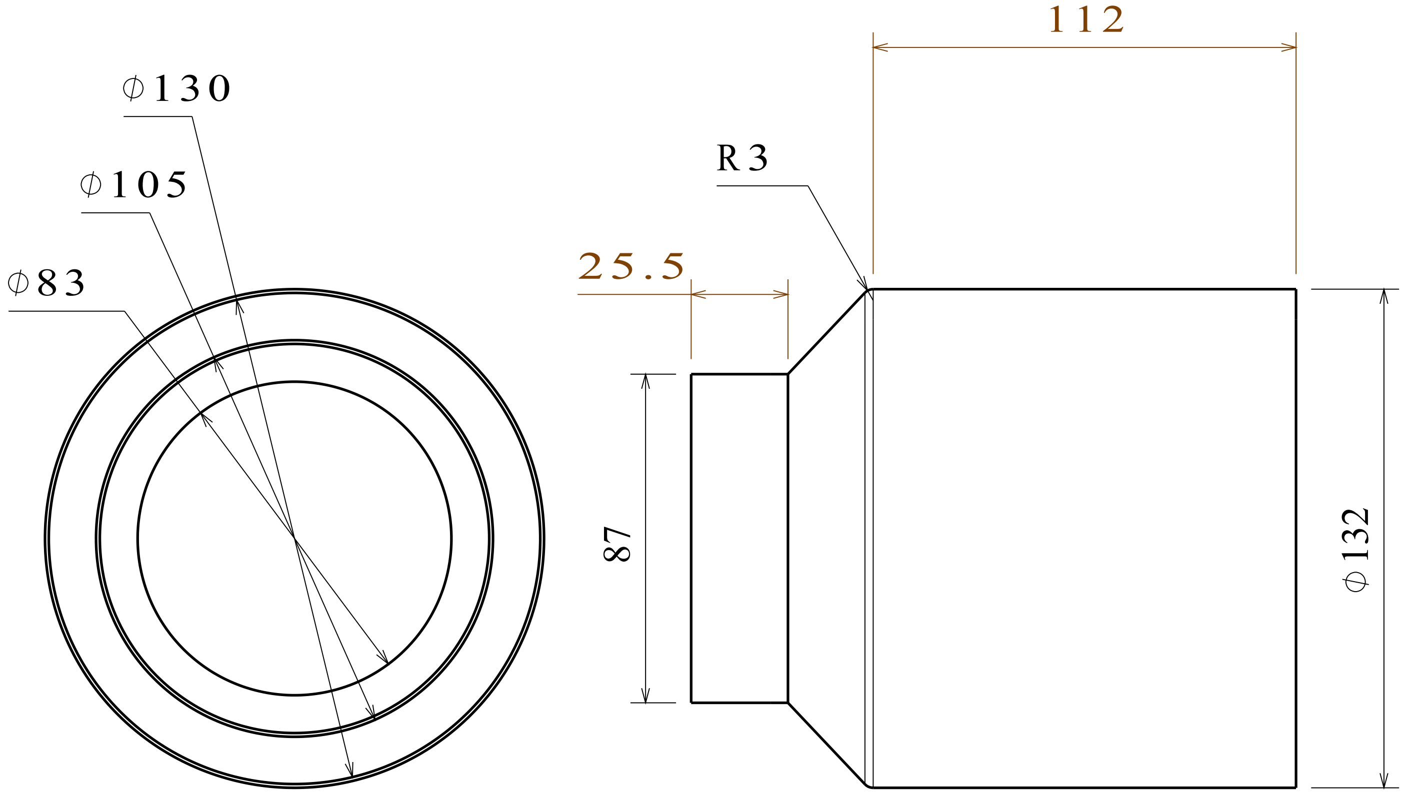

1 Grad	1 Nbr	Designation: **Outside engine structure**	Class: 5GA
Format: A4		**Olympus HP-E engine**	Drawn by: Jabri Ilhem Date:09/07/2023
		ESAT UNIVERSITY	Lader:1:3 Unit: mm

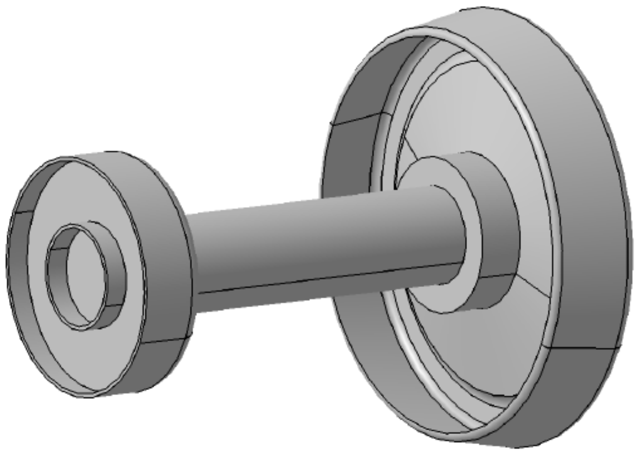

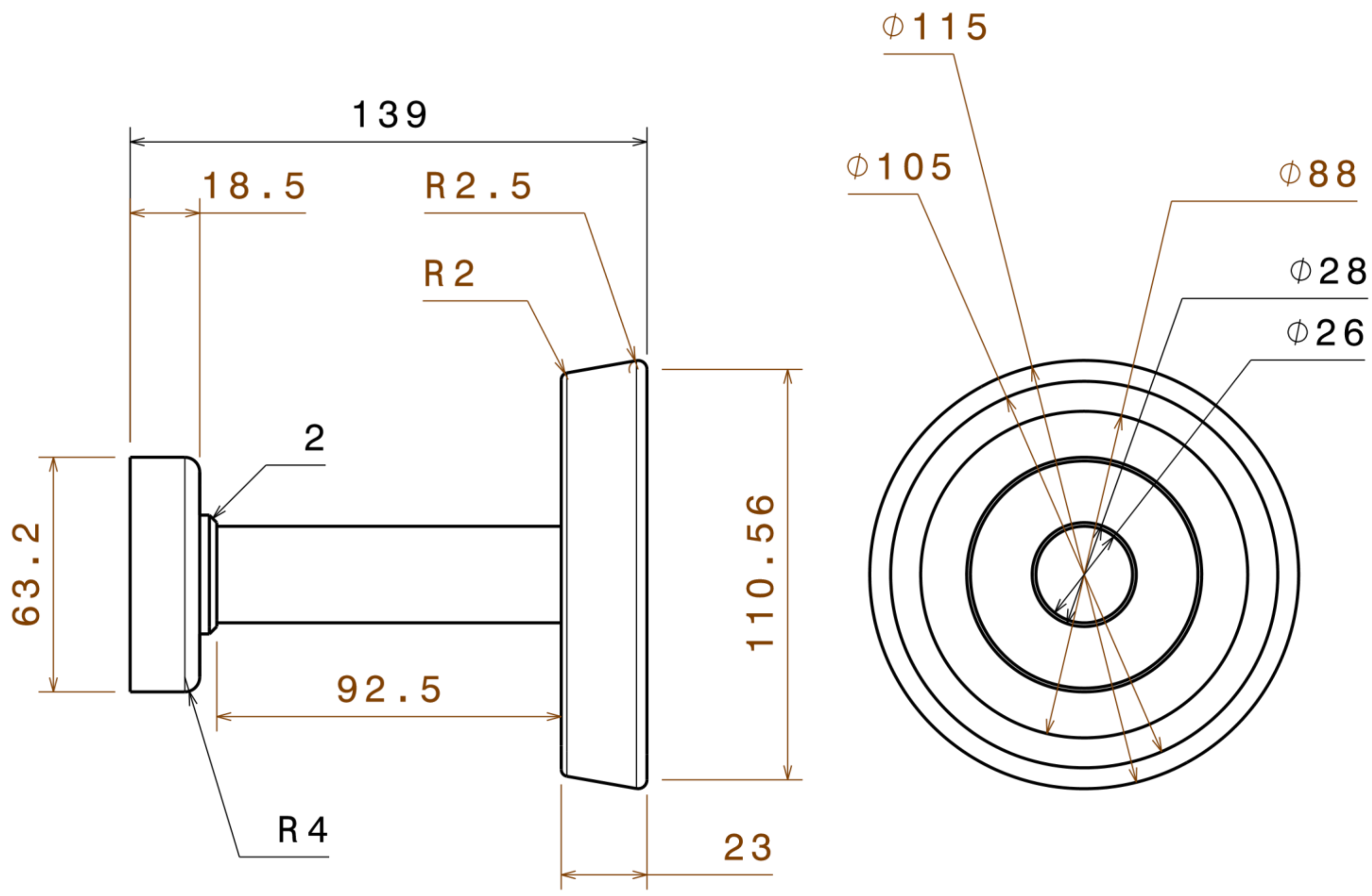

1 Grad	1 Nbr	Designation: **Middle piece**	Class: 5GA
Format: A4		**Olympus HP-E engine**	Drawn by: Jabri Ilhem Date:09/07/2023
		ESAT UNIVERSITY	Lader:1:3 Unit: mm

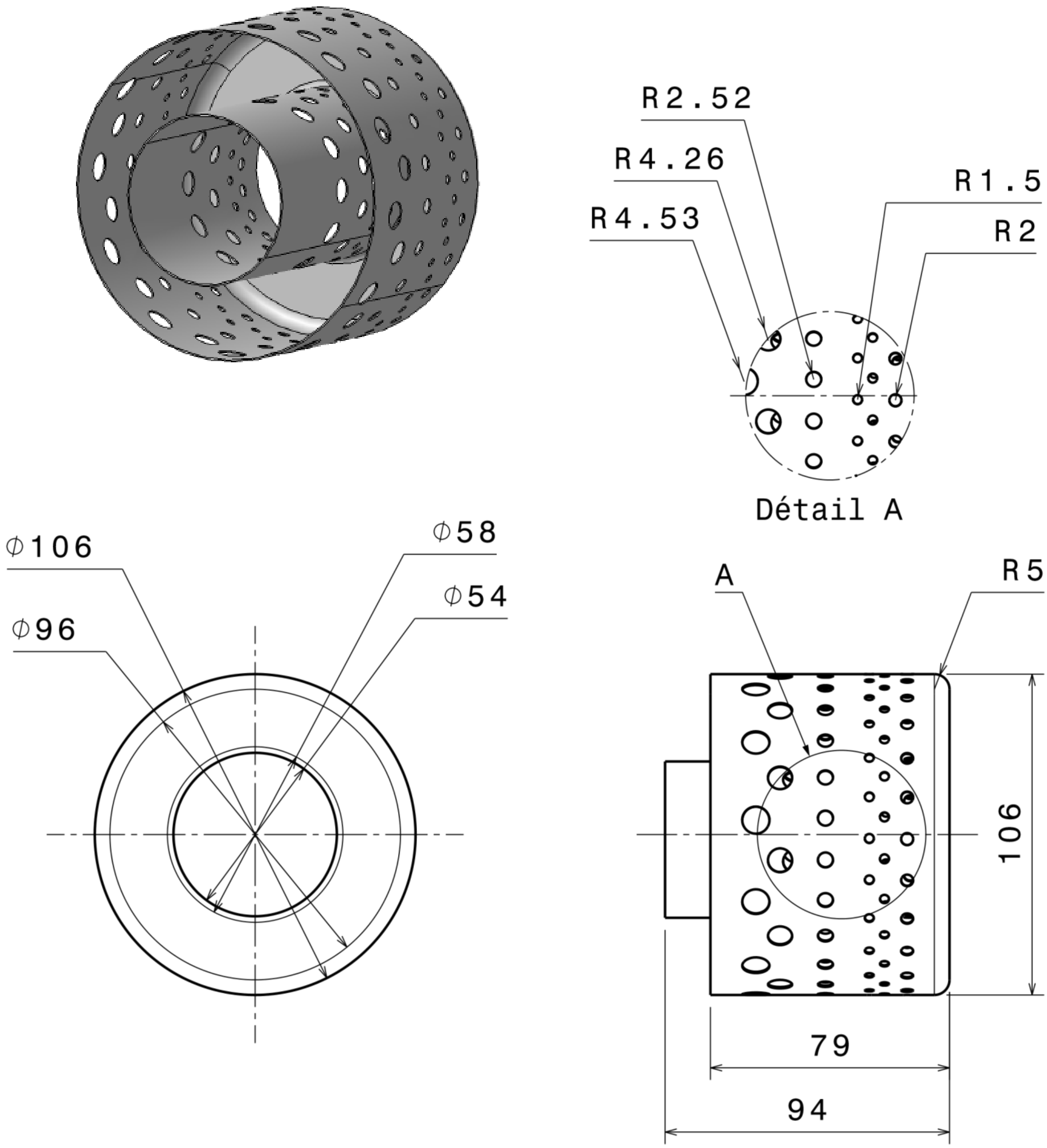

1 Grad	1 Nbr	Designation: **Combustion Chamber**	Class: 5GA
Format: A4		**Olympus HP-E engine**	Drawn by: Jabri Ilhem Date:09/07/2023
		ESAT UNIVERSITY	Lader:1:3 Unit: mm

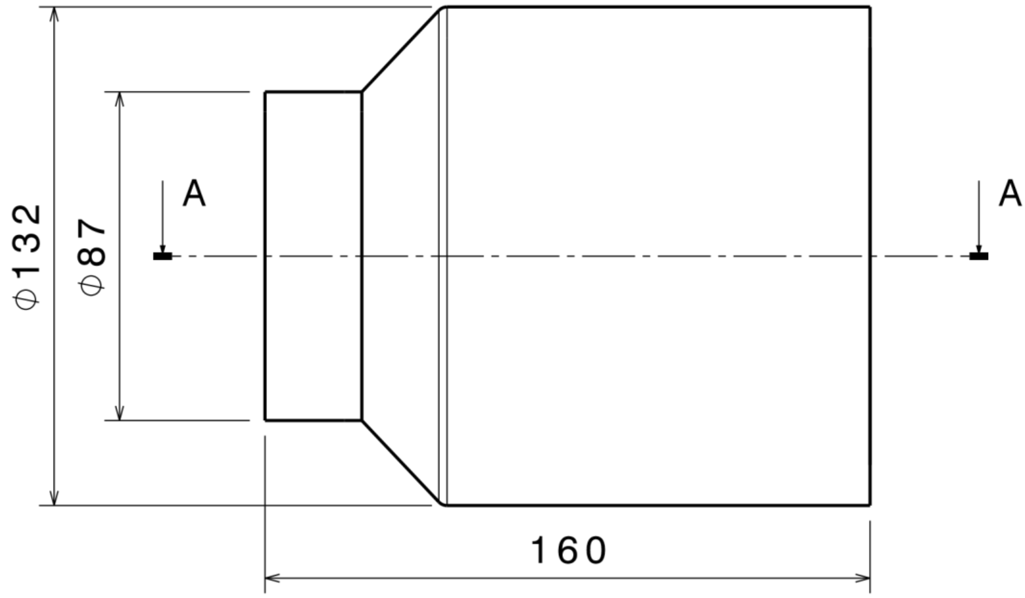

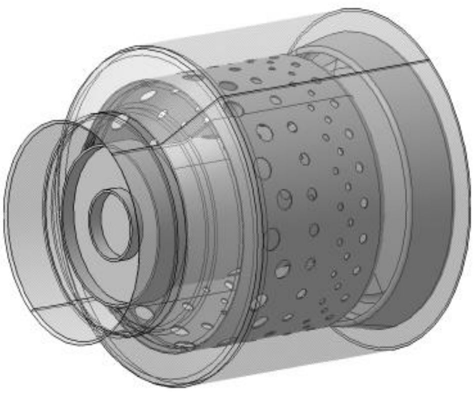

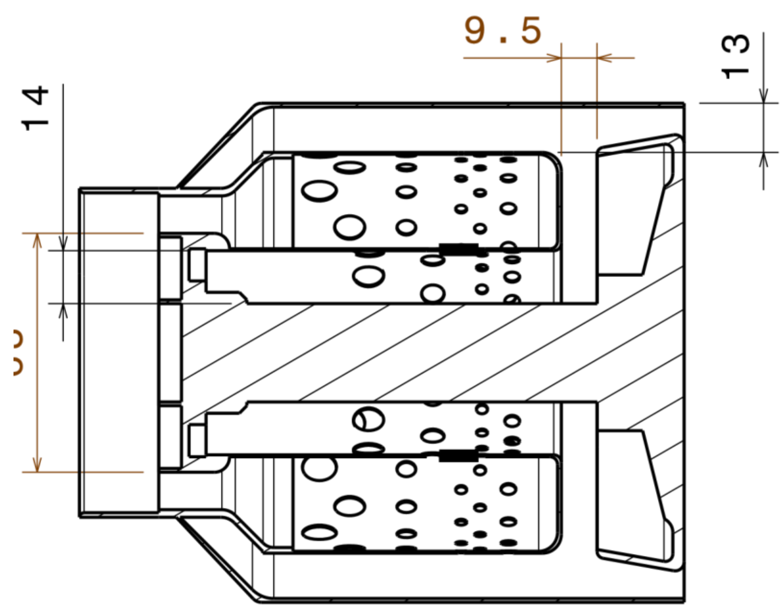

Coupe A-A

1 Grad	1 Nbr	Designation: **Combustion Chamber assembly**	Class: 5GA
Format: A4		**Olympus HP-E engine**	Drawn by: Jabri Ilhem Date:09/07/2023
		ESAT UNIVERSITY	Lader:1:3 Unit: mm

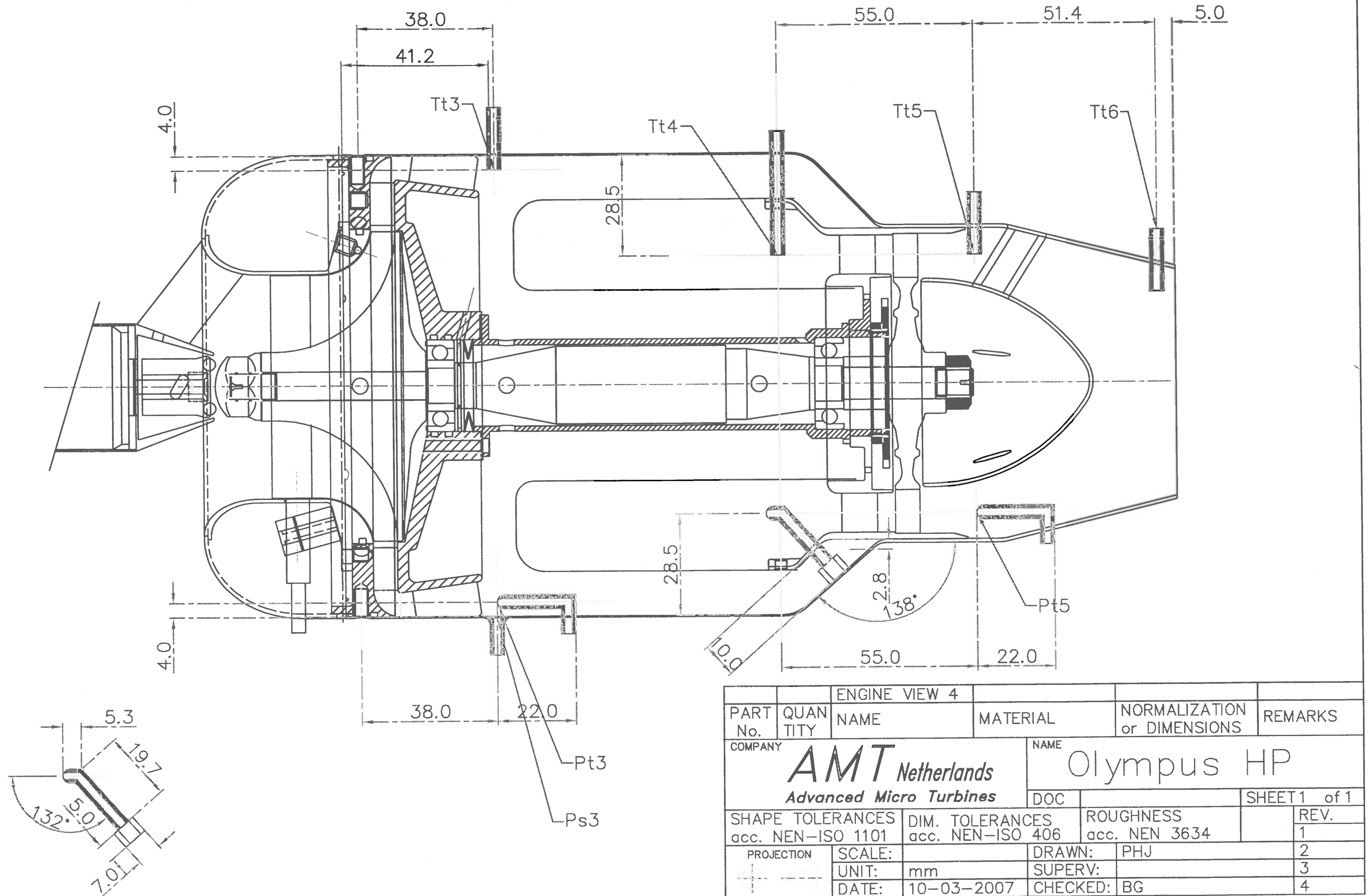

		ENGINE VIEW 4			
PART No.	QUANTITY	NAME	MATERIAL	NORMALIZATION or DIMENSIONS	REMARKS

COMPANY AMT Netherlands Advanced Micro Turbines		NAME Olympus HP		
		DOC		SHEET 1 of 1
SHAPE TOLERANCES acc. NEN-ISO 1101	DIM. TOLERANCES acc. NEN-ISO 406	ROUGHNESS acc. NEN 3634		REV. 1
PROJECTION	SCALE:	DRAWN:	PHJ	2
	UNIT: mm	SUPERV:		3
	DATE: 10-03-2007	CHECKED:	BG	4